UNIVERSITY OF OKLAHOMA

GRADUATE COLLEGE

SEASONAL INFLUENCES ON THE MOLECULAR AND METAL BINDING PROPERTIES OF GROUNDWATER AND SURFACE WATER DISSOLVED ORGANIC MATTER (DOM) IN AN ALPINE WATERSHED LOCATED IN CENTRAL COLORADO

A THESIS

SUBMITTED TO THE GRADUATE FACULTY

in partial fulfillment of the requirements for the

Degree of

MASTER OF SCIENCE

By

CHELSEY GALLAGHER

Norman, Oklahoma

2021

SEASONAL INFLUENCES ON THE MOLECULAR AND METAL BINDING PROPERTIES OF GROUNDWATER AND SURFACE WATER DISSOLVED ORGANIC MATTER (DOM) IN AN ALPINE WATERSHED LOCATED IN CENTRAL COLORADO

A THESIS APPROVED FOR THE

SCHOOL OF GEOSCIENCES

BY THE COMMITTEE CONSISTING OF

Dr. Kato T. Dee, Chair

Dr. Andrew S. Elwood Madden

Dr. Kyle E. Murray

ACKNOWLEDGEMENTS

First and foremost, I would like to thank my mentor for these past two years, Dr. Kato T. Dee. I would not be where I am today, with the knowledge base I now have, without the guidance of Dr. Dee. I would also like to thank my committee members, Dr. Andrew Elwood Madden, for his continuous encouragement, feedback, and willingness to assist in anything I needed and Dr. Kyle E. Murray, for his willingness to provide valuable feedback. In addition, I would like to thank my Geochemistry research group that encouraged, supported and helped me through the past two years. Specifically, Joy Foluso, who not only helped me with all my field and lab work but also was a friend and cheerleader to me. Lastly, my wonderful husband, for his constant love and support, and of course, willingness to move halfway across the United States to allow me to pursue my dreams.

TABLE OF CONTENTS

LIST OF FIGURES

LIST OF TABLES

ABSTRACT

The nature and behavior of surface water and groundwater chemistry in alpine watersheds is influenced by snowmelt-driven hydrology. This study investigated the effects of seasonal variability in groundwater and surface water dissolved organic matter (DOM) on trace metal binding behavior. Samples were collected from surface water and groundwater in an alpine watershed located in Central Colorado during the spring-snowmelt, summer, and fall seasons for general water chemistry and DOM characterization. We used the isolated fulvic acid (FA) component of DOM for spectroscopic characterization and Cu-DOM binding experiments to relate seasonal variability associated with groundwater DOM to its presence in surface water. Optical spectroscopy results of FA isolated from surface water had specific ultraviolet absorbance ($SUVA_{254}$) values that ranged from 4.00 to 4.71 L mg^{-1} m^{-1} during spring snowmelt and from 1.76 to 2.41 L mg^{-1} m^{-1} during baseflow, and the fluorescence index (FI) ranged from 1.35 to 1.38 during spring snowmelt and from 1.48 to 1.60 during baseflow. Groundwater $SUVA_{254}$ values ranged from 0.27 to 0.62 L mg^{-1} m^{-1} during baseflow and from 0.27 to 0.96 L mg^{-1} m^{-1} during spring snowmelt, while FI ranged from 1.77 to 2.73 during spring snowmelt and from 1.82 to 2.27 during baseflow in 2020. The range of spectroscopic indices suggests that DOM sources and associated molecular compositions in streams change from aromatic and allochthonous during spring/summer to lower aromaticity and autochthonous in fall/winter. DOM-Cu binding measurements using a cupric ion-selective electrode (ISE) showed that low-$SUVA_{254}$ values (0.62 to 2.05 L mg^{-1} m^{-1}) correspond to greater free copper ions in solution (17% Cu^{2+}) in comparison to higher $SUVA_{254}$ (2.18 to 4.71 L mg^{-1} m^{-1}) with a smaller proportion of free copper ions (ex. 3%) in surface water samples. The relationship between $SUVA_{254}$, Cu^{2+}, and seasonality indicates that DOM in streams during baseflow conditions exhibits similar

groundwater DOM characteristics. Our results indicate that seasonal variability exists in streams and is not as pronounced in groundwater. An improved understanding of variable DOM composition in streams related to snowmelt and baseflow conditions are important for the continued improvement of DOM parameterization in geochemical and toxicological models.

1 INTRODUCTION AND BACKGROUND

Mountainous watersheds are important sources of freshwater for the human economy, ecosystems, and biodiversity (Hauer et al., 1997). Historic hard-rock mining practices have impacted the water quality and aquatic life in many mountainous watersheds around the world because of the release of acid mine drainage (AMD) and associated elevated concentrations of toxic trace metals (Butler, Ranville, & Ross, 2008). AMD is created through pyrite oxidation reactions when water and oxygen interact with pyrite, common in sulfide mineral deposits, causing acidic runoff. The acidic runoff further mobilizes toxic metals such as copper by further dissolution of metal sulfide minerals (i.e., CuS, PbS, and ZnS) (Hutson, 2004).

The Leadville mining district, located in the headwaters of the Upper Arkansas River watershed (HUARW), produced several million tons of precious and commodity metals (i.e., Au, Pb, and Cu) extracted from sulfide ore deposits (K. S. Smith, Walton-Day, & Ranville, 2000). Decades of unregulated mining associated with the Leadville mining district resulted in widespread environmental contamination of soils, streams, and groundwater in the mountainous watershed. A study (Roline, 1988) found that heavy metal pollution of the Upper Arkansas River resulted in substantial impairment for aquatic life. Though decades of soil and water remediation has been completed in the HUARW, there are still lingering sources of toxic trace metals associated with AMD and mine tailings that continue to intermittently release toxic metals into streams and groundwater (K. S. Smith et al., 2000). Sares et al. (2004) found that the main stem of the Arkansas River, downstream of the Leadville mining district, contains disseminated tailings material deposited from fluvial processes that are a continuous source of metals loading into the Arkansas River. Previous research in the HUARW assessed water quality and the effects of heavy metal pollution (Dee, 2016; Kimball, Callender, & Axtmann, 1995; Roline, 1988; Sares et al.,

2004; K. S. Smith et al., 2000); however, research gaps still exist. Research has examined the presence of groundwater, as baseflow, in alpine streams during low-flow periods (Carroll et al., 2018; Godsey, Kirchner, & Tague, 2014); however, the contribution of groundwater solute concentration and distribution in surface water during fall and winter periods is relatively unknown. Specifically, to our current knowledge, research correlating dissolved organic matter (DOM) composition with metal binding affinity in surface water during fall and winter is not evident.

1.1 DOM source and characteristics

Natural organic matter (NOM) is a heterogeneous, complex mixture of organic compounds that originates from abiotic and biotic degradation of vegetation and aquatic organisms in soils and water. DOM is the soluble fraction of NOM (Fig. 1) that is operationally defined as the NOM fraction that passes through a 0.45 µm filter. The DOM pool (Fig. 1) is generally composed of hydrophobic (humic and fulvic acids) and hydrophilic (carbohydrates, proteins, and nucleic acids) organic components (E. Thurman, 1985).

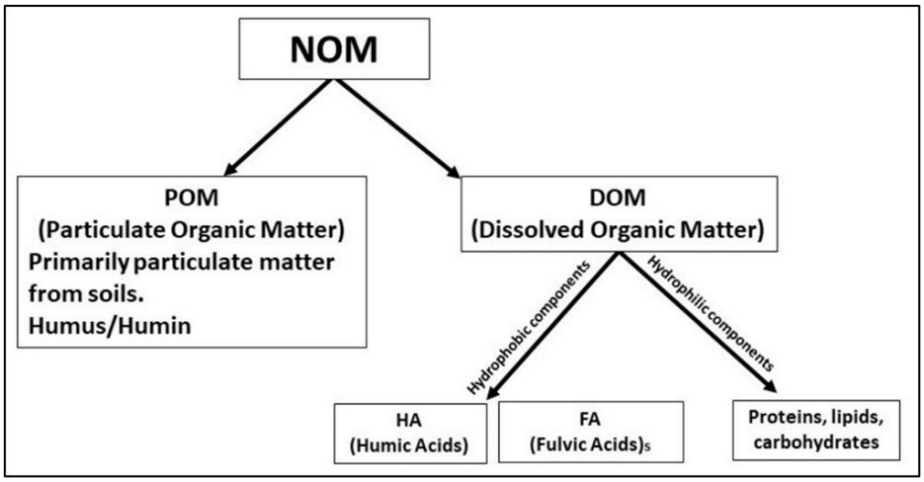

Figure 1. Major components of Natural Organic Matter (NOM).

DOM is ubiquitous and has many vital roles within aquatic ecosystems as a source of nutrients, an organic ligand for metals, absorption of UV light in aquatic systems, and regulating redox

reactions (Findley, 2003; Inamdar et al., 2012; McKnight et al., 2001). DOM in the environment originates from allochthonous and autochthonous sources, both widely applied terms to categorize the general source of DOM. Allochthonous DOM is often primarily composed of humic and fulvic acids (Fig. 2), whereas autochthonous DOM is primarily aliphatics, proteins, carbohydrates, and lipids (McKnight et al., 2001; E. Thurman, 1985). Allochthonous DOM found in aquatic systems commonly originates in soils and has characteristics of being optically dark, having high aromatic content and high molecular weight (Brooks, McKnight, & Bencala, 1999). In mountainous watersheds, the existence of nutrient-rich soils is often limited because of short growing seasons and extensive, cold winters that hinder the production of organic matter (Dwivedi et al., 2018). Although decomposition of organic matter slows down in the winter, it continues in soils because snowpack can provide an insulating layer that prevents freezing from extending too far downward. Autochthonous DOM originates from algae and the microbial breakdown of aquatic particulates (living organisms) within the water column and allochthonous DOM (Brooks et al., 1999). As a result of algae and microbial decomposition, autochthonous DOM is enriched in proteins (Inamdar et al., 2012) and typically has a low molecular weight, low aromatic content, and is optically light (E. Thurman, 1985). The distribution of DOM varies considerably among allochthonous and autochthonous environments. DOM concentrations are typically highest in soil pore water; however, DOM concentrations decrease dramatically because DOM is transported in percolating soil water from the upper soil horizons because of adsorption with minerals and microbial decomposition, resulting in noticeably smaller DOM concentrations in groundwater (Inamdar et al., 2012; Longnecker & Kujawinski, 2011).

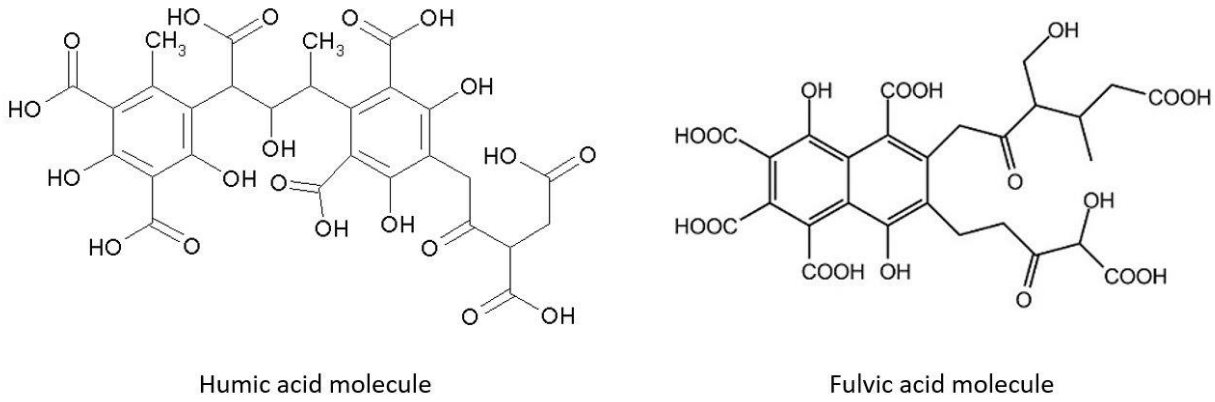

Figure 2. General humic and fulvic acid molecular structures. Image courtesy of: "Fulvic Acid" by Ronhjones and "Humic Acid" by Michal Sobkowski via Commons Wikimedia.

Fulvic acid (FA) can be a major component of the DOM pool (50—90% FA) (Al-Reasi, Wood, & Smith, 2013), and an important property of FA is how reactive it is and the ease at which it can form complexes with metal ions (Wood, Al-Reasi, & Smith, 2011). Within the FA molecule, aromatic structures bearing numerous oxygen-containing functional groups, including carboxylic and phenolic groups that ionize to release H^+, are known to strongly associate with metal ions (Ca^{2+}, Mg^{2+}, Cu^{2+}, Fe^{3+}, Cd^{2+}, Zn^{2+}, V^{2+}, and Ni^{2+}) (Saar & Weber, 1982). Therefore, the aromatic content of DOM is an important indicator of DOM reactivity related to metal-complexation (Baken, Degryse, Verheyen, Merckx, & Smolders, 2011). The aromatic property of organic molecules is related to the cyclic, planar structures with pi bonds in resonance, which can be very stable and allow for compounds to be highly reactive with other substances such that DOM is able to form a ligand (E. Thurman, 1985). Trace metal ions are known to form strong complexes with FA ligands and, as a result, alter the mobility and reactivity of metal ions (Saar & Weber, 1982). One important result of metals complexing with FA is a reduction in aquatic toxicity that is strongly correlated to the aromatic carbon content of DOM (Al-Reasi, Smith, & Wood, 2012).

Characterization of aquatic DOM composition is crucial to several fields, including climate change, ecology, and toxicology (Minor, Swenson, Mattson, & Oyler, 2014). Because of its

inherent heterogeneity and structural irregularity, DOM characterization at the individual molecular level is generally difficult or unattainable (Al-Reasi et al., 2012), therefore, most of the widely used techniques measure the overall molecular pool of DOM. The use of optical spectroscopic methods to molecularly characterize DOM has been used successfully in many studies (Al-Reasi et al., 2013; Dee, 2016; Inamdar et al., 2012; McKnight et al., 2001). For example, Dee (2016) focused on the variability in several spectroscopic indices of FA as a result of watershed source and season, revealing that FA from non-AMD streams shift from characteristics of being aromatic and allochthonous in the spring/summer to less aromatic and autochthonous in the fall/winter.

1.2 Groundwater DOM

The molecular properties and geochemical characteristics of surface water DOM is generally well known (Baken et al., 2011; Butler et al., 2008); however, groundwater DOM composition and role in surface waters is relatively unknown. Groundwater DOM has variable concentrations and composition that is controlled by recharge type and season, changes in flow rate and microbial activity (Longnecker & Kujawinski, 2011), as well as depth and geologic material. Groundwater DOM poses challenges related to compositional characterization related to surface water DOM because of the relatively low concentrations in groundwater (Inamdar et al., 2012; Shen, Chapelle, Strom, & Benner, 2015). Groundwater is generally the primary source of water for perennial streams during low flow periods (Carroll et al., 2018), and therefore it is expected that groundwater DOM likely contributes to the stream DOM pool during hydrologic baseflow periods. Hydrologic baseflow is defined as the time of year when streamflow is primarily sustained by groundwater and streams are low due to no liquid precipitation contribution. A study completed in the Rocky Mountains of Colorado (Boyer, Hornberger, Bencala, & McKnight, 1995)

measured DOC concentrations in the vadose zone, the saturated zone, and in streams, finding that concentrations of DOC in groundwater wells during baseflow were very similar to the nearby creek, suggesting that groundwater is the source of in-stream DOC during baseflow conditions. Previous studies examined the interaction between surface water and shallow groundwater (hyporheic zone and soil water) (Dwivedi et al., 2018; R. Smith, Moore, Weiler, & Jost, 2014) but have not considered deep groundwater. A study completed in a snow-dominated basin applied a multivariate statistical approach of end-member mixing analysis using a suite of daily chemical and isotopic observations (Carroll et al., 2018) found that there are substantial seasonal contributions of groundwater to streams with upwards of 50% groundwater contribution to streams during baseflow. Although the study considered deep groundwater as an endmember, it did not factor in the contribution of groundwater DOM to streams during baseflow.

The molecular composition of groundwater DOM is more similar to autochthonous DOM that is attributed to the microbial decomposition of allochthonous DOM. Early studies suggest that groundwater DOM originates as surface plant litter and soil NOM (Baker, Valett, & Dahm, 2000). However, recent studies have applied optical spectroscopy to show that the aromatic content in groundwater DOM were substantially less than surface water DOM, indicating removal of the plant-derived DOM during water percolation through the soil (Shen et al., 2015). As a result of DOM loss through infiltration, groundwater DOM contains lower proportions of humic and fulvic acids, and the bacterial community has a greater impact on the composition of DOM through microbial interactions (degradation and mineralization) and sorption in the unsaturated zone, resulting in molecular properties similar to autochthonous DOM (Inamdar et al., 2012; Longnecker & Kujawinski, 2011).

Groundwater DOM operates as a source of carbon and energy for heterotrophic metabolism (Baker et al., 2000) and can be important for redox reactions that control metal mobility in groundwater. Studies by Yang et al. (2020) and Jiang et al. (2014) found that DOM in groundwater systems is an important factor in the biogeochemistry of arsenic and chromium, playing a role in the mobility and speciation of trace metals, primarily as a transport mechanism for electrons and source of energy for microbes. Certain types of DOM play an important role in encouraging a reducing environment, such that it results in the mobilization of certain metals like As, Se, Sb, and Mo (Bauer & Blodau, 2006). Although groundwater DOM can be critical for the biogeochemistry of trace metals in aquifers, the role of groundwater DOM discharged into streams is not clearly understood (Bernal, Lupon, Catalán, Castelar, & Martí, 2018; Tiwari, Laudon, Beven, & Ågren, 2014; Yang et al., 2020). Specifically, the presence of groundwater DOM in streams during baseflow may be important in numerous biogeochemical processes, including metal transport and fate.

1.3 Spectroscopic Characterization of DOM

Characterization of DOM often focuses on molecular weight, elemental composition, and analysis of functional groups that comprise the molecular structure of DOM. Common techniques used to characterize isolated DOM include nuclear magnetic resonance mass spectrometry (NMR), Fourier transforms infrared spectroscopy (FTIR), mass spectrometry (MS), and optical spectroscopy such as ultraviolet-visible (UV-vis) light absorption and fluorescence. These laboratory approaches include measuring the intrinsic absorbance and fluorescence properties of DOM by optical spectroscopy, which is widely used to account for DOM source and likely aromatic content and reactivity (McKnight et al., 1992; Minor et al., 2014). Optical spectroscopic measurements only provide information on the DOM pool rather than detailed

structural information, therefore, isolation of certain primary DOM components (i.e., fulvic acids) are often needed to characterize specific components of the DOM pool (Minor et al., 2014).

The absorbance and fluorescence properties of DOM provide insight into the general molecular properties of DOM, including aromatic content, degree of decomposition, and likely source (Hansen et al., 2018). Results of UV absorbance coupled to fluorescence are applied to calculate a variety of spectral indices used to discern the general molecular properties of DOM. Specific UV-absorbance at the 254 nm wavelength ($SUVA_{254}$) is known to strongly correlate with DOM percent aromaticity as verified by ^{13}C-NMR (Fig. 3) and molecular weight (Chowdhury, 2013; Weishaar et al., 2003), for which increasing $SUVA_{254}$ values are associated with greater aromatic content and greater molecular weight (Hansen et al., 2016) and vice versa. The fluorescence index (FI) of DOM is commonly used to delineate likely DOM source and is easily calculated (Table 2) from excitation-emission matrices (EEMs) (Minor et al., 2014). The correlation between aromaticity and FI of isolated FA samples was used by McKnight et al. (2001) to distinguish between allochthonous and autochthonous DOM. Spectral slopes, such as $S_{275\text{-}295}$ and $S_{350\text{-}400}$, serve as a proxy for molecular weight and specific absorbance coefficient (SAC_{340}) as an aromaticity index (Al-Reasi et al., 2012). $S_{275\text{-}295}$ and $S_{350\text{-}400}$ values are also used as a general indicator of DOM source where $S_{275\text{-}295} > S_{350\text{-}400}$ is considered autochthonous and $S_{275\text{-}295} < S_{350\text{-}400}$ are allochthonous (Helms et al., 2008). Inamdar et al. (2012) used a suite of spectroscopic indices ($SUVA_{254}$, a_{254}, S_R, HIX, FI, % C3, % C5, % protein-like fluorescence, and tryptophan:tyrosine) to show that surficial watershed sources had high DOM concentrations with more humic-like DOM and high molecular weight, while deep groundwater sources were rich in protein-like fluorescence.

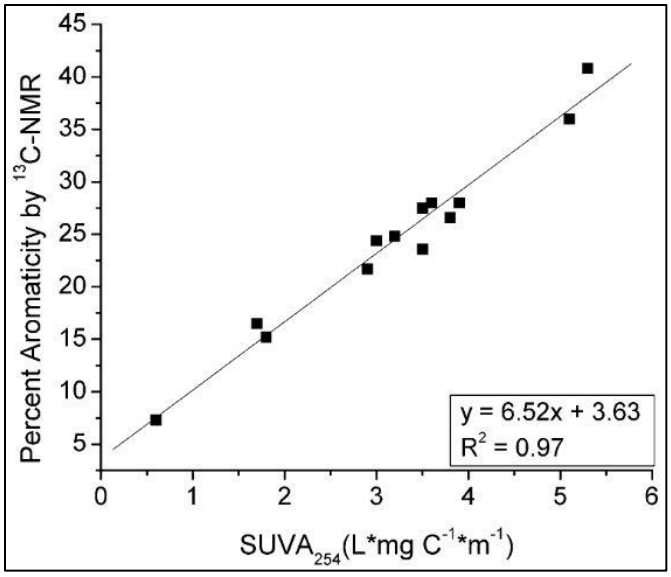

Figure 3. Correlation between $SUVA_{254}$ and percent aromaticity determined by ^{13}C NMR (Figure 1 from Weishaar et al. (2003)).

Other fluorescence measurements include the biological index (BIX), which is an indicator of autotrophic productivity where BIX values >1 correspond to microbial-derived, autochthonous DOM (Hansen et al., 2018) and humification index (HIX) as an indicator of the degree of humification where increasing values are proportional to higher degrees of humification (Hansen et al., 2018; Ohno, 2002). Bernal et al. (2018) used FI, BIX, and HIX to demonstrate that a riparian groundwater system displayed no change in the molecular composition throughout the year. However, during the leaf litter fall period (October-November/baseflow), FI was higher in streams than in groundwater, while HIX and BIX were generally greater in groundwater than in surface water but variable throughout the year. Multiple spectral indices are often paired to provide insight into changes in molecular composition as related to seasonality and source. For example, a study completed by Dee (2016) focused on examining changes in FA binding affinity and found that the variability in several spectroscopic indices was a result of watershed source and season, revealing FA from non-AMD streams shift

from being aromatic and allochthonous in the spring/summer to less aromatic and autochthonous in the fall/winter.

1.4 DOM variability in Mountainous watersheds

Seasonal variability of DOM in mountainous watersheds is generally related to transient snowpack and drought conditions (Singh, Inamdar, Mitchell, & McHale, 2014). Mountainous watersheds receive most of their annual water storage from seasonal snowpack, and as a result, water chemistry varies throughout the year (Boyer et al., 1995; McKnight & Bencala, 1990; Winnick et al., 2017). Several studies have linked DOM concentration in streams and groundwater to stream hydrology within alpine watersheds (Hornberger, Bencala, & McKnight, 1994; Pellerin et al., 2012). In spring, snowmelt transports detrital and enriched organic matter along the soil surface in surface runoff (the rising limb of hydrograph) and the stream channel is at or near flood stages (Boyer, Hornberger, Bencala, & McKnight, 1996; Butler et al., 2008; Longnecker & Kujawinski, 2011). DOM concentrations are greatest during spring snowmelt, generally followed by a decrease in concentration as the snowmelt influenced stream flow transitions to baseflow (Boyer et al., 1995). During baseflow, the general lack of liquid precipitation results in less terrestrial derived DOM in steams; therefore, the majority of DOM is most likely sourced from groundwater and hyporheic zones surrounding streams (Carroll et al., 2018; Dwivedi et al., 2018; Flerchinger, Cooley, & Ralston, 1992).

1.5 DOM-Metal binding

The concentrations and speciation of trace metals in natural waters are controlled by several geochemical processes, including complexation reactions with NOM. It is well known that NOM is a relatively strong ligand for trace metals, and the binding properties of NOM with metals is known to be influenced by NOM source and composition (Baken et al., 2011). Certain DOM

functional groups have a high affinity to bind with trace metals that may result in a decrease of free metal ion concentrations in aqueous solutions. Low metal affinity sites are commonly associated with carboxylic groups and low aromaticity, while high metal affinity sites are associated with phenolic groups and high aromaticity (Baken et al., 2011). DOM with a high molecular weight was found to be associated with strong binding affinities, while DOM with low molecular weight had weakened binding affinities (Chen, Smith, & Guéguen, 2013). Dee (2016) found that DOM's binding affinity can be related to spectroscopic indices, including $SUVA_{254,}$ where low values of $SUVA_{254}$ are related to greater free copper ions (as $\{Cu^{2+}\}$) whereas higher $SUVA_{254}$ resulted in less $\{Cu^{2+}\}$.

The presence of other ions in solutions influences the ability of DOM to complex with metals. Chemical factors include several impacts on metal bioavailability and competition, such as the ionic composition, pH, and redox reactions in the aquatic system. The effect of pH on complexation is attributed to the competition between H^+ and metal ions for anionic binding sites on DOM and the competition between OH^- and DOM for the cationic metal ion (Tchounwou, Yedjou, Patlolla, & Sutton, 2012) and can be affected if pH increases such that metal complexation with DOM results in decreased metal ion concentrations in solution (Saar & Weber, 1982). Metal-binding is also influenced by physical factors such as temperature, phase association, adsorption, and sequestration (Lu & Allen, 2002; Tchounwou et al., 2012). Specifically, Warren and Zimmerman (1994) observed through a series of multiple linear regressions for total and specific distribution coefficient estimates that temperature is one of the key environmental variables influencing trace metal partitioning such that a decrease in water temperature caused decreases in the accumulation of Cd, Cu, and Zn in the particulate pool, suggesting that during winter months, a higher proportion of these metals remain in the dissolved phase and are more bioavailable.

Trace metals enter aqueous systems through surface water runoff from soils, groundwater inflow, metal-enriched sediments, and leaching from agriculture, mine tailings, and industrial effluents (Thorslund et al., 2017). Certain trace metals are essential nutrients; however, at elevated concentrations, they can become toxic to aquatic organisms (Roline, 1988). Copper is an essential nutrient to most organisms, but at elevated levels, it can be highly toxic to aquatic organisms for which the ionic species $\{Cu^{2+}\}$ has the greatest bioavailability (Tchounwou et al., 2012). Cu is acutely toxic to freshwater fish at concentrations as low as 10-20 µg/L (Woody & O'Neal, 2012), with most U.S. aquifers having concentrations less than 10 µg/L (Lee & Helsel, 2005) and streams with average concentrations of 10 µg/L (Dorsey & Ingerman, 2004). Seasonality plays an important role on the copper concentrations in streams, as noted by Butler et al. (2008), where they observed a general trend of increased Cu concentration over baseflow months and dilution during higher flows during spring snowmelt. DOM plays an important role in the speciation of copper, however, there is still some uncertainty as to what controls the relationship of copper-DOM complexes (Craven, Aiken, & Ryan, 2012). Ca/Mg-Cu exchange experiments by Lu and Allen (2002) suggested that Ca and Mg are preferably bound by carboxyl sites over Cu, while Cu-DOM complexation is generally through the replacement of H^+ by Cu^{2+} at phenolic binding sites. At low pH, binding between Cu-FA is primarily affected by zero- (constant proportions) and first-order (concentration-dependent) components, and at high pH, it is primarily affected first- and second-order (concentration-dependent) (Cabaniss & Shuman, 1988). Because copper binding with NOM is well known, Cu is often used as a proxy for experiments that focus on the importance of DOM molecular variability as related to properties of DOM-metal binding.

1.6 Research Hypothesis and Objectives

Mountainous watersheds, such as the Headwaters of the Upper Arkansas River Watershed, are highly transient hydrologic systems signified by seasonal snowmelt-driven hydrology that results in variability in inorganic and organic solute composition, concentrations, distribution, and speciation. One important yet unexplored aspect of variable DOM composition is how it influences DOM-metal binding as an important control on trace metal bioavailability, mobility, and distribution in aqueous systems. Therefore, it is important to understand how seasonal hydrology influences DOM molecular properties and concentration, particularly during baseflow periods where groundwater DOM is likely present in streams. The importance of groundwater DOM in streams is rather unclear; however, understanding the role of baseflow in mountainous watersheds warrants further research. This study aims to investigate the role of seasonal effects of stream and groundwater DOM on trace metal binding. Therefore, we hypothesize that:

1. Dissolved organic matter concentrations and molecular properties are influenced by seasonal variability in streams, which results in groundwater-sourced DOM being present in streams during baseflow conditions.
2. The molecular composition and geochemical properties of DOM in streams are more representative of groundwater DOM than terrestrial sources during baseflow periods.
3. The geochemical properties of DOM in streams vary significantly due to seasonal influences, such that DOM during baseflow has diminished metal-binding affinity relative to snowmelt periods.

The objectives of this study include collecting groundwater and surface water samples from a mountainous watershed during the spring snowmelt and fall baseflow periods; to characterize bulk DOM and isolated FA composition and quality; and lastly, conduct a series of metal-DOM binding

experiments. This project provides information on the molecular level composition of DOM in groundwater and surface water as influenced by seasonality. A sampling event of groundwater and surface water occurred during the hydrologic baseflow, spring snowmelt, and summer recession periods in order to include seasonal effects on surface water DOM-metal binding properties, more specifically, the role of groundwater sourced DOM during baseflow. The seasonally collected samples were then isolated to capture the FA portion of DOM and characterized using a suite of optical indices, including UV-visible absorbance and fluorescence measurements. The measurements can be correlated to the DOM-metal binding experiments completed in the lab in order to examine the binding affinity of Cu with isolated FA and study the role of seasonal variability between groundwater DOM and surface water during baseflow.

2 GEOLOGIC AND HYDROLOGIC SETTING

2.1 Geology

The Headwaters of the Upper Arkansas River Watershed (HUARW) is located within Lake County, Colorado (Fig. 4). The Arkansas Valley graben is bound by two mountain ranges: the Sawatch and Collegiate Range in the west and the Mosquito and Ten Mile Range in the east. The valley floor primarily consists of quaternary alluvium and glacial deposits that reach depths down to approximately 1000 ft. Bedrock geology in the area consists of tertiary volcanic, Paleozoic sedimentary, and Precambrian metamorphic and igneous rocks (Fig. 5). The Paleozoic sedimentary units include approximately 2,500 ft of Cambrian through Mississippian quartzites and dolomites as well as Pennsylvanian black shale, quartzite, and arkose sandstone (Cappa & Bartos, 2007). The stratigraphic section is highly intruded by a series of Late-Cretaceous to early-Tertiary volcanic dikes, sills and plugs adding to the complex structure of Lake County. Several

main ore bodies formed from multiple intrusions. Six intrusive igneous rocks ranging in age from Late Cretaceous to early Tertiary, excluding Proterozoic granite basement, crop out in the Leadville Mining District (Cappa & Bartos, 2007). North-trending regional and local faults are present in the area and are widespread (Fig. 5). The faults play a role in both the distribution of ore bodies and act as conduits for groundwater (Cappa & Bartos, 2007; Geldon, 1989).

The Colorado Mineral Belt is a north/northeast-trending string of Tertiary intrusive rocks that are well-known sources of significant sulfide mineral ore and carbonate replacement deposits (Cappa & Bartos, 2007) that are approximately 39 million years in age. Common sulfide minerals associated with the deposits include galena (PbS), pyrite (FeS), chalcopyrite ($FeCuS_2$), sphalerite (ZnS), arsenopyrite (FeAsS), argentite (Ag_2S), and pyrrhotite ($Fe_{1-x}S$). The Leadville mining district contained one of the largest zinc-silver deposits globally, which produced more than $5 billion worth of metals (Wallace, 1993) over a span of 100 years. In addition to sulfide deposits, gold was also mined first as placer deposits and later as subsurface ore (Wallace, 1993).

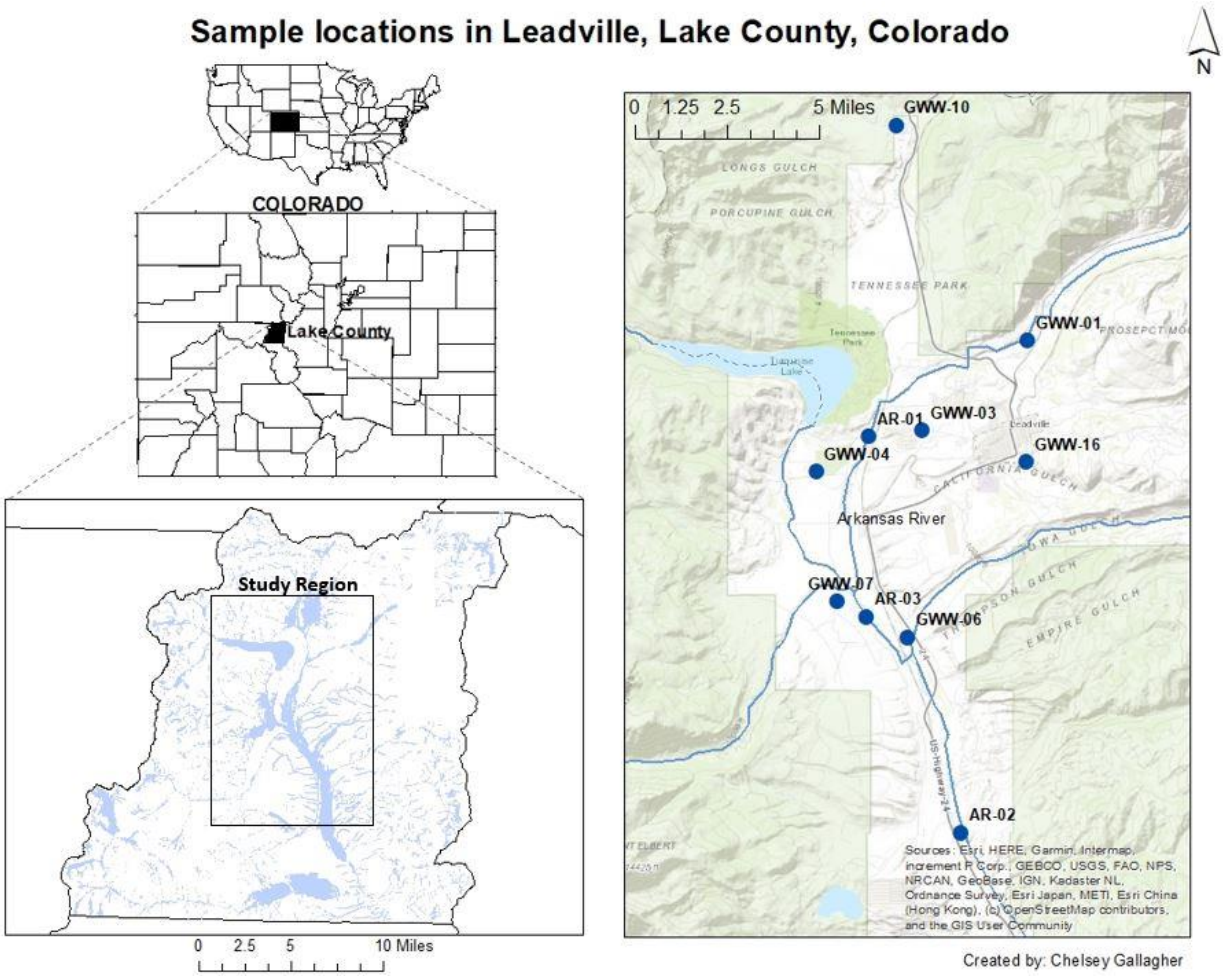

Figure 4. Map showing the location of the study area and sampling sites in Lake County, Colorado.

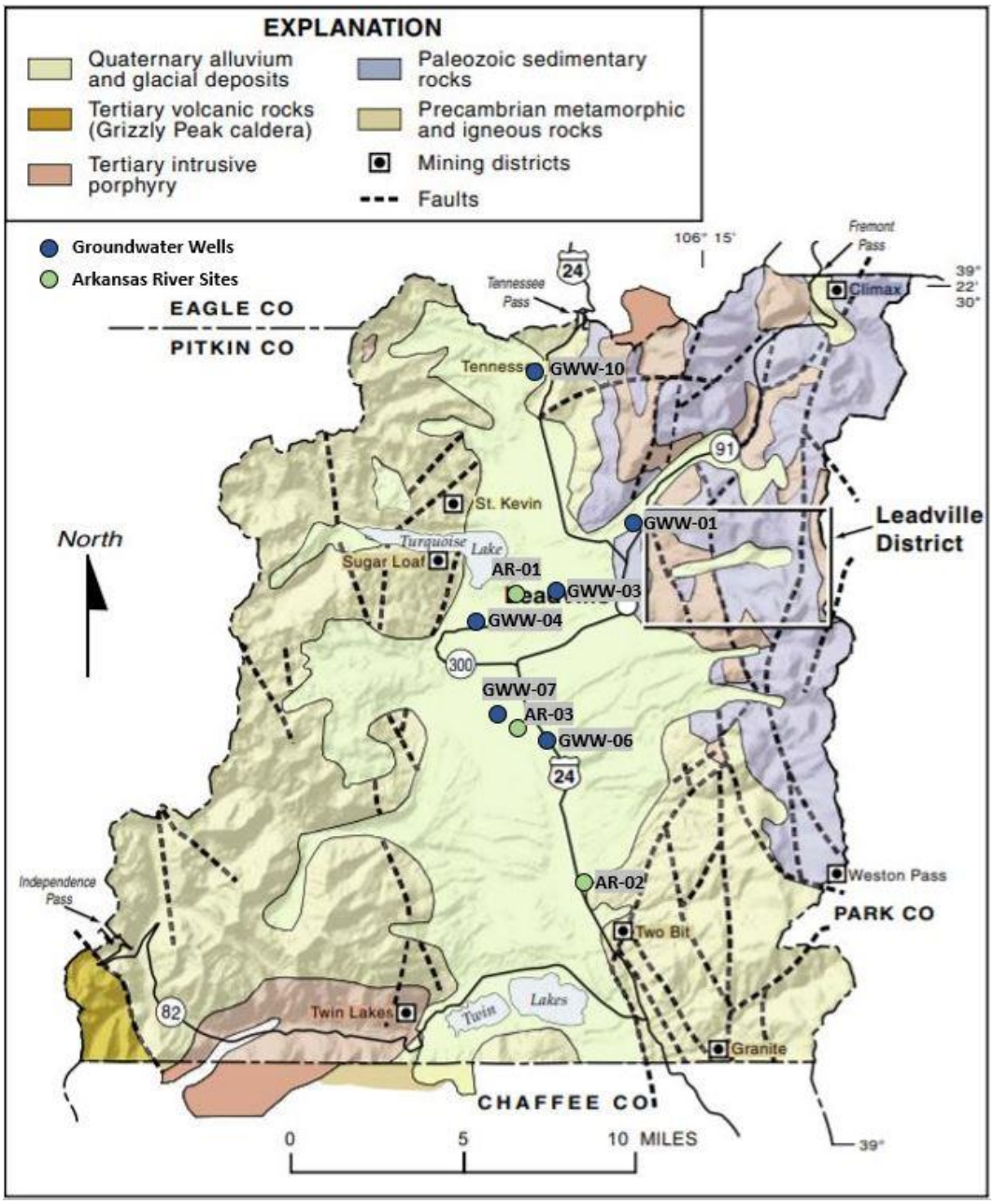

Figure 5. Geologic Map of Lake County, Colorado modified from Cappa and Bartos (2007). Sample sites are shown to include associated geology.

2.2 Hydrology

2.2.1 Climate

The climate in Lake County is classified as alpine to sub-alpine with characteristics of long-cold winters and mild summers. Average temperatures in Lake County range from 3°F to 31°F in

January and 38°F to 71°F in July (U.S. Climate Data, 2021). The average annual liquid water equivalence precipitation is 12 inches, with an average annual snowfall of 117 inches near Leadville (Western Regional Climate Center, 2021) which likely exceeds 400-inches near the Continental Divide. Most of the precipitation in this region falls as snow during the winter, with a smaller portion of sporadic liquid precipitation during the monsoon season in the summer. The snow generally incorporates atmospheric impurities, causing the snow's composition to reflect a similar composition to the atmosphere (aerosol particles, adsorbed and dissolved gases). The year 2020 is classified as having extreme drought conditions in the region (Fig. 7), where this region received little to no precipitation during the summer (Fig. 9), and snowpack (as snow water equivalence) conditions are around the 50th percentile compared to an average year (Fig. 6).

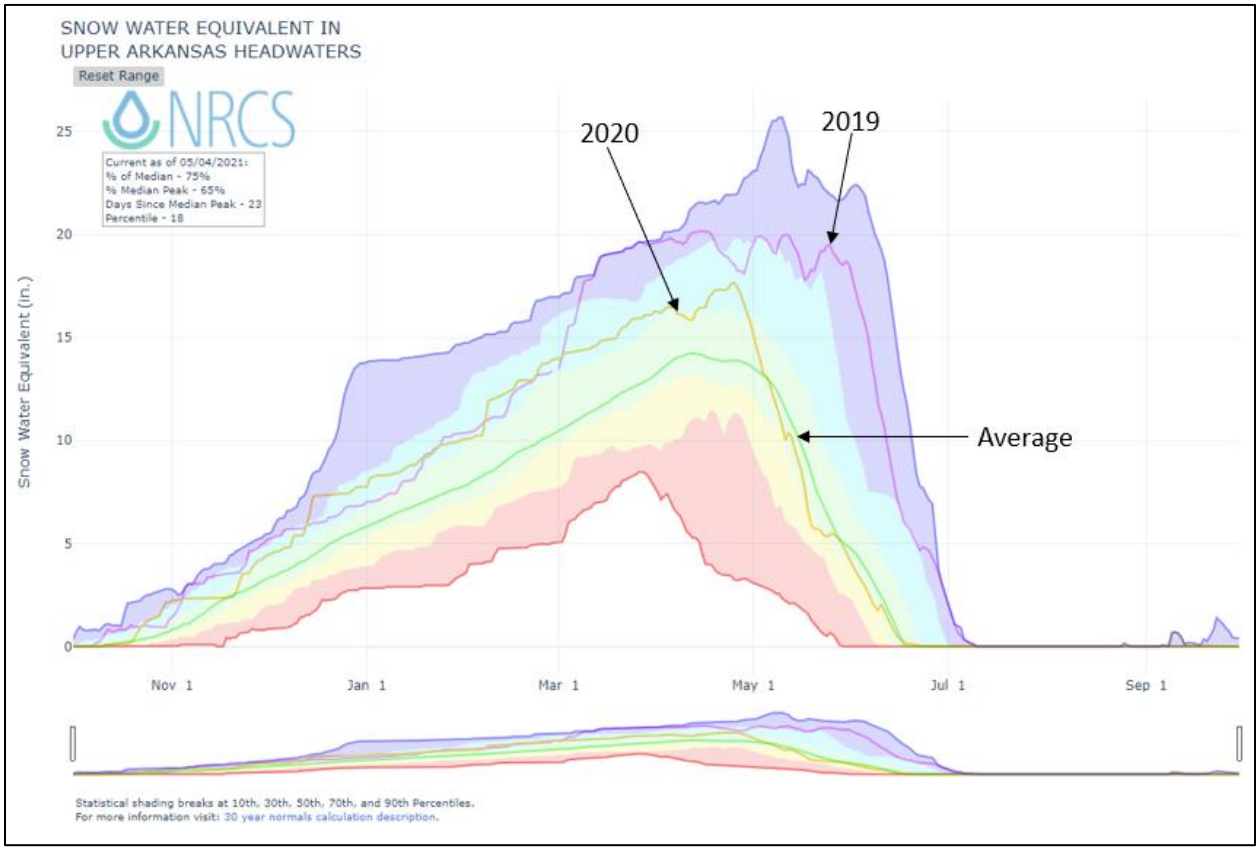

Figure 6. Snow water equivalent in the Upper Arkansas River Headwaters in 2019 and 2020 compared to median, minimum, and maximum years (United States Department of Agriculture, 2021).

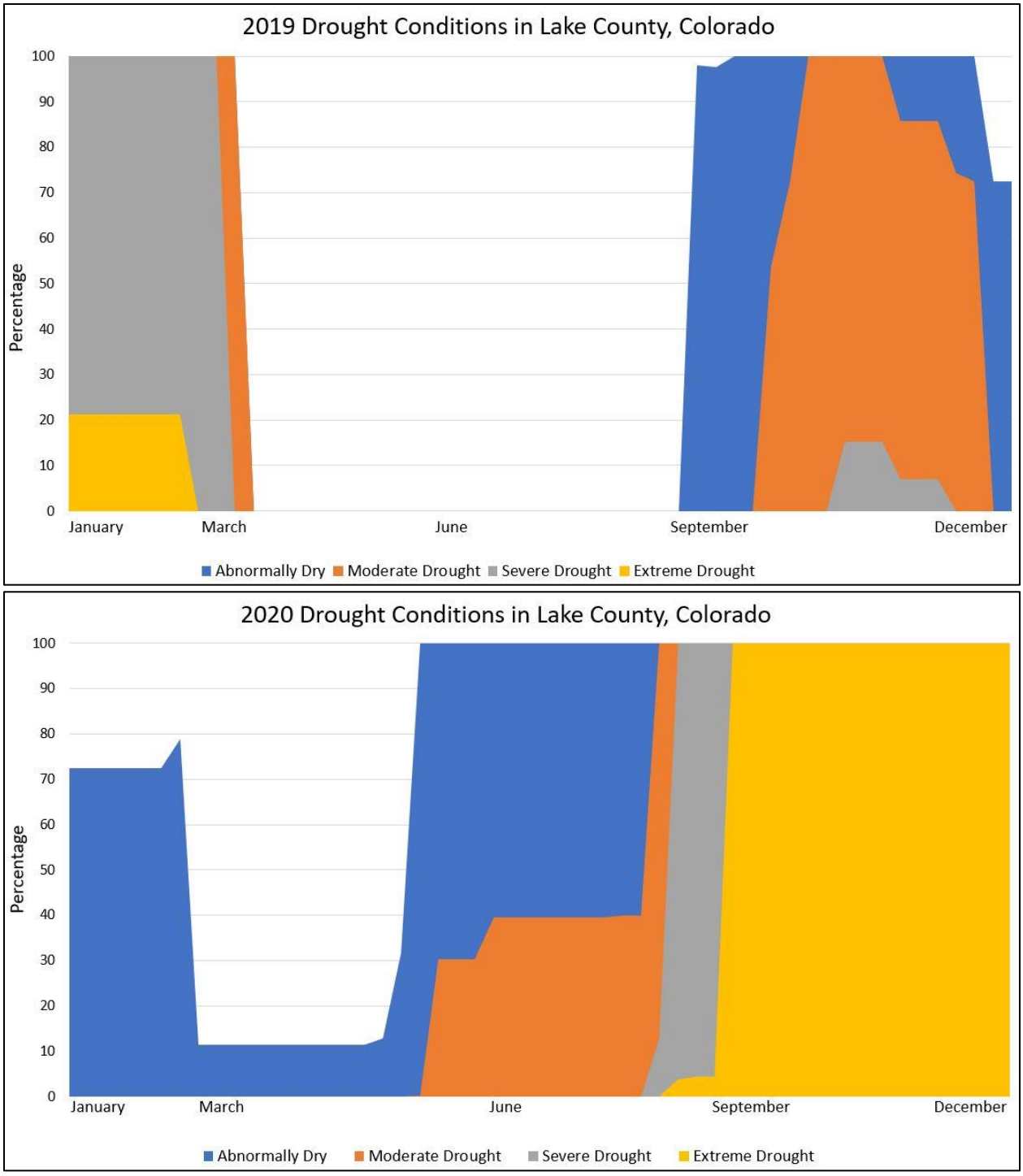

Figure 7. Graphs showing periods of extreme drought in Lake County, Colorado, from 2019 and 2020 (National Integrated Drought Information System, 2021).

2.2.2 Surface Hydrology

Hydrology of the Arkansas River is typical of streams located in mountainous watersheds, being defined by a deep, seasonally persistent snowpack that begins to melt in the spring resulting in a pronounced rise in stream discharge that reaches a maximum in late spring followed by a gradual decrease (summer recession) to baseflow in the late-summer to early-fall (Fig. 8). Hydrographs for USGS station #07081200, located in the Arkansas River near Leadville, are shown in Figure 9, showing that snowmelt run-off typically begins in late April and reaches peak discharge in late June. Climate variations related to drought (2020) and above-average snowpack (2019) result in a decrease in peak and summer recession discharge (Fig. 9). Estimated baseflow during the drought year shows that baseflow lasted until April and started again in August at the baseflow inflection (9 months) in 2020. However, during a wet year (2019), baseflow lasted until March and started again in September (7 months) (Fig. 9).

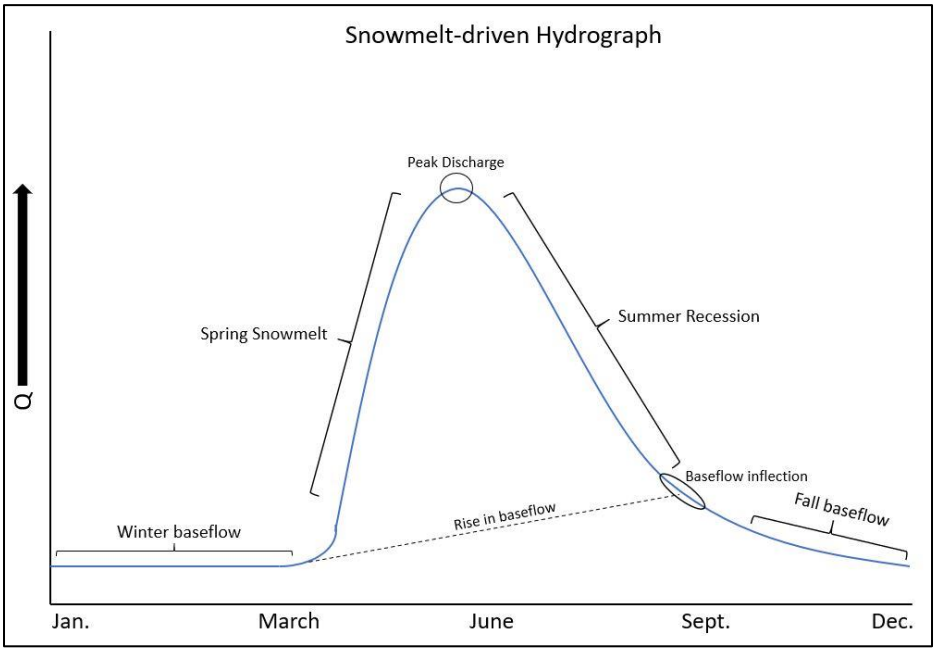

Figure 8. Generalized hydrograph depicting periods of snowmelt and baseflow.

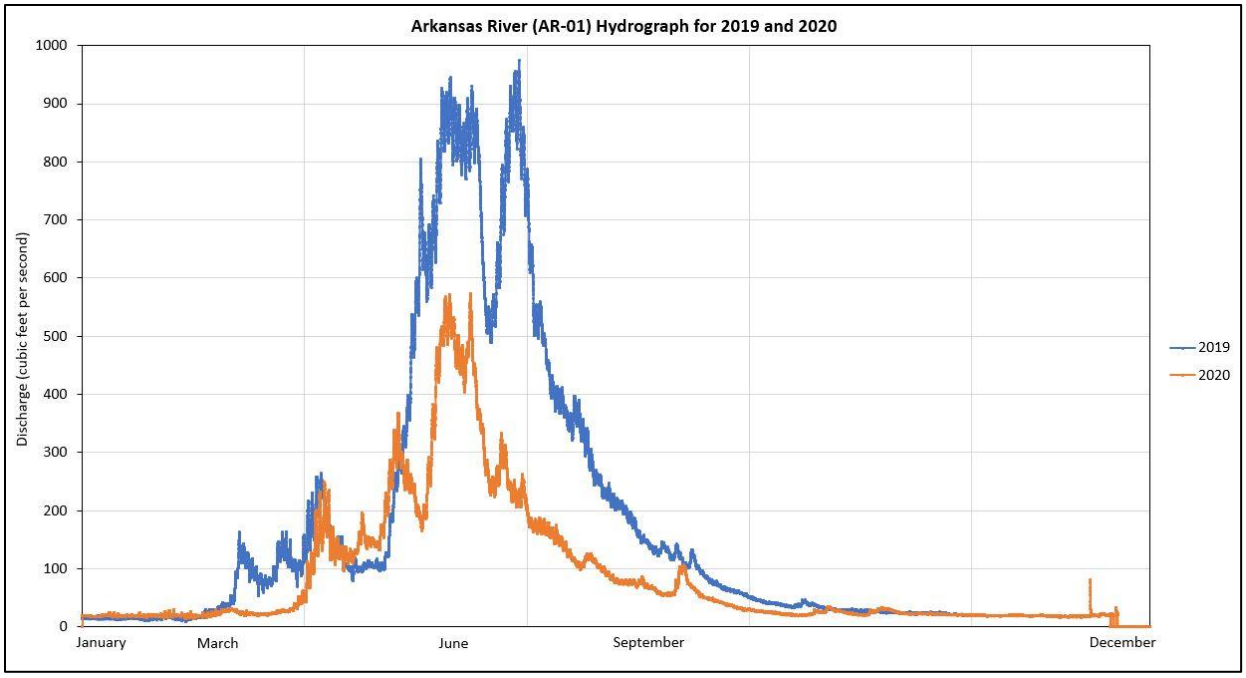

Figure 9. Hydrograph of data from the Upper Arkansas River USGS gaging station in 2019 and 2020 (United States Geological Survey, 2021).

2.2.3 Groundwater Hydrology

Groundwater occurrence and flow in the HUARW is controlled by topography, geology, mining features, streams, and quantity of recharge associated with each location (Wellman, Paschke, Minsley, & Dupree, 2011). There are two types of groundwater in the mountainous region: shallow, active groundwater flow supported by seasonal snowmelt and short residence times; and a deeper, inactive groundwater flow that can be recharged by snowmelt but has longer residence times (Walton-Day & Poeter, 2009). The valley-fill deposits in the HUARW form an unconfined shallow quaternary alluvium aquifer primarily comprised of unconsolidated sand and gravel with clay lenses reaching a depth as great as 260 feet in some areas (Wellman et al., 2011). Recharge to the Arkansas River alluvial aquifer is primarily through infiltration of snowmelt through the subsurface, areal recharge through faults, and deep recharge through fractured rock in the surrounding mountains (Barkmann et al., 2020; Walton-Day & Poeter, 2009; Wellman et al., 2011). The average annual groundwater recharge is assumed to be 30% of the average annual

precipitation (Wellman et al., 2011). A combination of stratigraphy, geologic structures such as fractures and fault networks, mine workings, and tunnels affect the groundwater table and flow direction in this region (Wellman et al., 2011). Depth to the water table ranges from about 5 to 30 feet below ground surface, dependent on the season and topography, with the highest water levels corresponding to spring snowmelt (Barkmann et al., 2020). Individual household, domestic, and public supply are the primary uses of groundwater (Barkmann et al., 2020; Wellman et al., 2011).

3 METHODS

3.1 Description of Study Sites and Sampling Approach

Sample sites consisted of six groundwater wells and three surface water sites in the Upper Arkansas River watershed in Central Colorado (Fig. 4). The sampling sites were chosen based on previous studies, stream and aquifer type, and ease of access. The Upper Arkansas River is a 1st-order perennial stream that begins near Fremont Pass located along the Continental Divide. The three surface water sites (AR-01, AR-02, and AR-03) are located within a 10-mile reach of each other in the headwaters of the Arkansas River, all located within Lake County, Colorado. With the exception of GWW-01, all remaining wells are screened in glacial till deposits and are located throughout Lake County within ~1.2 miles of the Arkansas River. GWW-01 is screened in fluvial and glacial deposits located in the Arkansas River floodplain northeast of Leadville. All sites are accessible by road or trail throughout the year, allowing ease of access.

Table 1 shows all sampling sites, their location, sampling date and description of the site. The groundwater sites represent a combination of private, domestic wells and one used by the Parkville Water District, all used for drinking water. Although the wells are not directly adjacent to the Arkansas River, they were chosen to represent groundwater DOM from the valley floor

glacial till that the Arkansas River flows through. All wells are in constant use, thereby negating any likely stagnant water from forming around the well screen resulting in relatively fast equilibrium conditions when sampled (verified by in-situ measurements). Untreated groundwater from the domestic wells were collected from outlets located before any in-line filtration or other sources of water treatment. Prior to collecting a groundwater sample, we allowed water to run from the sampling port until select water chemistry parameters (pH, temperature, conductivity) stabilized. Streams samples consisted of grab samples collected as far away from the stream bank as possible.

Table 1. Description of sampling sites located in Lake County, Colorado.

Sample Identifier	Latitude	Longitude	Elevation	Sample Date - Time	Description of Sample Site
AR-01	39.249026°	-106.348007°	9,694 ft	10/23/2019- 17:00 06/03/2020- 11:00 08/19/2020- 11:56 10/04/2020- 16:56	USGS gaging station (#07081200) present. Located to the west of County Rd 9D and County Rd 4 intersection in Lake County, Colorado.
AR-02	39.128647°	-106.311831°	9,197 ft	10/21/2019- 12:00 06/02/2020- 12:00 08/18/2020- 17:22 10/04/2020- 14:23	About 10 miles downstream of AR-01. Located to the east of Highway 24 and CO Rd 55 intersection in Lake County, CO.
AR-03	39.194239°	-106.348964°	9,421 ft	06/01/2020- 14:40 08/18/2020- 16:00 10/04/2020- 15:53	The site lies between AR-01 and AR-02. Located on the Smith Ranch in Lake County, CO.
GWW-01	39.278034°	-106.285661°	9,981 ft	05/30/2019- 11:20 10/21/2019- 12:00 06/03/2020- 14:00 10/06/2020- 09:00	The well depth is 140 ft; screened in fluvial and glacial deposits; Owned by Parkville Water District. Lies in the floodplains of the Arkansas River.
GWW-03	39.250335°	-106.327062°	9,866 ft	05/29/2019- 16:30 10/22/2019- 14:30 06/04/2020- 15:30 10/06/2020- 10:00	The well depth is 90 ft screened in glacial till; Personal well. Installed ~1.11 miles east of the Arkansas River.
GWW-04	39.238351°	-106.368735°	9,623 ft	05/29/2019- 09:00 10/23/2019- 11:00 06/05/2020- 08:30	The well depth is 40 ft; screened in glacial till; Personal well. Installed ~0.76 miles west of the Arkansas River.
GWW-06	39.187942°	-106.332934°	9,422 ft	05/30/2019- 15:30 10/20/2019- 10:30 06/01/2020- 15:30 10/06/2020- 12:00	The well depth is 55 ft; screened in glacial till; Personal well. Lies in the floodplains of the Arkansas River.
GWW-07	39.198788°	-106.360268°	9,513 ft	05/28/2019- 18:00 10/20/2019- 13:00 06/02/2020- 17:00 10/06/2020- 13:00	The well depth is 55 ft screened in glacial till; Personal well. ~0.35 miles west of the Arkansas River.
GWW-10	39.343301°	-106.337414°	10,308 ft	05/28/2019- 17:00 10/20/2019- 16:00 06/04/2020- 16:30 10/06/2020- 14:00	The well depth is 110 ft; screened in glacial till; Personal well. Installed ~0.54 miles west of a tributary to the Arkansas River, Tennessee Creek.

Snowmelt-driven hydrographs (Fig. 8) were used to determine when the snowmelt, summer recession, and baseflow periods generally occur within mountainous watersheds and then sampled during all three periods to include seasonal effects. Furthermore, the sample dates (Table 1) were also based off of previous sampling activity. Sampling included surface water and groundwater as part of the spring and fall events; however, we did not sample groundwater as part of the Summer 2020 event since this study focused on the spring snowmelt and fall baseflow periods. The chemistry of deep groundwater generally does not vary much throughout the year (Dhar et al., 2008), and the depths and locations of the wells in this study likely did not change from the spring sampling event to summer and fall. We included results collected in Spring 2019 from the same groundwater wells sampled in this study to see any differences in groundwater chemistry between a drought (2020) versus an above-average snowpack year (2019).

3.2 Water Chemistry

3.2.1 In-Situ Water Analysis

In-situ water chemistry measurements were used as part of general water chemistry and to aid in determining when equilibrium conditions have been met when sampling groundwater. Measured parameters include pH, Temperature (°C), Specific Conductivity (SC, µS/cm), Dissolved Oxygen (DO, mg/L), Oxidation Reduction Potential (ORP, mV), and Total Dissolved Solids (TDS, mg/L). A calibrated HANNA™ HI 9829 multiparameter meter was used for all in-situ stream and groundwater measurements. Instrument calibration consisted of using Orion Application Solutions (pH standards) with a pH of 7.00 (Orion 910107), 4.01 (Orion 910104), and 10.01 buffers (Orion 910110) along with conductivity/TDS standard solution (Orion 011007). In-situ measurements are the most accurate way to collect general water chemistry as they include how temperature affects pH, conductivity, D.O., and other parameters. Due to the

high rate of groundwater from the wells, a 5-gallon plastic bucket was utilized as a flow-through cell for the in-situ measurements. Care was taken to keep both the multi-parameter probes and hose (attached to the well sampling port) submerged in order to minimalize exposure to the atmosphere. At the stream sites, the multi-parameter probe was placed directly into the stream and recorded the values once it reached equilibrium. Equilibrium conditions were considered to be established when at least three consecutive in-situ measurements are within 10% of each other.

3.2.2 Anions

Samples collected from each site for anions were filtered through a 0.45 µm filter (Geotech™ Polyether sulfone 0.45 µm membrane) into pre-cleaned 60 ml HDPE sample bottles and stored at 4ºC until analysis. Anion analysis was completed by ion chromatography (IC) at the Colorado School of Mines (Golden, CO) AQWTEC laboratory within two weeks after samples were collected. Quality control (QC) included laboratory blanks (deionized, ultrapure water) and calibration check aliquots analyzed at the beginning and end of each analytical run, including after every group of 10 primary samples. Laboratory blanks checks are considered acceptable if results are below the detection limit, whereas calibration check results are also acceptable if the readings are within ±10% of the known concentration. Lastly, samples are diluted and rerun if the initial concentrations exceed the established calibration dynamic range of the IC. Anion analysis included fluoride (F^-), chloride (Cl^-), bromide (Br^-), nitrate (NO_3^-), phosphate (PO_4^{3-}), and sulfate (SO_4^{2-}) ions.

3.2.3 Carbonate Alkalinity

Alkalinity was measured in the field using a Hach™ digital titrator (Hach Method 8203: Phenolphthalein and Total Alkalinity) to avoid any potential temperature effects and

decomposition of bicarbonate/carbonate ions. The published (GmbH, 2014) detection limit is 10 to 4000 mg/L calcium carbonate ($CaCO_3$) equivalence. The bicarbonate (HCO_3^-) and carbonate (CO_3^{2-}) components of alkalinity were later quantified by inputting the field alkalinity results (as mg/L $CaCO_3$) into Visual MINTEQ version 3.1 (https://vminteq.lwr.kth.se/).

3.2.4 Major Cations and Trace Metal Analysis

Metal samples (major cations and trace) included the total recoverable (total) and dissolved (filtered) fractions. Total metals samples are unfiltered and collected in acid-washed 60 ml HDPE sample bottles. Dissolved metals are collected on-site by filtering sample water with a 60 ml syringe through a PVDF 0.1 µm filter (Millex-VV Syringe Filter: SLVVR33RS) directly into a 60 ml HDPE acid-washed sample bottle. Prior to collecting the dissolved metals sample, the filter was first conditioned by filtering and discarding approximately 10 mL of sample water. We used a 0.1 µm filter to remove a majority of colloidal material (i.e., suspended sediment, Fe- and Al-oxyhydroxides) in the sampled water. Samples were preserved with approximately 0.5 ml of 70% trace metal grade nitric acid (HNO_3) and refrigerated at 4ºC until analysis.

Metals samples were submitted to the Colorado School of Mines Atomic Spectroscopy Laboratory (Golden, CO) for metal analysis by Inductively Coupled Plasma Optical Emission Spectroscopy (ICP-OES). Metals measured included Ba, Be, Ca, Cd, Cu, Co, Cr, K, Li, Mg, Mn, Mo, Na, Ni, P, Pb, S, Sb, Se, Si, Sn, Sr, Ti, Tl, V, and Zn. Quality control (QC) consisted of measuring laboratory blanks, continuing calibration verification (CCV), and a NIST standard reference sample (NIST 1643f) throughout the entire run for all samples.

3.3 DOC Analysis and Spectroscopy

3.3.1 Bulk Dissolved Organic Carbon Analysis

Bulk DOC samples (DOC-01) were collected by filtering site water through a 0.45 µm nominal pore size filter (Geotech™ Polyether sulfone 0.45 µm membrane) into pre-combusted (8 hours at 550°C) and pre-cleaned (soaked in 5% HNO_3 followed by rinsing with DI water) 60 ml glass amber sample bottles and stored at 4ºC until DOC analysis in the OU AGL. DOC analysis was completed by high-temperature combustion with NDIR detection (Shimadzu™ TOC-L). DOC analysis in this study used a non-purgeable organic carbon (NPOC) method to negate interferences by inorganic carbon (IC) by acid volatilization of IC followed by a 30-second purge with purified air. The NPOC method has an estimated MDL of 20 to 30 µg C/L, which is sufficient for groundwater DOC concentrations (<1.0 mg C/L). A blank (deionized, ultrapure water) is analyzed at the beginning and end of the analytical run (~20 samples) to ensure the readings are below the detection limit. Various known concentrations of KPH (potassium hydrogen phthalate) are used as the calibration check standards (R^2 ~ 0.9999), and the total calibration and analyzed at the beginning of each group run. The concentrations are acceptable if they fall within ±10% of the known concentration.

3.3.2 Fulvic Acid (FA) Isolation

A widely used isolation procedure first described by E. M. Thurman and Malcolm (1981) was used to isolate the FA component of DOM collected in this study. Sample water for FA isolation was collected by filtering site water with a 0.45 µm high-capacity capsule filter (Geotech™, dispos-a-filter, #73050004) into pre-cleaned (rinsed with DI water) stainless-steel canisters (50L). We collected 50L samples at the AR sites, GWW-01 and GWW-06, based on their location and how close they are to the Arkansas River. However, sites that did not include

50L collection still went through FA isolation on a smaller scale (1L) as these locations were further away from the Arkansas River. The large volume was collected to ensure that the necessary mass of FA is recovered for spectroscopic characterization and lab DOM-metal binding experiments. FA isolation was completed shortly upon collection in the field (within 24 hours) to minimalize any potential DOM decomposition. Filtered water samples were first transferred into pre-cleaned (triple rinsed with distilled water) glass carboys and acidified with concentrated HCl (pH <3.0) in order to protonate the FA prior to beginning FA isolation. Refer to Appendix C for a detailed summary of the FA isolation procedure. The final isolated FA (DOC-03) was refrigerated for subsequent spectroscopic analysis and Cu-DOM binding experimentation.

3.3.3 Spectroscopic analysis

DOM molecular characterization was completed using a Horiba Aqualog™ Spectrofluorometer in the OU Aqueous Geochemistry Laboratory (AGL) to measure the UV-visible absorbance and fluorescence properties of the isolated FA (DOC-03) and Bulk DOC (DOC-01), generally within two weeks of field collection and FA isolation. Prior to spectroscopic analysis, the concentrated FA (DOC-03) obtained from the isolation process was diluted down to a concentration of 3 mg of C/L to minimize interferences, including saturation of the detector and inner-filter effects (IFE) related to high DOC concentrations (Hansen et al., 2018).

Excitation-Emission and absorption data were collected by scans (double-grating monochrometer) covering a range from 240 to 600nm with a 5-nm bandpass and in 2 nm increments. Emission spectra collected (charge-coupled device) ranged from 245 to 830 nm with a 5-nm bandpass at a resolution of 4 pixels. Suwannee River Fulvic Acid (SRFA) (available

through the International Humic Substance Society, IHSS) is well-characterized and therefore is used as a reference material to account for accuracy and stability in measurements. The Raman peak position and intensity were measured using a NIST certified (Starna scientific, type: 3/Q/10/WATER) nano-pure blank. Particles and other inorganic species that absorb light, like iron and nitrate, can interfere with the UV absorbance of DOC (Weishaar et al., 2003), therefore, a few steps are in place to minimize potential interferences. A blank containing DI water in a quartz cuvette (Starna scientific, Spectrosil® Quartz 10mm path length. Catalog #3-Q-10) used for sample analysis was measured for sample blank subtraction and ensuring proper cleaning of the sample cuvette. Between measurements, the sample cuvette was rinsed ten times with DI water.

3.3.4 Spectroscopic Indices

Ultra-violet – Visible (UV-Vis) absorbance and excitation-emission matrices (EEMs) data from the spectroscopic analysis was used to calculate the spectroscopic indices listed in Table 2 for both DOC-03 and DOC-01 samples. UV-Vis and EEM data reduction consisted of a series of steps to reduce the absorbance and fluorescence scans. Absorbance scans are depicted in a two-dimensional array with wavelength (nm) on one axis and amount of light absorbed on the other axis, while fluorescence scans have three axes; excitation wavelength (nm) on first, emission wavelength (nm) on second, and fluorescence intensity on third (Hansen et al., 2018). Further detail of dating reduction can be found in Appendix C. Several spectral indices were calculated as part of this study and are shown in Table 2. Specific absorbance ($SUVA_{254}$) and fluorescence index (FI) measurements were chosen to characterize DOM aromaticity and general source. Several other indices (Table 2) are also used to provide information on the molecular weight, degree of humification, and relative freshness of the DOM.

Table 2. DOM optical indices used in this study.

DOM quality index	Reference	Calculation	Purpose
		UV	
Specific UV absorbance ($SUVA_{254}$) [L mg C^{-1} m^{-1}]	Weishaar et al. (2003), Chowdhury (2013)	(Abs@254nm/DOC concentration) *100	Absorbance per unit of carbon. Generally, a more significant number is associated with greater aromatic content. It can act as a proxy for molecular weight as well.
Absorbance coefficient a_{254} [m^{-1}]	Green and Blough (1994)	(UV absorbance at 254nm) x 2.303 x 100	Measure of aromaticity of DOM
Spectral Slopes ($S_{275-295}$, $S_{290-350}$, $S_{350-400}$) [nm^{-1}]	Helms et al. (2008)	The nonlinear fit of an exponential function to the absorption spectrum/wavelength range.	Higher S values generally indicate low molecular weight material &/or decreasing aromaticity.
Spectral Slope Ratio (S_R)	Helms et al. (2008)	Spectral slope $S_{275-295}$/spectral slope $S_{350-400}$	May be negatively correlated to DOM molecular weight & typically increases through irradiation.
		Fluorescence	
Fluorescence index (FI)	Cory, Miller, McKnight, Guerard, and Miller (2010); McKnight et al. (2001)	EM 470nm:EM 520nm @ EX 370nm	Used to identify the relative contribution of both terrestrial and aquatic sources of DOM.
Humification Index (HIX)	Hansen et al. (2018)	The area under the EM spectra (435-480 nm) divided by the peak area (300-345 nm + 435-480 nm)	Indicator of humic substance content or extent of humification. The higher values indicate increasing humification.
Biological Index (BIX)	Hansen et al. (2018)	The ratio of emission intensity at 380 nm over 430 nm at excitation 310 nm.	Indicator of autotrophic productivity. Values greater than one suggest recently produced DOM of autochthonous origin.
Freshness Index	(Hansen et al., 2018)	The ratio of emission intensity at 380 nm divided by the maximum emission intensity between 420 & 432 nm at excitation 310 nm.	Indicator of recently produced DOM. Greater values equal greater proportion of fresh DOM.

3.4 Cu Binding Experiments

Metal-binding experiments consisted of a series of solutions containing isolated FA (~3 mg of C/L) in synthetic moderately hard water (MHW, Table 3) and varying concentrations of Cu^{2+} at a pH of ~6. It is well known that copper binds well with organic matter (Al-Reasi et al., 2012; Baken et al., 2011; Lu & Allen, 2002), and we used Cu^{2+} as a proxy for all DOM-metal binding experiments. DOM from all Arkansas River sites and one groundwater site (GWW-06) from Spring 2020 and Fall 2020 were used in the Cu-DOM binding experiments. Because groundwater DOM concentrations are low, most groundwater samples were not able to be used as part of the experiment. 10 L of MHW was created (Table 3) for all binding experiments to ensure

consistency in water chemistry and the same solution was used for all eight experiments. MHW was chosen to buffer the acidic DOC-03 solutions used in the experiments. An ionic strength adjuster (ISA) was not added to the test solutions because MHW provides the necessary background electrolytes.

Table 3. Water chemistry of synthetic moderately hard freshwater (MHW) (EPA-821-R-02-013, 2002).

Final Water Chemistry (mg/L)							**Final Water Quality**		
Ca^{2+}	**Mg^{2+}**	**K^{+}**	**Na^{+}**	**Cl^{-}**	**SO_4^{2-}**	**HCO_3^{-}**	**pH**	**Hardness**	**Alkalinity**
17.64	12.12	2.10	26.30	1.90	90.24	69.70	7.4-7.8	80-100	57-64

A cupric ion-selective electrode (Cu-ISE) (Thermo Orion ionplus Sure-Flow Cupric Electrode, #9629BNWP) was used for all Cu-DOM measurements based on the relative ease of use and sufficient sensitivity the ISE provides at the Cu concentrations used in this study. The sensitivity of the Cu-ISE generally diminishes at Cu concentrations $<10^{-7}$ M Cu (Jenne, 1979; Saar & Weber, 1982; Xue & Sunda, 1997) and therefore, measurements beyond this concentration are excluded. Prior to Cu-DOM measurements, a calibration curve was established in order to calculate the $\{Cu^{2+}\}$ in each Cu-DOM test solution. Details (i.e., Cu^{2+} concentrations, pH, etc.) of the calibration solutions and Cu-DOM binding experimental procedure are located in Appendix D.

Concentrations of Cu^{2+} (from Orion ionplus Application Solution 942906: 0.1 M Cu^{2+} Cupric Standard) from 10^{-7} M to 10^{-5} M Cu^{2+} standards were chosen for both calibrations and Cu-DOM measurements as this is the likely range of environmental copper in freshwater systems and AMD-impacted streams (Woody & O'Neal, 2012). A FA concentration (as DOC) of 3 mg C/L was chosen for Cu-DOM binding as it represents likely FA amounts in natural waters (Cabaniss & Shuman, 1988). Temperature and pH were recorded with every measurement because these parameters may

affect the readings if unstable. Each test solution (10^{-8} M through 10^{-5} M Cu) was measured at room temperature five times, and each set of solutions was measured three times to ensure reproductivity of the ISE measurements. New calibration standard solutions are created for each test batch to ensure minimal cross-contamination. ISE readings were considered acceptable when an R^2 ~0.99 was generated. A follow-up Cu analysis on an Atomic Absorbance Spectrophotometer (AAS) was completed to verify Cu concentrations from calibration solutions and determine concentrations of total copper in test solutions, in contrast to free copper measurements recorded by the ISE. The measurement of cations is done with an ICP-OES through CREW Laboratories at OU to ensure consistency in the water chemistry between different solutions and explain any anomalous ISE results. There was no anion analysis of the Cu-DOM solutions as they can be calculated based on the cation results as we know the concentrations of the salts that were added to the solutions.

The cupric ISE does not directly report Cu^{2+} as concentration (mg/L) but as potential (mV) reading requiring the use of the aforementioned calibration curve. Total Cu results from AAS measurements of the calibration solutions were used in conjunction with the ISE readings to create a calibration curve (Fig. 10). An exponential regression formula is produced from the calibration solutions to calculate $\{Cu^{2+}\}$ with the use of the mV readings produced on the Cu-ISE as the "x" value, explained further in Appendix D.

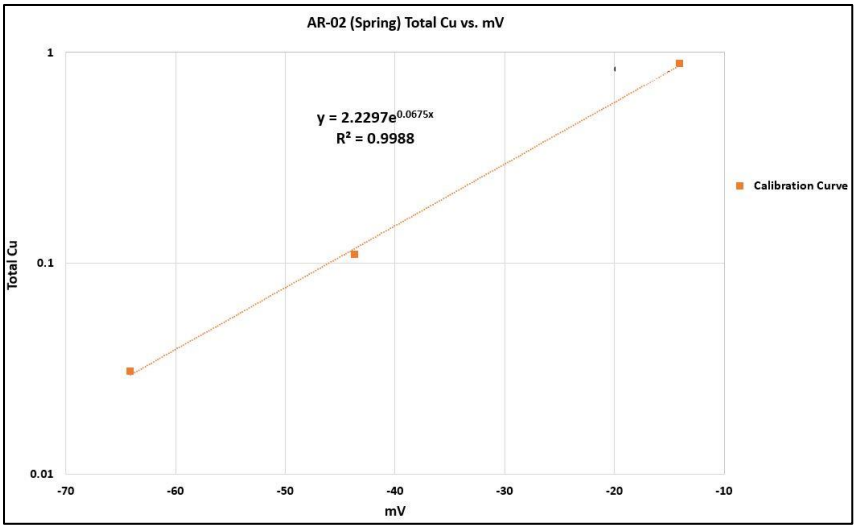

Figure 10. Example calibration curve from the Cu-DOM binding experiments for the Spring AR-02 sample.

4 RESULTS

4.1 Water Chemistry

Field and laboratory results for all the sampled sites are shown in Table 4. Comprehensive water chemistry results for all the surface and groundwater sites sampled in this project are found in Appendix B. Surface water alkalinity, and pH values were generally smaller during spring snowmelt than during the fall and summer sampling periods, with pH being nearly one unit less. For example, the pH during Spring 2020 at AR-03 was 7.15 while it was 8.01 during Fall 2020 (Table 4). The alkalinity at AR-03 during spring and fall were 22 and 52 mg/L as $CaCO_3$, respectively (Table 4). This trend is the same for AR-01 and AR-02 samples and is likely related to snowmelt during the spring. The conductivity and total dissolved solids (TDS) were much less during spring snowmelt compared to baseflow in surface water. The conductivity ranged from 76 to 107 µS/cm at the three surface water sites during spring and 210 to 271 µS/cm during fall, while the TDS ranged from 38 to 53 ppm in spring and 105 to 136 ppm in fall. Anions and cations in surface water are dilute in the spring and more concentrated during

baseflow months. For example, Ca^{2+} and SO_4^{2-} were 8.30 and 9.60 mg/L at AR-01, respectively, during Spring 2020, while they were 26.33 and 44.70 mg/L in Fall 2020 (Table 4). This trend is the same for Mg^{2+}, Na^{+}, and Cl^{-}, however, there is no major change in K^{+} between seasons in surface water. This is likely due to an influx of snowmelt into streams, diluting ionic concentration, whereas water level is lower in fall, causing higher concentration of ions. There is little to no variability in water chemistry between samples collected in Summer 2020 and Fall 2020 related to lack of precipitation, causing baseflow to start earlier in the year.

In general, groundwater chemistry does not vary much by site, however, distinct variability does exist among all wells sampled in this study. On average, the pH varies between 7.0 and 8.0 between the wells, however, GWW-04 experienced more variability with a pH of 6.40 during Spring 2019 and 5.60 during Fall 2019 (Table 4). The alkalinity in groundwater varies slightly between seasons, with greater alkalinity typically during baseflow and lesser alkalinity during spring snowmelt. For example, GWW-01 was 89 mg/L as $CaCO_3$ in Spring 2020 and 127 mg/L as $CaCO_3$ in Fall 2020. Each individual well showed relatively little variation throughout the year, as shown by the conductivity and TDS values, however, variability between wells exists. For example, GWW-06 had a conductivity value of approximately 357 µS/cm, while GWW-07 was approximately 90 µS/cm throughout the year. Concentrations of cations and anions in groundwater for each well do not change significantly between seasons (average of ±1.0 or less) but differ between sites. GWW-04 is the only groundwater well with greater variability between seasons as seen with pH (6.40 in Spring 2019 and 5.60 in Fall 2019) and alkalinity values (43 mg/L as $CaCO_3$ in Spring 2019 and 8 mg/L as $CaCO_3$ in Fall 2019) as well as conductivity (79 µS/cm in Spring and 44 µS/cm in Fall 2019) and TDS (39 ppm in Spring and 22 ppm in Fall 2019).

Stiff diagrams (Fig. 11) for all research sites are used to show how the ionic composition of water changes over time and by location. Dilution resulting from snowmelt is apparent in Stiff diagrams for the Arkansas River sites (AR-01, AR-02, and AR-03), as evident by the smaller ionic concentration relative to baseflow (Fig. 11a-11c). The surface water samples during baseflow have an increased ionic concentration (Fig. 11a-11c). In general, the ionic composition of groundwater does not vary among the sampling dates at each site (Fig. 11d-11i); however, there is variability between the groundwater wells. GWW-04 and GWW-07 tend to have lower ion concentrations than the other groundwater wells.

Piper diagrams are used to graphically display how hydrogeochemical facies change based on shifts in their water types (surface water or groundwater). Piper diagrams for all seasons used in this study are shown in Figure 12. The Piper diagrams suggest the water chemistry does not change significantly between seasons. However, surface water sites may show a slight shift from being primarily calcium-bicarbonate waters towards calcium-sulfate waters from spring snowmelt to baseflow (Fig. 12c and 12e). GWW-04 also shifts through seasons from calcium-bicarbonate waters to calcium-sulfate waters from Spring 2019 to Fall 2019 and Spring 2020.

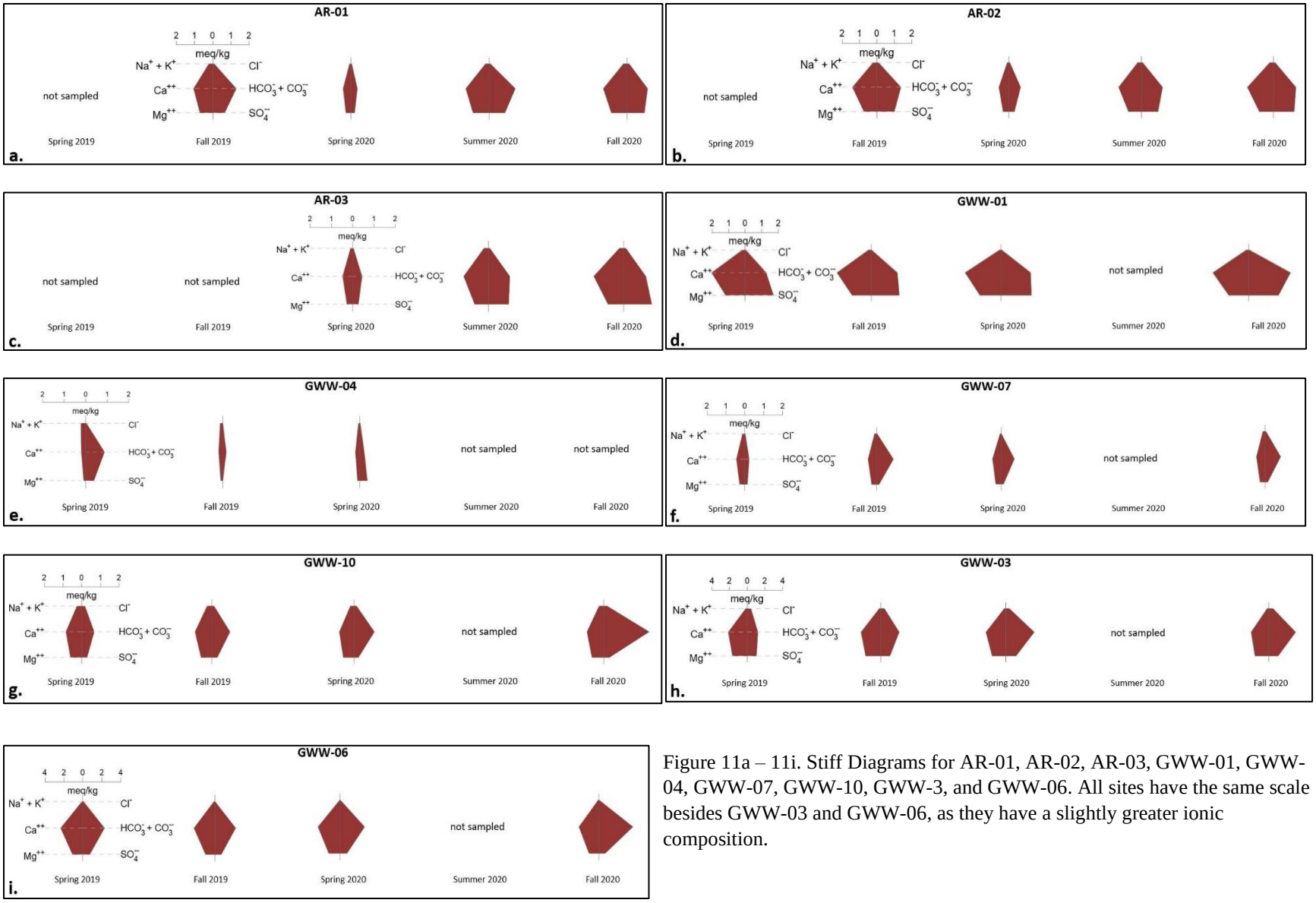

Figure 11a – 11i. Stiff Diagrams for AR-01, AR-02, AR-03, GWW-01, GWW-04, GWW-07, GWW-10, GWW-3, and GWW-06. All sites have the same scale besides GWW-03 and GWW-06, as they have a slightly greater ionic composition.

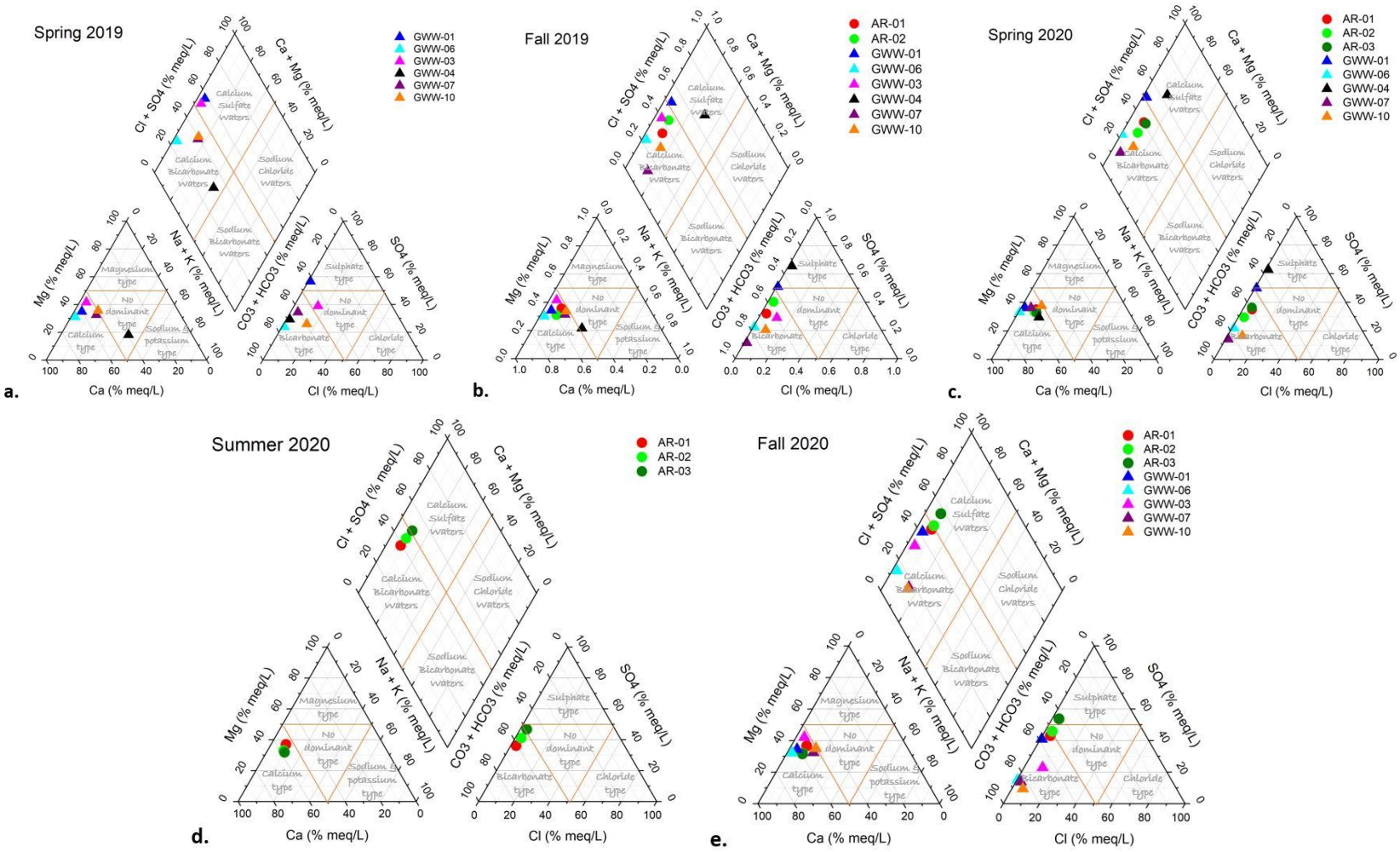

Figure 12. Piper diagrams for all seasons included in this study. Figure 12a-12e is Spring 2019, Fall 2019, Spring 2020, Summer 2020, and Fall 2020.

Dissolved organic carbon (DOC) concentrations tend to be greater during the spring snowmelt months compared to the baseflow months in surface water samples (Table 4), supported by box plots showing that the greatest concentrations are found in Spring 2020 compared to Summer and Fall 2020 (Fig. 13). For example, during Spring 2020, the Arkansas River sites had a mean DOC concentration of 3.89 mg C/L while the mean concentrations for Summer and Fall 2020 were 1.47 and 1.02 mg C/L, respectively (Table 5). Overall, DOC concentrations in surface water were greater during baseflow in 2019 compared to baseflow in 2020, likely related to 2019 experiencing an above-average snowpack. DOC concentrations in groundwater were much greater in Spring 2019 compared to Fall 2019, such that concentrations were between 1.68 and 4.30 mg C/L during spring snowmelt and between 0.35 and 1.38 mg C/L during baseflow. However, DOC concentrations between spring snowmelt and baseflow in 2020 do not vary greatly. For example, GWW 10 had concentrations of 0.39 mg C/L during Spring 2020 and 0.32 mg C/L in Fall 2020. Even with a drought year (2020), the baseflow DOC concentrations are still less than the spring snowmelt concentrations in groundwater and surface water. Box plots comparing groundwater and surface water during spring and fall in 2020 (Fig. 13) support the fact that groundwater DOC concentrations do not vary significantly throughout the year, and surface water samples during fall show similar concentrations to groundwater.

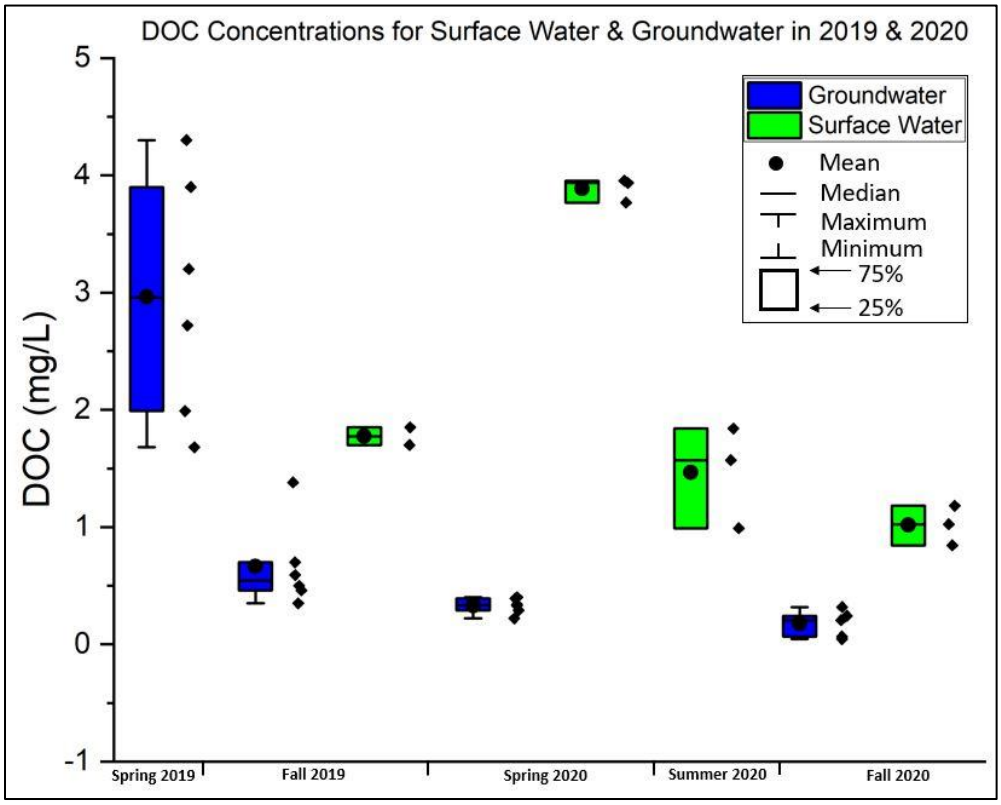

Figure 13. DOC concentrations in surface water and groundwater during the Spring and Fall of 2019 and 2020. The plots show that there are greater concentrations of DOC during Spring snowmelt in surface water compared to the groundwater samples and surface water during fall. Individual data points are shown to the right of each box plot.

Table 4. Water Chemistry Results for Streams and Groundwater sites located in Lake County, Colorado.

Site	*Season*	*pH* [a]	*Alkalinity* [b]	*Cond.* [f]	*TDS* [g]	*Bulk DOC* [c]	*Diss Ca* [d]	*Diss Mg* [d]	*Diss Na* [d]	*Diss K* [d]	*Cl^-* [d]	*SO_4^{2-}* [d]
AR-01	Fall 2019	8.09	65	210	105	1.70	21.6	8.2	4.1	1.0	2.3	30.7
	Spring 2020	7.73	17	76	38	3.95	8.3	3.2	1.2	0.8	1.1	9.6
	Summer 2020	8.28	73	240	120	0.99	25.3	10.2	3.9	0.9	2.5	41.4
	Fall 2020	8.34	57	253	126	0.84	26.3	10.9	4.2	1.0	3.2	44.7
AR-02	Fall 2019	8.00	68	258	129	1.85	28.1	8.7	4.8	0.9	2.9	46.7
	Spring 2020	7.70	33	107	53	3.77	11.4	4.0	1.7	0.9	1.2	14.0
	Summer 2020	8.75	64	237	118	1.84	25.5	8.7	4.0	0.8	2.7	45.3
	Fall 2020	8.48	65	271	136	1.18	29.8	9.9	4.4	1.0	3.6	57.0
AR-03	Spring 2020	7.15	22	87	43	3.94	9.1	3.1	1.6	1.0	1.3	13.0
	Summer 2020	7.91	50	219	110	1.57	23.2	7.6	4.1	0.9	2.6	45.4
	Fall 2020	8.01	52	255	128	1.02	28.1	9.0	4.1	1.0	3.2	62.5
GWW-01	Spring 2019	8.04	63	346	173	4.30	36.4	12.8	3.0	1.0	1.4	81.6
	Fall 2019	8.20	79	348	173	0.35	40.8	13.7	3.2	1.0	1.0	80.2
	Spring 2020	8.08	89	372	186	0.22	42.9	15.1	1.5	0.9	1.2	86.5
	Fall 2020	7.88	127	363	181	0.07	43.0	14.5	2.8	1.2	1.1	85.5
GWW-03	Spring 2019	7.59	60	412	206	2.72	41.6	17.9	3.1	0.8	13.6	48.6
	Fall 2019	7.40	102	412	206	0.50	44.4	19.6	3.6	0.7	13.3	47.5
	Spring 2020	7.53	162	411	206	0.40	44.3	18.4	3.4	1.0	14.4	54.7
	Fall 2020	7.67	152	387	193	0.24	39.4	18.6	3.2	1.1	16.3	49.8
GWW-04	Spring 2019	6.40	43	79	39	1.68	4.3	1.1	4.7	0.8	0.9	17.6
	Fall 2019	5.60	8	44	22	0.46	3.8	1.0	2.3	0.6	0.4	15.8
	Spring 2020	6.57	10	80	40	0.33	4.1	1.3	0.9	0.5	0.3	16.9
GWW-06	Spring 2019	7.44	114	357	178	3.20	44.4	12.3	1.5	1.1	1.7	34.9
	Fall 2019	7.46	109	328	164	0.70	43.5	11.8	1.5	1.1	0.6	30.6
	Spring 2020	7.35	131	357	179	0.34	46.4	13.9	BDL [e]	1.1	1.5	35.8
	Fall 2020	7.59	178	325	163	0.21	42.0	12.4	1.4	1.2	0.5	30.3
GWW-07	Spring 2019	6.92	11	90	45	1.99	8.4	2.9	2.4	0.6	0.6	6.0
	Fall 2019	7.00	44	90.0	45	0.59	9.1	3.1	2.6	0.5	0.6	5.4
	Spring 2020	7.02	35	91	46	0.29	8.9	3.3	0.9	0.3	0.5	5.6
	Fall 2020	6.93	41	93	47	0.04	9.2	3.4	2.4	0.8	1.0	6.5
GWW-10	Spring 2019	7.26	33	180	90	3.90	16.0	6.8	4.5	1.8	5.6	13.8
	Fall 2019	7.60	49	189	94	1.38	17.4	7.2	4.9	1.9	4.2	13.5
	Spring 2020	7.39	55	167	83	0.39	15.5	6.9	3.2	1.6	4.7	11.7
	Fall 2020	7.63	121	196	98	0.32	18.1	7.5	4.8	2.0	6.1	13.0

a. Standard Units
b. mg $CaCO_3$/L
c. Bulk DOC filtered through a 0.45µm membrane filter, mg/L
d. Filtered through a 0.1 µm membrane filter, mg/L
e. Below Detection Limit
f. Conductivity in units of µS/cm
g. Total Dissolved Solids (TDS) in units of ppm

Table 5. Mean values for DOC concentration, alkalinity, pH, conductivity, and sulfate concentration (SO_4^{2-}).

Site		*DOC (mg/L)*	*Alkalinity (mg $CaCO_3$/L)*	*pH*	*Conductivity (µS/cm)*	*SO_4^{2-} (mg/L)*
Groundwater	Spring 2019	2.97	54	7.28	244	33.73
	Fall 2019	0.66	65	7.21	235	32.15
	Spring 2020	0.33	80	7.32	246	35.19
	Fall 2020	0.18	124	7.54	273	37.02
Surface Water	Fall 2019	1.78	67	8.05	234	38.72
	Spring 2020	3.89	24	7.53	90	12.20
	Summer 2020	1.47	62	8.31	232	44.07
	Fall 2020	1.02	58	8.28	260	54.73

4.2 DOM Optical Spectroscopy Results

Spectroscopic indices, including $SUVA_{254}$, fluorescence index (FI), humification index (HIX), and freshness index, were chosen to highlight the molecular properties of DOM in this study and are shown in Table 6. Box plots are used to statistically show how significant (or not) the spectroscopic indices vary among the sites (groundwater and surface water) and by season in 2020 (Fig. 14 and Fig. 15). $SUVA_{254}$ values for isolated FA (DOC-03) stream samples ranged from 4.71 L mg^{-1} m^{-1} during spring snowmelt to 1.76 L mg^{-1} m^{-1} during baseflow (Fig. 14a). Summer values were as low as 1.29 L mg^{-1} m^{-1} in the Arkansas River samples. Bulk DOC (DOC-01) had the same trend in surface waters, with higher $SUVA_{254}$ values during spring snowmelt periods (Fig. 15a); however, the difference was not as significant. For example, $SUVA_{254}$ during Spring 2020 in AR-01 was 4.17 L mg^{-1} m^{-1} and 3.84 L mg^{-1} m^{-1} during Fall 2020, while the values were 4.39 L mg^{-1} m^{-1} and 4.35 L mg^{-1} m^{-1} at AR-03 during spring snowmelt and baseflow, respectively. The FI in the Arkansas River isolated FA samples are greatest during baseflow, with summer values being similar and lowest during spring snowmelt (Fig. 14b). The values ranged from 1.35 during spring snowmelt to 1.60 during baseflow, with summer values as great as 1.65. The same trend was seen in bulk DOC samples, showing greater values during baseflow than spring snowmelt (Fig. 15b). The freshness index in surface water samples does not vary greatly between seasons (±0.10) but does show a slight decrease during

spring snowmelt in the isolated FA (Fig. 14d) and bulk DOC (Fig. 15d) samples. The humification index (HIX) in the isolated FA (Fig. 14c) and bulk DOC (Fig. 15c) samples in surface water indicated a slightly greater degree of humification during spring snowmelt compared to baseflow.

The lowest $SUVA_{254}$ values were observed in groundwater samples with a mean of less than 1.0 L mg^{-1} m^{-1} for both bulk DOC and isolated FA. Groundwater $SUVA_{254}$ values for isolated FA varied considerably between years (Fig. 16). In 2019, the $SUVA_{254}$ values were greatest during baseflow, however, during 2020, the variability between spring snowmelt and baseflow months was minimal, such that the difference was non-existent to approximately ±0.10. Groundwater $SUVA_{254}$ values for bulk DOC were extremely low (Spring 2019) to non-existent (Spring 2020) in the spring snowmelt samples, while the baseflow samples were greater (between 2.08 and 3.39 L mg^{-1} m^{-1}) (Fig. 16). FI for isolated FA and bulk DOC groundwater varied with values greatest during spring snowmelt in some groundwater wells, and others are greatest during baseflow (Fig. 14b and 15b). Bulk DOC FI values in groundwater ranged from 1.87 to 2.36 during baseflow and between 1.98 to 3.01 during spring snowmelt in 2020 (Fig. 15b). The isolated FA FI values were in the range of 1.82 to 2.27 during baseflow and between 1.77 to 2.73 during spring snowmelt in 2020 (Fig. 14b). The freshness index in groundwater samples does not vary greatly between seasons. Overall, the freshness index values for bulk DOC are greater in 2020 than in 2019. Freshness index values for isolated FA samples showed variability, with baseflow values greater than spring snowmelt in certain groundwater wells and nearly the same throughout the year in other groundwater wells (Fig. 14d). The Humification Index (HIX) does not vary much between seasons at each groundwater well in isolated FA (Fig. 14c). Bulk DOC HIX values were greater during spring snowmelt (Fig. 15c). Where variability

exists, there is no significant pattern. Unlike the water chemistry discussed in 4.1, the molecular characteristics of DOM did not vary greatly between each individual groundwater well between seasons, however, there is variability between all the wells.

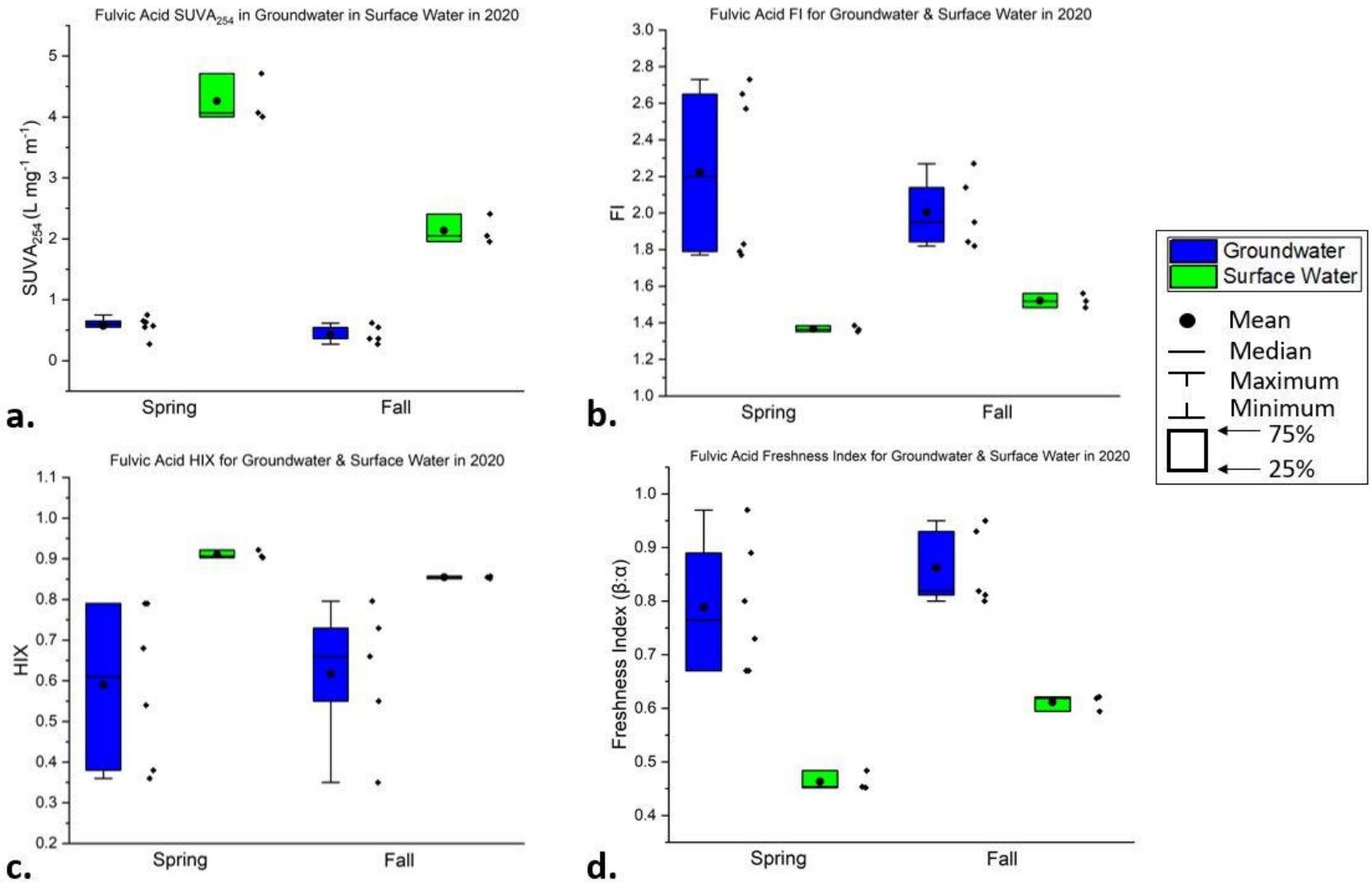

Figure 14a-14d. Box Plots for the spectroscopic indices used in this study for the isolated fulvic acid samples in groundwater and surface water during spring and fall of 2020. Individual data points are shown to the right of each box plot.

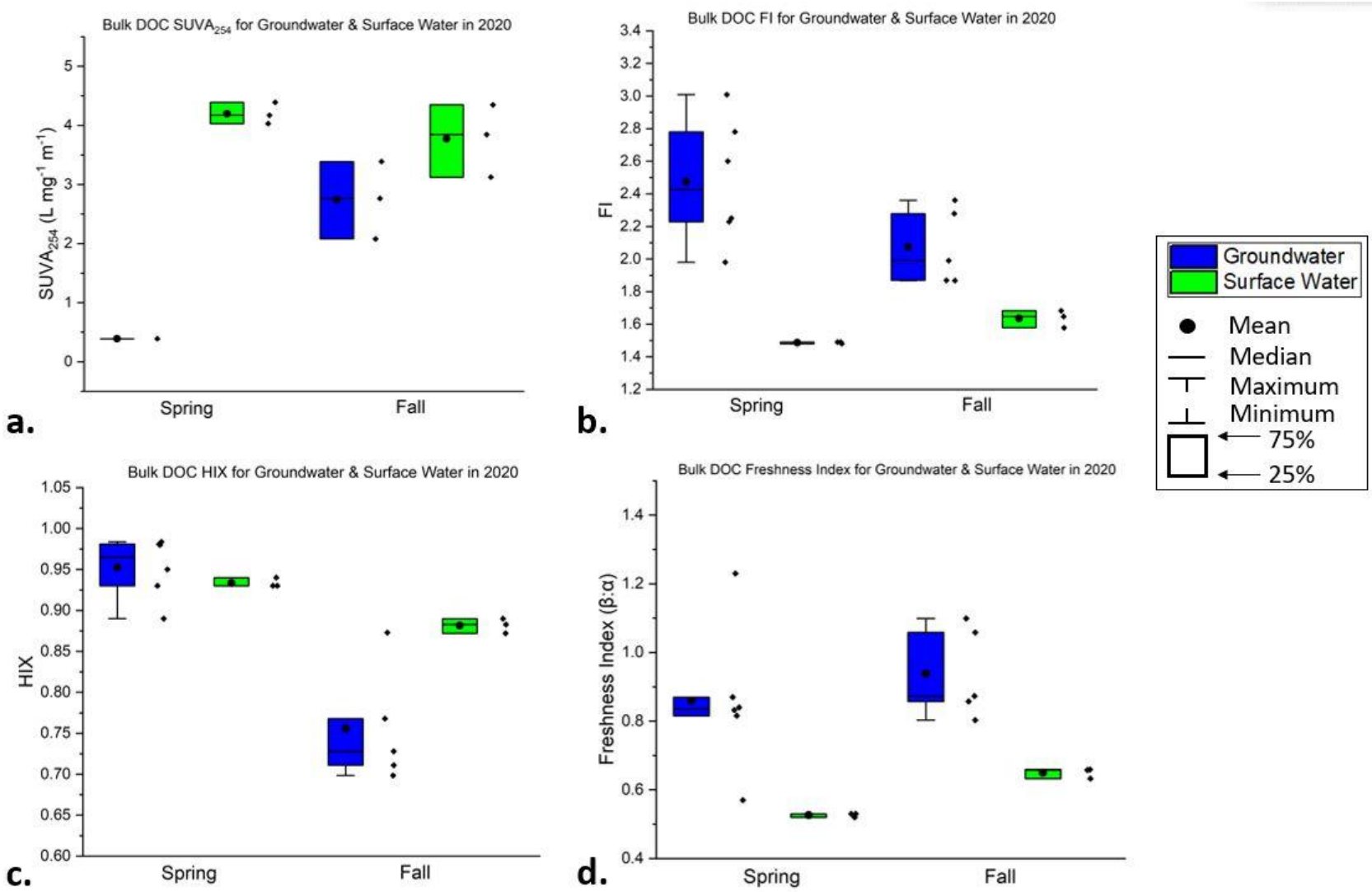

Figure 15a-15d. Box Plots for the spectroscopic indices used in this study for the bulk DOC samples in groundwater and surface water during spring and fall of 2020. Individual data points are shown to the right of each box plot.

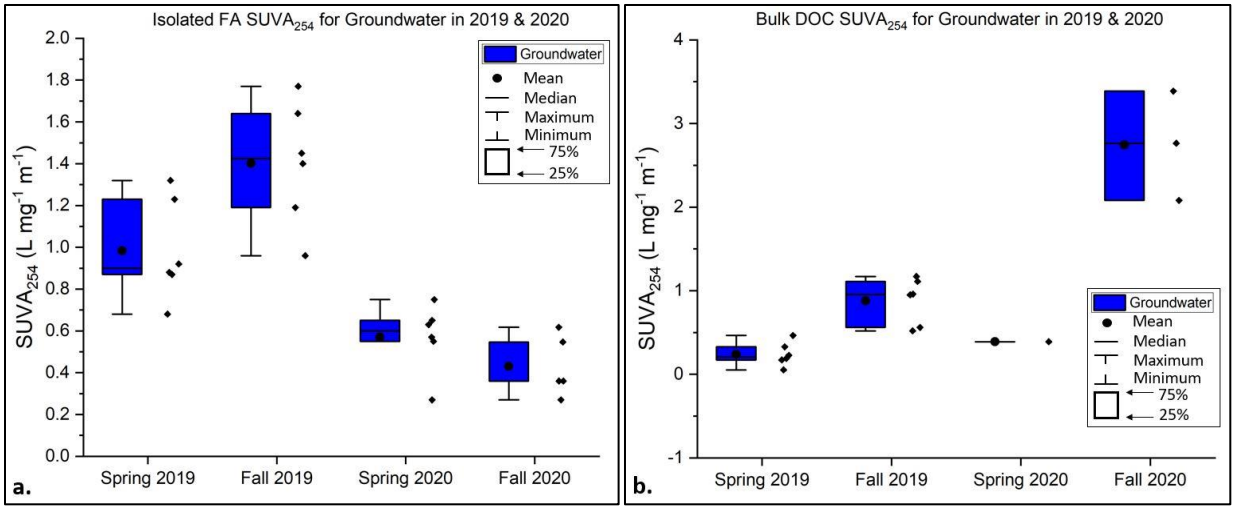

Figure 16. Box plots for isolated FA (right) and bulk DOC (left) $SUVA_{254}$ values in groundwater during 2019 and 2020. Individual data points are shown to the right of each box plot.

Table 6. Spectroscopic Indices used in this study for bulk DOC (DOC-01) and isolated FA (DOC-03).

		Bulk DOC (DOC-01)				*Isolated FA (DOC-03)*			
Site	*Season*	*$SUVA_{254}$*	*FI*	*HIX*	*Freshness Index (β:α)*	*$SUVA_{254}$*	*FI*	*HIX*	*Freshness Index (β:α)*
AR-01	Fall 2019	2.22	1.62	0.84	0.60	1.76	1.60	0.80	0.64
	Spring 2020	4.17	1.49	0.94	0.52	4.71	1.35	0.91	0.45
	Summer 2020	2.96	1.64	0.89	0.59	1.29	1.65	0.69	0.75
	Fall 2020	3.84	1.68	0.89	0.66	2.05	1.56	0.85	0.62
AR-02	Fall 2019	1.8	1.58	0.87	0.65	2.06	1.59	0.81	0.68
	Spring 2020	4.03	1.49	0.93	0.53	4.07	1.38	0.92	0.45
	Summer 2020	2.79	1.66	0.85	0.63	1.79	1.52	0.80	0.66
	Fall 2020	3.12	1.65	0.87	0.66	1.95	1.48	0.85	0.62
AR-03	Spring 2020	4.39	1.48	0.93	0.53	4.00	1.36	0.90	0.48
	Summer 2020	3.32	1.61	0.86	0.63	2.21	1.44	0.84	0.61
	Fall 2020	4.35	1.58	0.88	0.63	2.41	1.52	0.86	0.59
GWW-01	Spring 2019	0.05	2.27	0.81	0.60	0.88	1.81	0.65	0.77
	Fall 2019	1.17	1.63	0.81	0.55	1.45	2.26	0.64	0.92
	Spring 2020	---	3.01	0.98	0.83	0.55	1.77	0.79	0.67
	Fall 2020	---	2.36	0.73	0.80	0.55	1.95	0.73	0.81
GWW-03	Spring 2019	0.33	1.96	0.82	0.87	1.32	2.00	0.63	0.95
	Fall 2019	1.11	1.51	0.83	0.76	1.40	1.82	0.69	0.97
	Spring 2020	---	2.60	0.98	1.23	0.63	2.65	0.54	0.97
	Fall 2020	3.39	1.87	0.77	1.10	0.36	2.14	0.66	0.93
GWW-04	Spring 2019	0.46	1.28	0.55	0.53	0.92	1.57	0.49	0.7
	Fall 2019	0.56	1.47	0.76	0.68	0.96	1.87	0.70	0.95
	Spring 2020	---	2.78	0.95	0.57	0.57	2.73	0.38	0.73
GWW-06	Spring 2019	0.19	1.72	0.88	0.78	0.87	1.79	0.67	0.81
	Fall 2019	0.52	1.86	0.93	0.79	1.64	1.96	0.73	0.92
	Spring 2020	---	2.23	0.98	0.82	0.75	1.83	0.79	0.67
	Fall 2020	2.08	1.99	0.87	0.86	0.62	1.84	0.80	0.82
GWW-07	Spring 2019	0.17	2.65	0.84	0.81	0.68	1.86	0.67	0.71
	Fall 2019	0.96	1.66	0.77	0.41	1.77	2.40	0.55	0.94
	Spring 2020	---	1.98	0.93	0.87	0.65	1.79	0.68	0.80
	Fall 2020	---	2.28	0.70	0.87	0.27	2.27	0.35	0.80
GWW-10	Spring 2019	0.23	1.68	0.59	0.78	1.23	1.78	0.54	0.87
	Fall 2019	0.95	1.99	0.33	0.97	1.19	1.87	0.58	1.02
	Spring 2020	0.39	2.25	0.89	0.84	0.27	2.57	0.36	0.89
	Fall 2020	2.76	1.87	0.71	1.06	0.36	1.82	0.55	0.95

4.3 Statistical Analysis

Principal Component Analysis (PCA) was used to indicate which parameters, including DOC concentration and spectral indices ($SUVA_{254}$, FI, freshness index, and HIX), are most influential in the observed variability between groundwater and surface water. These spectral indices were used to demonstrate if the samples were influenced by molecular weight or aromaticity ($SUVA_{254}$), by DOM source (FI), how freshly produced is the DOM (freshness index), or by the degree of humification (HIX) the sample had undergone. DOC concentrations were included because the concentrations can affect the spectral indices and vary throughout the year. Origin 2021™ was used for PCA, and the results were transferred to Excel to create PCA plots. The PCA analysis for the isolated FA and bulk DOC components is shown in Figures 17 and 18, respectively. The PCA results account for 83% of the variability in the isolated FA samples and 61% of the variability for bulk DOC samples. $SUVA_{254}$, FI, and freshness index seem to influence the first principal component greatly, and all surface water samples tend to plot along the principal component axis one.

In general, much of the variability between groundwater and surface water samples throughout the year is explained by spectral indices and bulk DOC concentrations. The PCA diagram for the isolated FA component of DOM (Fig. 17) shows that distinct clustering of surface water samples exists along PC1 that are strongly related to $SUVA_{254}$, FI, and freshness index. The PCA diagram for isolated FA (Fig. 17) shows that Spring 2020 surface water samples cluster together while baseflow months and summer samples group together. There is an apparent shift during baseflow (and summer) in the surface water samples that is strongly influenced by $SUVA_{254}$, FI, and freshness index, which causes the samples to have a more similar molecular composition to groundwater than to spring surface water samples.

Groundwater samples display a similar shift due to seasonality, with DOC concentrations and HIX also influencing the way the samples group. The greater distribution of groundwater samples appears to be more of a factor of variability among individual well chemistry rather than seasonality. For example, GWW-03 and GWW-04 may be more influenced by FI and freshness index than other groundwater samples. There is a clear grouping between spring snowmelt/summer samples and baseflow samples besides two outliers (Spring 2020 GWW-03 and GWW-04).

The bulk DOC PCA shows a similar distribution as the isolated FA samples in surface water samples, where spring surface water samples are clustered separately from the fall and summer surface water samples along PC1 (Fig. 18). The fall and summer samples display slight compositional overlap with the spring groundwater samples and a few fall (Fall 2019) groundwater samples. The first principal component axis is influenced greatly by FI and DOC concentration. DOC concentrations appear to factor more into the variability of surface water samples and Spring 2019 groundwater samples. Spring 2020 groundwater samples cluster and are more influenced by FI. In contrast, there is more spread among the groundwater samples with slight clustering between seasons that is likely a factor of differing DOM among the wells sampled in this study.

Pearson correlation was used to determine significant correlations among multiple parameters and are shown in Table 7. A strong correlation exists for coefficient values that lie between ±0.50 and ±1; medium correlation is between ±0.30 and ±0.49, and small correlation is less than ±0.29. The isolated FA indices in groundwater mostly have a small to no correlation with one another. Bulk DOC concentrations appear to have a medium correlation with FI (-0.37), while $SUVA_{254}$ has a medium correlation with the freshness index (0.39). The only strong

correlation (between the indices we picked) is a negative correlation between FI and HIX (-0.59). However, isolated FA indices in surface water show strong correlations with all indices used in this study (Table 7). For example, there is a very strong negative correlation between FI and $SUVA_{254}$ (-0.89) and a positive correlation between $SUVA_{254}$ and DOC concentrations (0.92), and thus, if $SUVA_{254}$ values increase, DOC concentrations are also increased, and FI is decreased. Bulk DOC spectral indices in groundwater have a similar trend to isolated FA samples, with a majority of the correlations being small or medium. $SUVA_{254}$ has a medium correlation with bulk DOC concentration (-0.30) and HIX (-0.33), FI has a medium correlation with HIX (0.45), and the freshness index has little to no correlation with the indices used in this study. Surface water for bulk DOC samples shows strong correlations for nearly all samples, similar to the isolated FA samples, aside from $SUVA_{254}$, which shows medium correlations with DOC concentrations (0.42) and freshness index (-0.49).

Supporting statistics for isolated FA and bulk DOC spectroscopic indices are given in Table 8. Isolated FA $SUVA_{254}$ and FI values show that the mean groundwater $SUVA_{254}$ is 0.85 with a variance of 0.19, and the mean surface water $SUVA_{254}$ is 2.57 with a much greater variance of 1.28. The mean groundwater FI is 2.01 with a variance of 0.10, and the mean surface water FI is 1.50 with a variance of 0.01.

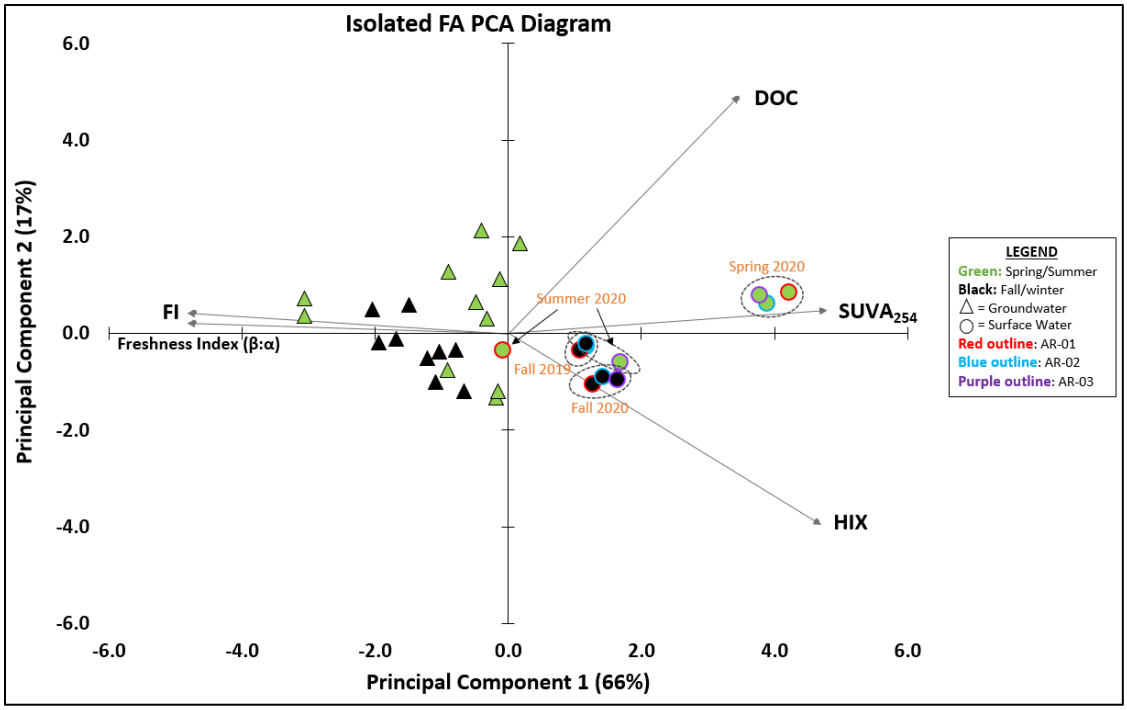

Figure 17. PCA Diagram for isolated FA samples (DOC-03). The loading vectors include the molecular composition of DOC through spectral indices such as FI, freshness index, $SUVA_{254}$, and HIX, as well as DOC concentrations. These vectors can indicate seasonal variability as related to DOC source and composition. Dashed ovals indicate clustering between surface water samples. Specifically, Summer 2020 samples overlay some of the Fall 2019 samples.

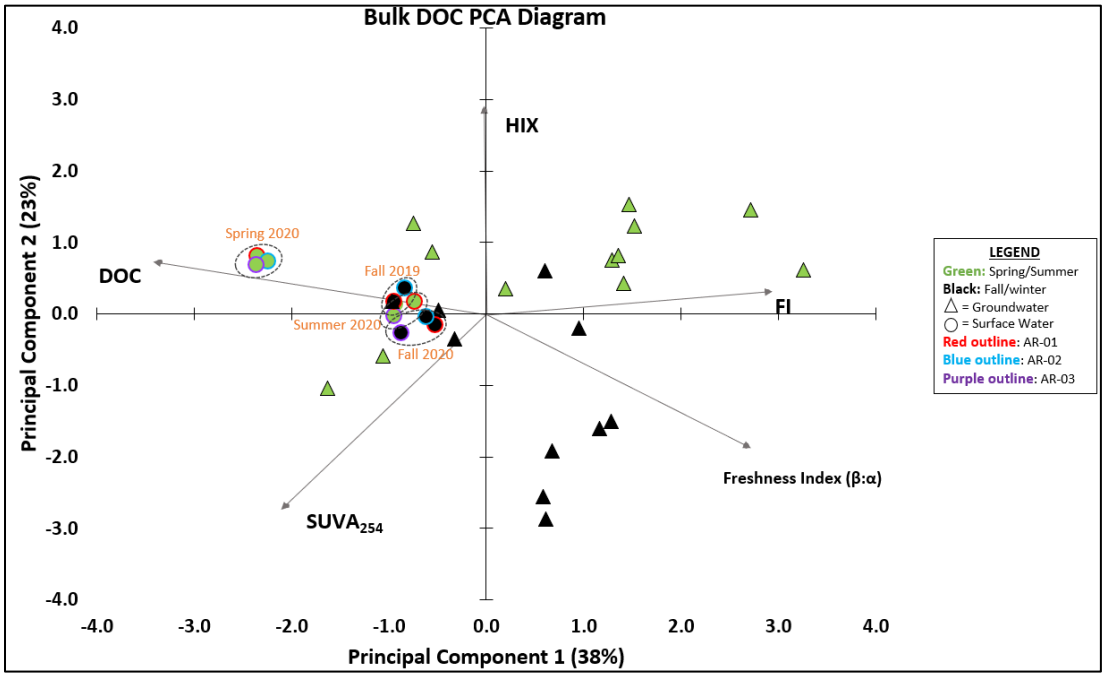

Figure 18. PCA Diagram for bulk DOM samples (DOC-01). The loading vectors include the molecular composition of DOC through spectral indices such as FI, freshness index, $SUVA_{254}$, and HIX, as well as DOC concentrations. These vectors can indicate seasonal variability as related to DOC source and composition. Dashed ovals indicate clustering between surface water samples.

Table 7. Groundwater Pearson correlation coefficient data from 2019 and 2020 isolated FA (DOC-03) and bulk DOC concentrations, created using Origin 2021.

	Bulk DOC (DOC-01)		**Isolated FA (DOC-03)**	
	Streams	**Groundwater**	**Streams**	**Groundwater**
DOC -- $SUVA_{254}$	0.42	-0.30	0.92	0.29
DOC – FI	-0.91	-0.16	-0.81	-0.37
DOC – HIX	0.75	-0.25	0.66	-0.01
DOC -- Freshness Index	-0.89	-0.20	-0.85	0.09
$SUVA_{254}$ – FI	-0.50	0.00	-0.89	-0.13
$SUVA_{254}$ – HIX	0.74	-0.33	0.82	0.22
$SUVA_{254}$ – Freshness Index	-0.49	0.15	-0.96	0.39
FI -- HIX	-0.77	0.45	-0.86	-0.59
FI – Freshness Index	0.84	0.29	0.92	0.24
HIX – Freshness Index	-0.77	0.04	-0.92	-0.12

High degree: If the coefficient value lies between ± 0.50 and ± 1, then it is said to be a strong correlation.
Moderate degree: If the value lies between ± 0.30 and ± 0.49, then it is said to be a medium correlation.
Low degree: When the value lies below ± 0.29, then it is said to be a small correlation.

Table 8. Mean values for spectral indices ($SUVA_{254}$, FI, HIX, and freshness index) included in this study for bulk DOC and isolated FA.

Site	***Season***	***Bulk DOC (DOC-01)***				***Isolated FA (DOC-03)***			
		$SUVA_{254}$ (L mg^{-1} m^{-1})	***FI***	***HIX***	***Freshness Index (β:α)***	***$SUVA_{254}$ (L mg^{-1} m^{-1})***	***FI***	***HIX***	***Freshness Index (β:α)***
Groundwater	Spring 2019	0.24	1.93	0.75	0.73	0.98	1.80	0.61	0.80
	Fall 2019	0.88	1.69	0.74	0.69	1.40	2.03	0.65	0.95
	Spring 2020	---	2.47	0.95	0.86	0.57	2.22	0.59	0.79
	Fall 2020	2.74	2.07	0.76	0.94	0.43	2.00	0.62	0.86
	Total Mean:	**1.29**	**2.04**	**0.80**	**0.80**	**0.85**	**2.01**	**0.62**	**0.85**
	Variance:	**0.96**	**0.20**	**0.02**	**0.04**	**0.19**	**0.10**	**0.02**	**0.01**
Surface Water	Fall 2019	2.01	1.60	0.86	0.63	1.91	1.60	0.81	0.66
	Spring 2020	4.20	1.49	0.93	0.53	4.26	1.37	0.91	0.46
	Summer 2020	3.02	1.64	0.87	0.61	1.76	1.54	0.78	0.67
	Fall 2020	3.77	1.64	0.88	0.65	2.14	1.52	0.85	0.61
	Total Mean:	**3.36**	**1.59**	**0.89**	**0.60**	**2.57**	**1.50**	**0.84**	**0.60**
	Variance:	**0.77**	**0.01**	**0.00**	**0.00**	**1.28**	**0.01**	**0.00**	**0.01**

4.4 Cu-DOC Binding

Results for eight Cu-DOC binding experiments are shown in Table 9, representing isolated FA from all three surface water samples and one groundwater sample collected in Spring 2020 and Fall 2020. The target concentration of approximately 3 mg C/L was obtained in most spring samples; however, fall samples ranged from ~2 to 3 mg C/L (Table 9). The two greatest Cu concentration solutions in both GWW-06 samples have a DOC concentration ~1.0 mg/L greater than the other solutions. The mean pH of the solutions in the experiments was ~6.5, however, there are test solutions where pH reaches ~7.0 or falls below 6.0, likely affecting $\{Cu^{2+}\}$ of the test solutions. Specifically, the experiments using DOM collected from AR-03 in Spring 2020 have pH values near 5.5. The likely cause of the variability in pH is potentially a factor of increased acid or base addition in the experimental solutions used to reach the desired ~6.5 pH value. The stock MHW created for use in all experimental solutions had ion concentrations of 14.80 mg/L Ca^{2+}, 3.23 mg/L K^{+}, 10.97 mg/L Mg^{2+}, 19.76 mg/L Na^{2+}, and 78.88 mg/L SO_4^{2-}. The Cu-DOM test solutions generally had Ca^{2+} and Mg^{2+} concentrations that were very close to the expected MHW concentrations (per EPA-821-R-02-013 (2002)) (Table 3). However, K^{+} and Na^{+} concentrations were greater than the published EPA MHW values. The elevated K^{+} and Na^{+} concentrations are likely due to the electrode filling solution (made of DI water, KNO_3, and NaCl) bleeding, and excess Na may have originated from NaOH used during the FA isolation process (NaOH used to remove the FA from the DAX-8 resin), or NaOH added to the FA isolate solutions to raise the pH prior to adding into the test solutions. The initial pH and alkalinity of the main MHW batch (10L) were 7.9 and 60 mg/L, respectively. The concentrations of anions and cations, the pH, temperature, alkalinity, and DOC concentrations are found in Table 9 for all the experiment solutions.

All Total Cu versus mV plots can be found in Appendix D. Total copper and free copper values are listed in Table 9. Plots comparing the experimental solutions for each season are shown in Figure 19 (Spring 2020) and Figure 20 (Fall 2020), while plots of each site are shown in Figure 21. There is a clear separation between the surface water samples and the groundwater sample in the Spring 2020 set (Fig. 19), where surface water samples have higher $\{Cu^{2+}\}$ compared to groundwater. For example, AR-01, AR-02, and AR-03 have 9%, 8%, and 12% $\{Cu^{2+}\}$ in the lowest copper solutions, respectively, while GWW-06 has 0% $\{Cu^{2+}\}$. The GWW-06 site had a greater pH than the other three sites, resulting in less $\{Cu^{2+}\}$ in solution, likely due to complexation with carbonate/bicarbonate. The Fall 2020 set of experimental solutions clustered together so that there was no distinct separation between groundwater and surface water samples (Fig. 20). Two out of the three surface water samples and the groundwater sample showed more free copper in solution in the Fall samples than the Spring samples (Fig. 21). AR-03 showed more free copper during Spring than in Fall (Fig. 21), likely due to the pH being less than 6.0 from a lab error (potentially added too much acid).

Table 9. Results of total Cu and free Cu from all experimental solutions.

	Season	*Total Cu (µg/L)*	*{Cu^{2+}} (µg/L)*	*% {Cu^{2+}}*	*DOC Conc. (mg C/L)*	*pH*	*Temp. (℃)*	*Alkalinity (mg/L as $CaCO_3$)*	*Ca^{2+}*	*Mg^{2+}*	*K^{+}*	*Na^{+}*	*SO_4^{2-}*
AR-01	Spring 2020	38.19 104.99 693.69	3.28 3.19 18.26	9% 3% 3%	3.08 2.86 2.78	6.74 6.74 6.76	19.6 19.6 19.6	25.0	15.79	12.10	60.59	35.30	85.71
	Fall 2020	18.68 83.45 737.44	0.32 14.18 546.61	2% 17% 74%	2.10 1.90 1.97	6.54 6.24 6.33	20.0 20.0 20.0	75.0	15.40	11.93	15.32	37.55	84.12
AR-02	Spring 2020	39.20 140.32 696.89	2.95 18.40 75.06	8% 13% 11%	2.93 2.74 2.66	7.24 6.86 6.75	19.9 19.6 19.6	30.0	15.61	12.13	30.81	27.97	85.39
	Fall 2020	51.82 114.91 840.58	5.47 62.71 797.24	11% 55% 95%	1.95 1.75 1.73	7.14 6.37 5.87	20.3 20.2 20.3	57.5	14.05	10.47	16.60	55.80	75.09
AR-03	Spring 2020	33.44 101.48 782.21	3.85 40.96 630.73	12% 40% 81%	2.51 2.53 2.43	5.73 5.56 5.53	19.9 19.9 19.9	30.0	16.25	12.74	13.73	21.30	89.33
	Fall 2020	19.85 237.40 774.29	0.15 4.09 451.68	1% 2% 58%	2.43 2.23 2.24	6.84 6.88 6.67	20.1 20.0 20.1	45.0	14.79	11.23	10.13	42.00	79.88
GWW -06	Spring 2020	28.10 80.93 505.93	0.00 0.06 19.56	0% 0% 4%	2.11 2.12 3.04	7.58 7.42 7.02	19.7 19.7 19.7	66.0	14.54	10.96	34.64	37.13	78.22
	Fall 2020	27.59 87.32 776.47	0.36 2.99 56.67	1% 3% 7%	1.52 1.37 3.16	7.05 7.22 7.24	19.9 20.0 20.0	90.0	14.00	10.34	12.93	80.57	74.50

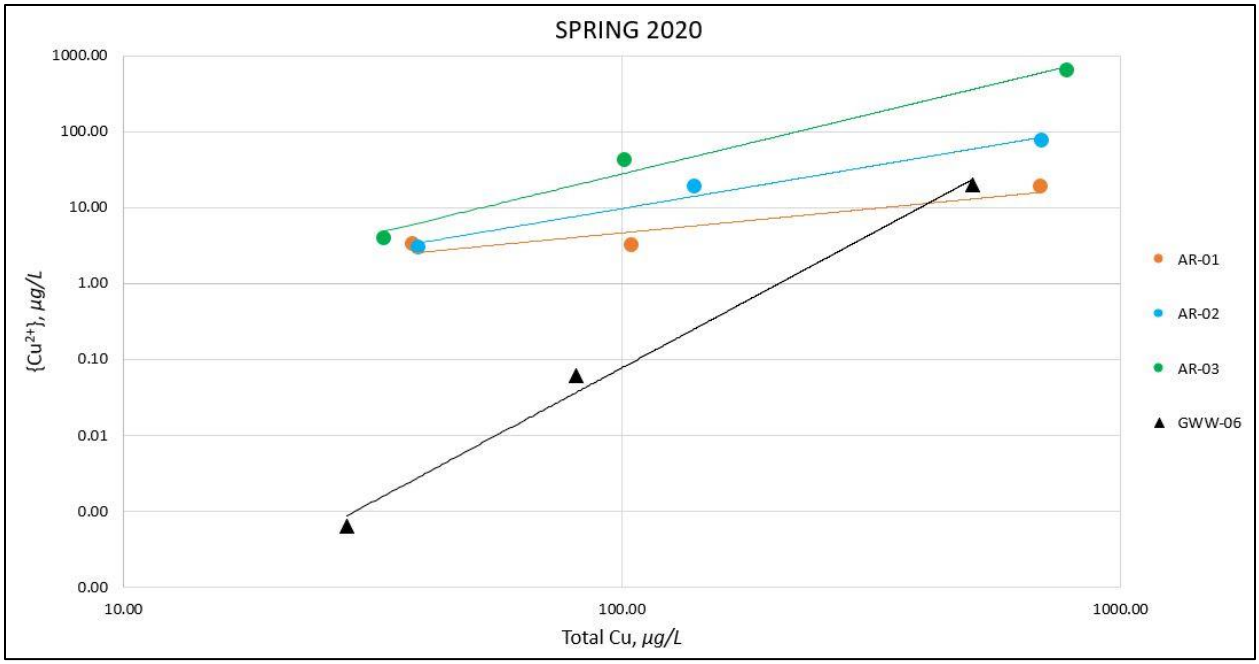

Figure 19. Spring 2020 total Cu versus free Cu in experimental Cu-DOC solutions in µg/L.

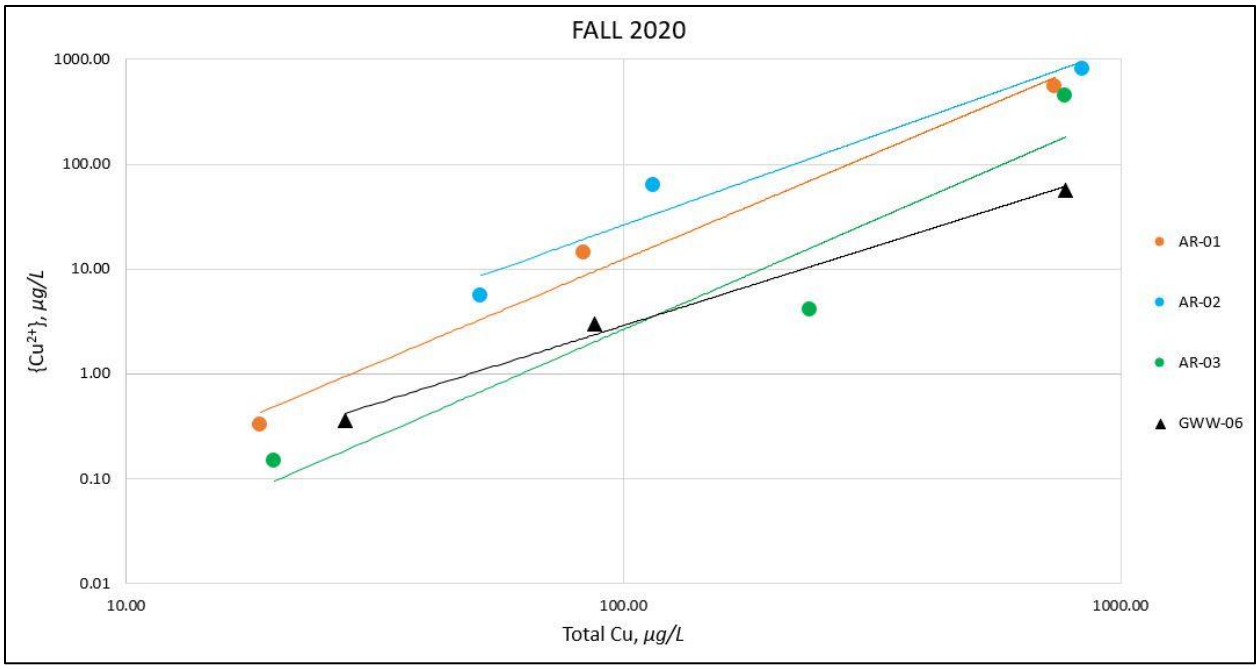

Figure 20. Fall 2020 total Cu versus free Cu in experimental Cu-DOC solutions in µg/L.

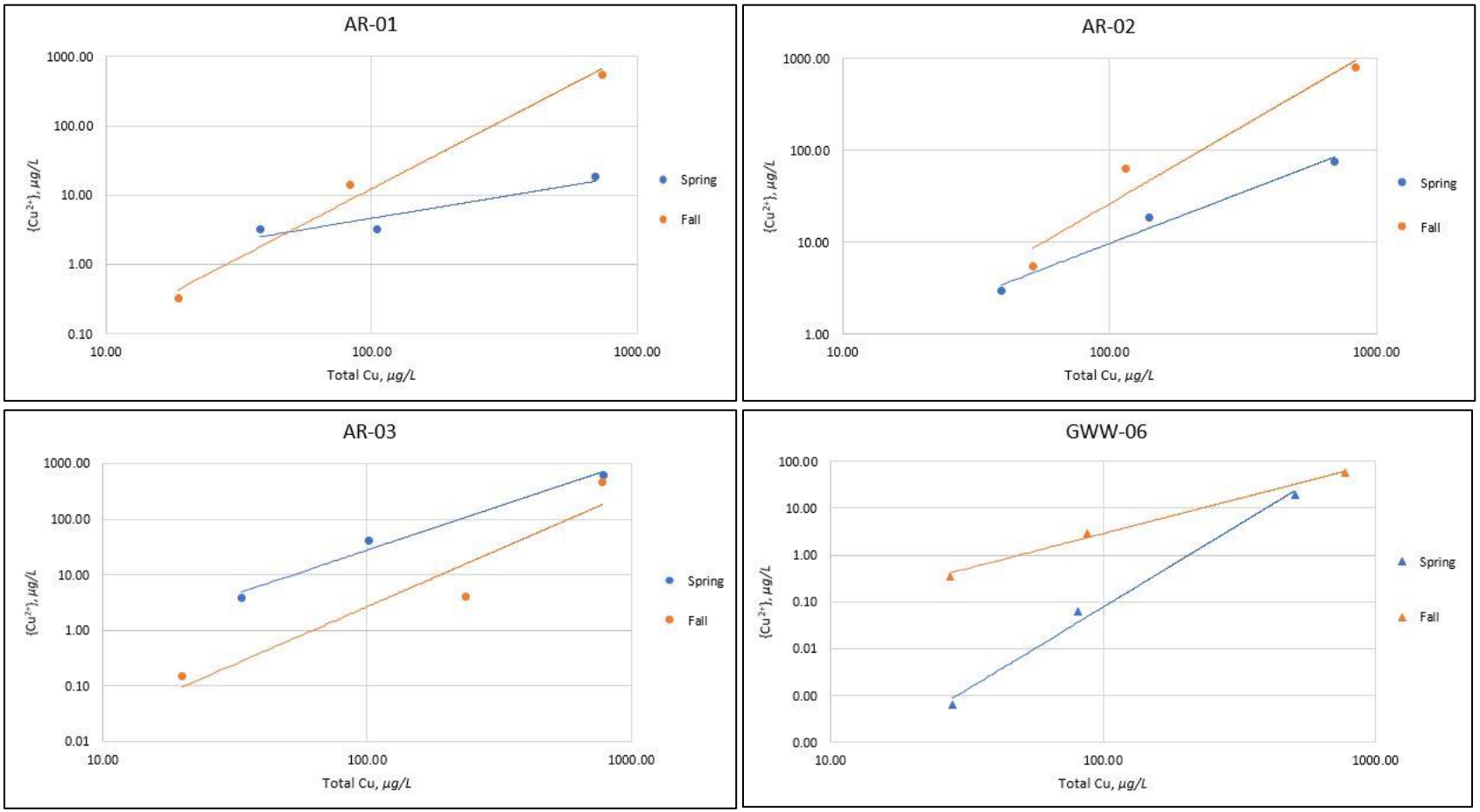

Figure 21. Spring and Fall 2020 experimental Cu-DOC solutions comparison with the total Cu versus $\{Cu^{2+}\}$ concentrations in µg/L for AR-01, AR-02, AR-03, and GWW-06.

5 DISCUSSION

5.1 Seasonal Influences on Solute Concentration and Distribution

Hydrologic seasonal variability related to transient snowpack is the primary influence on hydrology and water chemistry variability in mountainous watersheds. Although snowmelt dominates as the primary source of water feeding streams for 48% to 74% of the year (Carroll et al., 2018), recent studies suggest high relief watersheds are also dependent on groundwater based on the age of water found in streamflow (Jasechko, Kirchner, Welker, & McDonnell, 2016). A study on the Sierra Nevada Mountains in California showed low flow periods were primarily sustained by groundwater that was previously recharged during snowmelt (Godsey et al., 2014). We are able to build upon these studies by including seasonal effects on solute concentrations and distribution related to surface water and groundwater interactions during different seasons. Changes in water chemistry are more pronounced during spring snowmelt, where the mean pH in surface water was 7.53, and mean alkalinity was 24 mg/L as $CaCO_3$ (Table 5) and can be attributed to spring snowmelt runoff. During baseflow, the mean pH was 8.28, with a rise in alkalinity of 58 mg/L as $CaCO_3$ (Table 5). During Spring, surface water samples had a decrease in pH, likely due to snowmelt contributing acidity, while the decrease in alkalinity may be due to increased acidity (potentially from AMD) and dilution, as supported by Butler et al. (2008), where they associated the lower pH and alkalinity to the combined effects of AMD input and snowmelt in the North Fork of Clear Creek in Clear Creek County, CO. In contrast, during baseflow, we notice greater alkalinity and pH, more closely related to the groundwater chemistry (Fig. 22). Groundwater pH and alkalinity are relatively stable within each groundwater well throughout the year, with an overall greater alkalinity than what is seen in surface water.

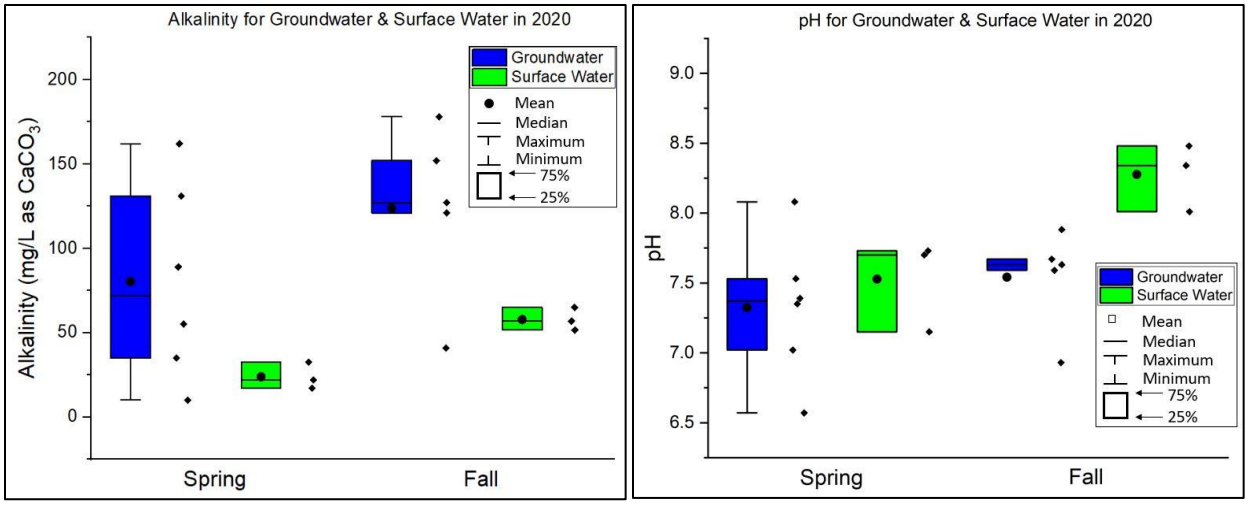

Figure 22. Alkalinity and pH for groundwater and surface water in 2020. Individual data points (found in Table 4) are shown to the right of each box plot.

The reduced conductivity and TDS in surface water during spring snowmelt appears to be due to dilution from increased water discharge in the river. During baseflow, the river discharge is much lower, resulting in more concentrated TDS and conductivity and had similar values measured in groundwater that did not vary much throughout the year. The differing concentrations of major anions and cations between seasons are due to dilution. The lowest concentrations are linked to the highest flows (spring snowmelt), while the highest concentrations are linked to low flow (baseflow) as supported by stiff diagrams (Fig. 11) and by a study from Butler et al. (2008) where they observed metals increase in concentration over baseflow months and saw dilution during spring snowmelt. The piper diagrams (Fig. 12) suggested that the water type among the surface water and groundwater sites did not change markedly between seasons. However, the surface water sites did show a slight shift from being calcium bicarbonate water during spring snowmelt towards calcium sulfate water in baseflow, likely attributed to sulfide ore deposits interacting with groundwater, which indicates that there is another source of water contributing to streams during baseflow, potentially deep groundwater. Within the East River of Colorado, Carroll et al. (2018) found that annually, nearly one-third of the streamflow during baseflow can be attributed to groundwater contribution through concentration-discharge relationships and

multivariate statistical approaches. There are greater concentrations of sulfate found in groundwater, as seen in Figure 23, where the mean concentration in groundwater falls between 32.15 and 37.02 mg/L throughout 2019 and 2020, however, in surface water, the mean concentration is 12.20 mg/L during spring snowmelt and increases significantly (54.73 mg/L) during 2020 baseflow. This is likely attributed to this region having great amounts of sulfide ore deposits which are diminished during Spring snowmelt due to dilution, causing greater concentrations of sulfate in surface water during baseflow when groundwater contributes to streamflow.

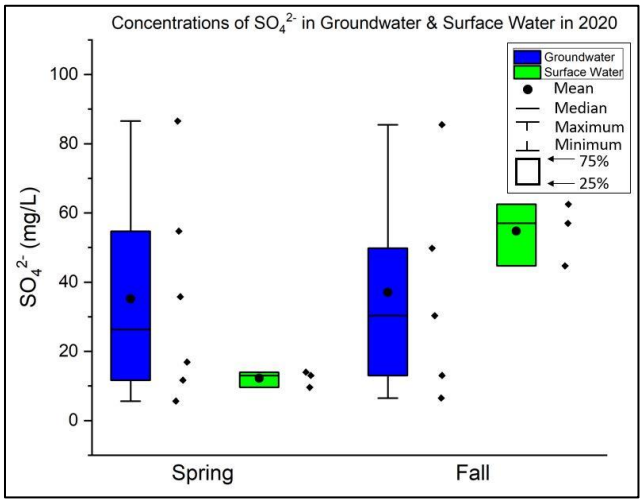

Figure 23. Concentrations of sulfate (SO_4^{2-}) in mg/L in groundwater and surface water during 2020. Individual data points are shown to the right of each box plot.

DOC concentrations also demonstrated similar seasonal variations as to what was seen in general water chemistry. Several studies conducted in similar watersheds in Central Colorado (Boyer et al., 1996; Brooks et al., 1999; Hornberger et al., 1994) show DOC concentrations in surface water increased during snowmelt due to flushing of terrestrial DOC that had accumulated in soils during the fall-winter periods. The greatest DOC concentrations in this study were observed in surface water during the start of spring snowmelt with a decrease in concentration as melting moves into baseflow (Fig. 13), which is likely due to DOC input originating from shallow soil and plants being carried along in snowmelt runoff into the river (Boyer et al., 1996; Butler et

al., 2008; Longnecker & Kujawinski, 2011). Consequently, the lack of substantial soil water moving through the subsurface during baseflow periods is related to cold temperatures causing the precipitation to exist as snowfall. Thus, without runoff or soil percolation to mobilize terrestrial DOM, a majority of DOM contributing to streams during baseflow is likely sourced from groundwater which is supported by Carroll et al. (2018), where they observed groundwater contributions of approximately 50% to streams during baseflow in the East River of Colorado. Similar seasonal effects were observed in DOC concentrations in both groundwater and surface water samples in 2020 compared to 2019, likely due to drought, such that seasonal effects are not as pronounced in 2020 compared to 2019. The mean DOC concentration in groundwater from Spring 2019 was 2.97 mg/L, and the mean in Spring 2020 was 0.33 mg/L (Table 5), which is nearly a 160% difference in mean values. A similar seasonal effect on DOC concentration is also observed in surface water, where the mean DOC concentration from Fall 2019 was 1.78 mg/L, and the mean value in Fall 2020 is 1.02 mg/L (Table 5). The year 2019 in Central Colorado experienced above-average snowpack, which is likely why greater DOC concentrations in groundwater during spring snowmelt and fall were measured. Groundwater DOC concentrations did not vary greatly in 2020, with a mean concentration in spring of 0.33 mg/L and 0.18 mg/L in baseflow (Table 5). Overall, DOC concentrations decreased from surface water to deep groundwater, with the sharpest decrease during spring snowmelt periods, supported by Boyer et al. (1996), where they saw the greatest concentrations of DOC in surface water during spring snowmelt with lower concentrations of DOC during baseflow in groundwater and surface water.

5.2 Hydrologic Effects on DOM Molecular Variability

This study suggests that the molecular composition of DOM in streams and groundwater within mountainous watersheds is strongly influenced by seasonality and water source, which is

similar to what Lynch et al. (2019) observed where optical fluorescence properties of DOM and DOC concentrations were strongly related to in-stream flows. Spectroscopic characterization of DOM has successfully been completed through spectroscopic measurements (Baken et al., 2011; Inamdar et al., 2012; McKnight et al., 2001) used to discriminate seasonal changes in DOM composition related to hydrologic factors such as snow melt. It is important to note the difference between bulk DOC and isolated FA spectral indices described below. The bulk DOC spectral indices results include the entire DOM pool and all ions in solution, such that greater ionic strengths in water may influence the absorbance and fluorescence measurements. Whereas the isolated FA spectral indices results only include DI water and the FA component of DOM, which can give us values with less potential interferences and can be related to the Cu-DOM binding experiments.

The use of FI is commonly used to identify the likely source of DOM where values between 1.2-1.5 are considered terrestrial or allochthonous sources and values between 1.7-2.0 are microbial or autochthonous in source (Inamdar et al., 2012; McKnight et al., 2001). We observed that DOM in surface water during spring snowmelt is allochthonous, originating from surficial sources such as soils. The FI in spring surface water DOM falls within the range of 1.2-1.5 (1.35-1.38 for FA and 1.48-1.49 for bulk DOC), indicating the DOM source originates from allochthonous sources for isolated FA and bulk DOC. Whereas FI in baseflow surface water DOM was slightly greater (1.48-1.60 for FA and 1.58-1.68) and were more similar to FI values of groundwater DOM in 2020 baseflow (1.82-2.27), suggesting that surface water DOM during baseflow may be more autochthonous (Inamdar et al., 2012; McKnight et al., 2001) and have a similar source to what was measured in groundwater (Fig. 14b and Fig. 15b).

The isolated FA and bulk DOC surface water $SUVA_{254}$ values in the spring snowmelt samples were generally greater (~4.3 L mg^{-1} m^{-1}) than samples collected in the summer and fall periods (~2.2 L mg^{-1} m^{-1} for FA and ~3.7 L mg^{-1} m^{-1} for bulk DOC) indicating that the spring snowmelt sourced DOM had greater aromatic content and molecular weight than summer and baseflow samples (Fig. 14a and Fig. 15a). These seasonal differences are similar to a study by Inamdar et al. (2012), where they observed a similar decrease in $SUVA_{254,}$ which is also supported by Hansen et al. (2016), where they linked high $SUVA_{254}$ values to high molecular weight and aromatic content. The summer $SUVA_{254}$ values for isolated FA from the stream samples ranged from 1.29 to 2.21 L mg-1 m-1 that is likely related to extreme drought and potentially autochthonous DOM being produced by increased microbial activity due to increased warm weather. A study completed in the Yukon River (Striegl, Aiken, Dornblaser, Raymond, & Wickland, 2005) observed increased microbial input with a decrease in DOC during the summer to surface water, supporting our study where we notice low $SUVA_{254}$ values from low DOC concentrations in the summer (similar to baseflow), suggesting DOC has low aromatic content and low molecular weight in the summer. The surface water baseflow $SUVA_{254}$ values are also low compared to spring snowmelt. We also observed that surface water DOC had a greater degree of humification (HIX) during spring snowmelt periods compared to baseflow periods (Fig. 14c and Fig. 15c), indicating that the DOC in surface water during spring snowmelt is primarily composed of humic and fulvic acids, and thus, allochthonous in source, supported by E. Thurman (1985) and McKnight et al. (2001). The freshness index (β:α) in surface water during spring snowmelt was lower compared to baseflow, having a lower proportion of fresh DOC as seen in box plots (Fig. 14d and Fig. 15d). This is not surprising as much of the DOC is

produced during fall and winter when DOC builds up the soil profile and is flushed into surface water during spring snowmelt (Boyer et al., 1996; Brooks et al., 1999; Hornberger et al., 1994).

Overall, spectral indices suggest that the groundwater DOM has attributes of being autochthonous throughout the year. McKnight et al. (2001) saw that microbially derived FAs have low aromatics and FI of 1.7 to 2.0, which we also observed in our groundwater samples. FI values for groundwater DOM generally fall within the range of 1.7 to 2.0, with some samples being greater than 2.0. This is the case for isolated FA and most bulk DOC samples. The groundwater $SUVA_{254}$ values for isolated FA samples throughout the year were generally small, with low molecular weight and low aromatic content. The groundwater bulk DOC $SUVA_{254}$ values were slightly greater during baseflow months than spring snowmelt (Fig. 15a), which is likely related to low DOC concentrations and the more complex solute chemistry in bulk DOC samples (causing enhanced absorbance by ions in solution). $SUVA_{254}$ in groundwater was much greater overall during 2019 than 2020 (Fig. 15a), which can be attributed to the snowmelt signature moving through the watershed in the above-average snowpack year (2019), causing greater concentrations of DOC. The HIX in isolated FA samples showed little variability between seasons at each groundwater site (Fig. 14c), with values less than surface water during spring snowmelt but similar to surface water during baseflow, having less humic-like signatures. The reduced HIX in groundwater indicates a protein-like signature that suggests the source of DOC in groundwater is autochthonous, supported by Al-Reasi et al. (2013), in which they observed autochthonous DOMs have a higher proportion of protein-like substances. The freshness index values also support the autochthonous composition of groundwater DOM by having a higher proportion of fresh DOC, indicating the organic matter was recently produced by microbial activity and potentially due to fractionation with soil solids causing more aromatic components to be removed by adsorption,

leaving the autochthonous DOC pool remaining in groundwater. This is supported by Hansen et al. (2016), who used freshness index values as an indicator for the presence of autochthonous DOM, with greater values representing fresher DOM, and thus is autochthonous DOM.

The range of spectroscopic indices suggests that DOM source and associated molecular composition in streams change from aromatic and allochthonous during spring to lower aromaticity and autochthonous in fall. The $SUVA_{254}$ values for DOM in surface water during baseflow were very similar to groundwater DOM, suggesting that DOM from groundwater may be present in surface water during baseflow (and drought) periods which is supported by Carroll et al. (2018), where they note that groundwater contributions to surface water during baseflow are significant (~50%). Whereas groundwater DOM composition does not vary much throughout the year, having primarily autochthonous spectral indices values of low $SUVA_{254}$ and HIX and greater FI and freshness index.

Principal Component Analysis (PCA) supports the differences in DOM composition and characteristics, controlled by watershed source and seasonality (Fig. 17 and Fig. 18). A distinct clustering occurred between Spring 2020 surface water samples, where the isolated FA PCA plot (Fig. 17) was controlled by $SUVA_{254,}$ and the bulk DOC PCA plot (Fig. 18) was controlled primarily by bulk DOC concentration. During baseflow and summer, the surface water samples plotted away from the spring snowmelt samples and clustered with or near several groundwater samples in both plots. The orientation of the surface water DOM samples during baseflow suggests a strong influence of microbial activity and possibly protein-like fluorescence indices, with a weak influence of aromaticity similar to what Inamdar et al. (2012) observed in groundwater DOM. Because there was a strong correlation (>0.50) between nearly all quality indices in surface water (Table 7), it is clear that a series of components can influence DOM in surface water, as evidenced

by PCA results accounting for 83% variability in isolated FA samples (Fig. 17) and Pearson correlations (Table 7).

There is seasonal grouping between groundwater sites as well, however, less pronounced. In the bulk DOC plot (Fig. 18), groundwater samples from Spring 2019 and Fall 2019 are grouped close to the surface water samples from baseflow and summer, likely related to a larger volume of water from snowpack moving through the watershed being influenced by greater concentrations of DOC and is more similar to terrestrial DOM. Groundwater samples in 2020 also cluster but are more influenced by freshness index in baseflow samples and FI in spring snowmelt samples (Fig. 17 and Fig. 18). In contrast to the high correlations seen between surface water spectral indices, DOM in groundwater relies more on protein-like fluorescence indices, which matches the study from Inamdar et al. (2012), where they saw the same trend. In general, correlations between groundwater spectral indices are minimal as specific indices may influence specific sites based on their depth and interactions in the subsurface (Table 7). The PCA differences between isolated FA and bulk DOC are likely due to the greater ionic strength of the bulk DOC aliquots, known (Weishaar et al., 2003) to affect absorbance and fluorescence properties of the DOM solutions. Regardless, the distribution of streams and groundwater in the PCA plot is similar between the isolated FA and bulk DOC.

5.3 Seasonal Effects on Cu-DOM Binding Properties

DOM found within natural water systems is an important organic ligand that will bind with metals, therefore, the role of seasonality and water source may be important factors in metal-DOM binding behavior. In this study, Cu-DOM binding using isolated FA from surface water and groundwater samples in the HUARW during Spring 2020 and Fall 2020 showed possible variability due to factors of seasonality and source. The relationship between DOC concentration

and Cu binding is well known, as demonstrated by Craven et al. (2012), where increasing DOM (as quantified by DOC) results in increased removal of Cu from solution. While DOC concentration is important for metal binding, the inherent variability of DOC composition in streams and groundwater may be just as important in regards to reactivity and binding affinity with metals (Hansen et al., 2016; Minor et al., 2014). An important result of Cu^{2+} complexing with FA is a reduction in aquatic copper toxicity, which is strongly correlated to the aromatic carbon content of DOM and can be estimated with spectroscopic indices such as $SUVA_{254}$ (Al-Reasi et al., 2012). $\{Cu^{2+}\}$ values from four samples used in this experiment are plotted against associated $SUVA_{254}$ values for isolated FA and show a negative correlation, also observed by Dee (2016), who correlated low $SUVA_{254}$ to lower binding affinity, resulting in higher concentrations of $\{Cu^{2+}\}$ (Fig. 24). FA-Cu binding measurements showed that low $SUVA_{254}$ values (0.62 to 2.05 L mg^{-1} m^{-1}) generally seen in Fall 2020 samples correspond to greater free copper ions in solution (7% to 95%), whereas higher $SUVA_{254}$ (2.18 to 4.71 L mg^{-1} m^{-1}) showed a smaller proportion of free copper ion (0% to 11%) in surface water samples as seen in Figure 24. GWW-06, AR-01, and AR-02 during baseflow and AR-03 during spring snowmelt had greater $\{Cu^{2+}\}$ than the opposing season and is reflected this in Figure 21. The samples for the Spring 2020 AR-03 had a pH of less than six that likely resulted in greater $\{Cu^{2+}\}$ due to a competition effect between H^+ and Cu^{2+} complexing with DOM. Lu and Allen (2002) found that Cu-DOM complexation has a pH dependence, where at acidic pH, the replacement of Cu^{2+} by H^+ will occur. In general, DOM in surface water and groundwater during baseflow has diminished metal-binding affinity. A study by Al-Reasi et al. (2012) found that aromatic, allochthonous DOM with higher humic-like content are more protective against Cu toxicity, agreeing with our study where we see less free copper in solution in the Spring 2020 samples when the primary source of DOM in streams is allochthonous.

The contribution of groundwater DOM in streams during baseflow periods is unclear, however, as demonstrated by PCA and the hydrograph indicating baseflow conditions in our summer and fall samples, groundwater DOM is likely present. Comparing other findings to our study regarding copper-binding with DOM in surface water and groundwater during different seasons in a mountainous watershed proves challenging due to the lack of comparable studies. Our results contradict a study done by Macoustra, Jolley, Stauber, Koppel, and Holland (2020), where they note that DOM was more protective and, thus, binds better with copper during dry seasons and less protective during wet seasons, however, this study was completed in a tropical freshwater setting, and ours is in a mountainous watershed. Kramer, Jak, Van Hattum, Hooftman, and Zwolsman (2004) observed no differences in copper toxicity by surface water location or season; however, this study only analyzed a lake. We found that there is more $\{Cu^{2+}\}$ in surface water and groundwater during baseflow (dry period), and thus, DOM is less protective than DOM in surface water and groundwater during spring snowmelt (wet period), otherwise noted as allochthonous DOM. Typically, allochthonous DOM is associated with lower metal toxicity, explained by humic- and fulvic-like components having more metal-binding sites compared to the protein-like component (Macoustra et al., 2020; Perdue, 1998), which agrees with our findings.

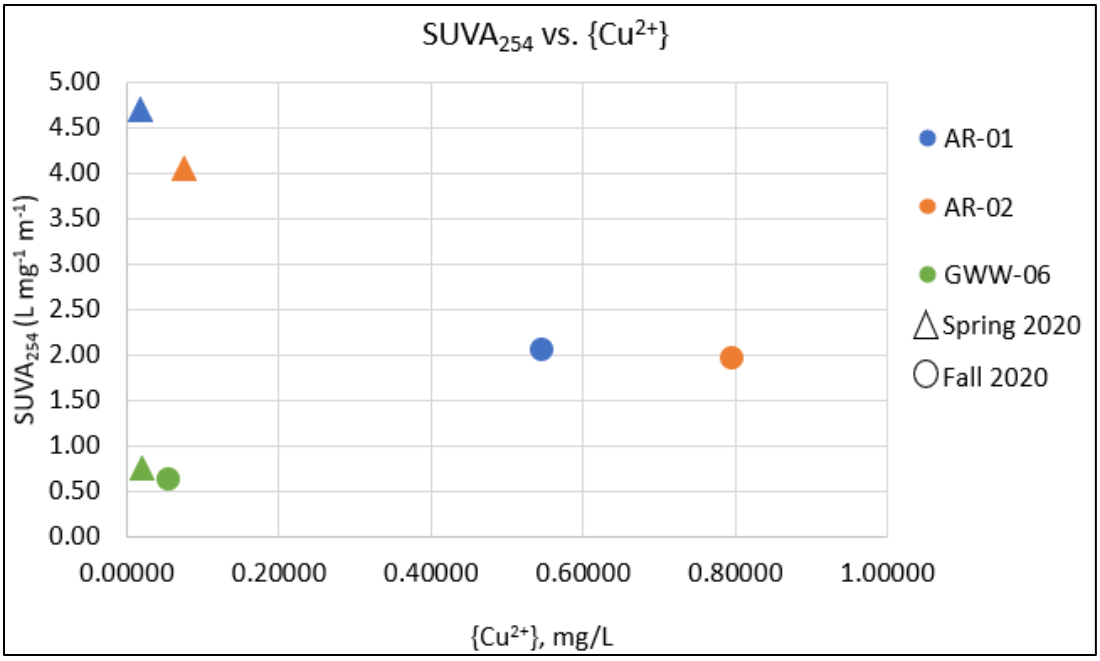

Figure 24. Graph of $\{Cu^{2+}\}$ in 10^{-5} M Cu^{2+} solutions versus $SUVA_{254}$ values from isolated FA.

6 SUMMARY AND CONCLUSIONS

Mountainous watersheds are signified by their transient hydrologic systems, defined by snowmelt-driven hydrology, resulting in highly variable solute concentrations, composition, distribution, and speciation. This study focused on evaluating DOM concentrations and quality in groundwater and surface water in a mountainous watershed over a two-year period using a suite of optical indices, general water chemistry, and metal-binding experiments. We found that DOM from the Upper Arkansas River watershed has variable sources related to the transient, seasonal hydrology. Surface water sources had high DOM concentrations, higher molecular weight and aromaticity, and were more humic-like during spring snowmelt periods, suggesting the source of DOM is allochthonous. While DOM originating from deep groundwater sources throughout the year and DOM in surface water during baseflow were autochthonous, having low DOC concentrations, low molecular weight and aromaticity, and were less humic-like and more protein-like. Our Cu-DOM binding experiments demonstrated that DOM in surface water and

groundwater during baseflow had diminished metal-binding affinity relative to snowmelt periods where DOM in surface water and groundwater in spring snowmelt samples had less $\{Cu^{2+}\}$ in solution, proving DOM is more protective against copper toxicity during spring snowmelt. The importance of likely groundwater DOM in streams during baseflow is the reduced metal binding affinity related to groundwater DOM that may result in increased aquatic metal toxicity. It is important to note that the groundwater samples used in this study were selected to demonstrate alluvial groundwater DOM composition and reactivity in the HUARW. It is beyond the scope of this study to determine any direct connection between the streams and groundwater from the wells sampled. However, our results indicate that, during baseflow periods, groundwater DOM in the streams sampled in this study are likely present and have a similar composition as samples included in this study. Overall, this study supported our hypotheses: DOM concentrations and molecular properties are influenced by seasonal variability in surface water, resulting in groundwater-sourced DOM being present in surface water during baseflow; the molecular composition of DOM in streams is similar to groundwater DOM during baseflow, and DOM during baseflow has a diminished metal-binding affinity.

6.1 Contributions to the Field

The results of this study provide more insight into ongoing research attempting to further understand groundwater DOM contributions to surface water during low-flow periods in snow-dominated mountainous watersheds. Our work adds to a continuous body of literature, providing further information on the differing molecular compositions and metal-binding characteristics of groundwater and surface water bulk DOC and isolated fulvic acid during spring snowmelt, summer, and baseflow periods. Specifically, the importance of groundwater DOM in surface water during low-flow periods as a potential ligand for trace metals. This research also

demonstrates the complexities associated with measuring Cu^{2+} in solutions that are similar to natural waters. This information is valuable for future use of Cu-DOM complexation research and can be used to improve geochemical and toxicological modeling.

6.2 Recommendations and Suggestions for Future Research

Conclusions from this research suggest further characterization of Cu-DOM binding and a different analytical approach for measuring Cu^{2+} is necessary to provide better data quality and understand the variability in complexation between Cu^{2+} and seasonal DOM. A new isolation procedure such as reverse osmosis (RO) would be much more efficient in terms of time and recovery of DOM mass. We also suggest collecting samples from the hyporheic zone, alluvial aquifer, and bedrock aquifer near the Arkansas River to understand better the interaction between DOM found in surface water during spring snowmelt, summer, and baseflow. Collecting DOM at a greater frequency would also prove useful to understand better how DOM molecular composition and metal-binding ability differ throughout the year.

APPENDIX A

RESEARCH SITE PHOTO DOCUMENTATION

Figure A1. Arkansas River Site 1 (AR-01) during the Spring sampling event (June 2020).

Figure A2. Arkansas River Site 1 (AR-01) during the Summer sampling event (August 2020).

Figure A3. Arkansas River Site 1 (AR-01) during the Fall sampling event (October 2020).

Figure A4. Arkansas River Site 2 (AR-02) during the Fall sampling event (October 2019).

Figure A5. Arkansas River Site 2 (AR-02) during the Spring sampling event (June 2020).

Figure A6. Arkansas River Site 2 (AR-02) during the Fall sampling event (October 2020). You can see rocks exposed where they are covered during Spring.

Figure A7. Arkansas River Site 3 (AR-03) during the Spring sampling event (June 2020).

Figure A8. Arkansas River Site 3 (AR-03) during the Fall sampling event (October 2020).

APPENDIX B

ANALYTICAL RESULTS FOR SITE WATER SAMPLES

Table B1. Water quality data for all research sites. Anions left out include Br^-, NO_2^-, and PO_4^{3-} because they are nearly always below the detection limit.

Site	*Season*	*Temp. (°C)*	*D.O.*	*ORP*	*F^-*	*NO_3^-*	*Total Ca d*	*Total Mg d*	*Total Na d*	*Total K d*	*Diss Al*	*Total Al*	*Diss As*	*Total As*
AR-01	Fall 2019	4.63	7.64	189.6	0.15	0.45	20.87	8.28	4.11	0.88	BDL	BDL	0.01	BDL
	Spring 2020	7.24	7.99	162.5	0.10	0.26	8.45	3.23	1.20	0.82	0.06	0.26	0.02	0.03
	Summer 2020	14.06	6.77	181.8	0.16	0.33	25.52	10.36	3.96	0.88	0.00	0.19	0.02	0.02
	Fall 2020	11.39	6.55	177.1	0.27	0.19	26.16	10.48	4.13	0.95	BDL	0.01	0.03	0.02
AR-02	Fall 2019	3.06	7.79	186.6	0.16	0.88	28.15	8.78	4.78	0.85	BDL	0.00	BDL	BDL
	Spring 2020	11.15	7.48	160.3	0.15	BDL	11.61	4.06	1.70	0.90	0.04	0.21	0.03	0.02
	Summer 2020	16.51	6.65	176.8	0.17	0.35	25.70	8.75	4.01	1.07	BDL	0.02	0.01	0.02
	Fall 2020	10.61	7.56	206.2	0.26	0.39	29.75	9.56	4.31	1.13	BDL	0.02	0.01	0.01
AR-03	Spring 2020	10.14	7.77	167.2	0.13	0.29	9.22	3.22	1.61	0.83	0.05	0.25	0.03	0.03
	Summer 2020	15.05	6.41	176.8	0.18	0.99	23.02	7.59	4.04	0.94	BDL	0.01	0.02	0.01
	Fall 2020	11.254	6.44	174.5	0.24	0.83	28.12	8.93	4.08	1.07	0.01	0.02	0.02	0.03
GWW-01	Spring 2019	8.54	3.71	204.6	BDL	BDL	40.34	14.02	3.07	1.04	BDL	BDL	0.00	BDL
	Fall 2019	8.24	4.85	184.6	0.08	0.58	41.34	13.92	3.21	1.13	BDL	BDL	0.01	0.01
	Spring 2020	8.74	3.65	172.9	BDL	BDL	42.94	15.11	1.53	0.88	BDL	BDL	BDL	BDL
	Fall 2020	13.71	2.86	174.4	0.16	0.59	42.95	14.47	2.84	1.23	BDL	BDL	0.02	0.02
GWW-03	Spring 2019	6.50	5.36	202.4	BDL	23.11	42.57	19.64	3.28	0.91	BDL	BDL	BDL	BDL
	Fall 2019	5.99	6.03	198.2	0.07	18.19	44.88	20.72	3.83	0.94	BDL	BDL	0.01	0.01
	Spring 2020	5.82	5.77	180.3	BDL	14.92	44.25	18.35	3.35	1.01	BDL	BDL	0.04	0.04
	Fall 2020	10.39	5.48	177.9	0.13	16.12	39.44	18.64	3.24	1.07	BDL	BDL	0.02	0.02
GWW-04	Spring 2019	6.83	2.29	214.1	BDL	0.34	4.15	1.14	4.65	0.75	0.00	0.01	BDL	BDL
	Fall 2019	7.80	6.73	237.0	0.11	0.34	3.79	1.01	2.32	0.66	BDL	BDL	BDL	BDL
	Spring 2020	6.99	1.64	170.9	0.12	BDL	4.09	1.29	0.90	0.49	0.01	0.01	BDL	BDL
GWW-06	Spring 2019	8.42	7.11	208.1	BDL	0.98	46.90	13.10	1.50	1.21	BDL	0.01	BDL	BDL
	Fall 2019	8.05	3.63	190.3	0.14	0.28	43.93	11.78	1.50	1.14	BDL	BDL	0.01	0.0095
	Spring 2020	7.59	9.05	181.9	0.13	0.94	46.38	13.89	BDL	1.05	BDL	BDL	BDL	BDL
	Fall 2020	10.52	3.88	176.8	0.22	0.18	42.00	12.44	1.36	1.21	BDL	BDL	0.02	0.02
GWW-07	Spring 2019	7.10	4.85	194.2	BDL	1.68	8.76	3.27	2.49	0.68	BDL	BDL	BDL	BDL
	Fall 2019	6.63	5.20	184.30	0.11	1.22	8.98	3.12	2.54	0.49	BDL	BDL	BDL	BDL
	Spring 2020	6.93	7.95	171.0	0.10	0.94	8.89	3.33	0.86	0.34	BDL	BDL	BDL	BDL
	Fall 2020	12.00	4.13	166.8	0.16	3.75	9.20	3.36	2.39	0.79	BDL	BDL	0.01	0.01
GWW-10	Spring 2019	5.39	4.41	193.5	BDL	9.87	16.81	7.23	4.55	1.85	BDL	0.01	BDL	BDL
	Fall 2019	4.60	5.01	185.00	0.12	7.66	17.80	6.91	4.65	1.76	BDL	0.02	BDL	BDL
	Spring 2020	5.89	3.66	174.0	0.12	7.56	15.46	6.86	3.20	1.57	BDL	BDL	BDL	BDL
	Fall 2020	11.73	4.28	172.5	0.18	11.03	18.09	7.52	4.76	2.00	BDL	BDL	0.01	0.01

Site	*Season*	*Diss B*	*Total B*	*Diss Ba*	*Total Ba*	*Diss Cd*	*Total Cd*	*Diss Cu*	*Total Cu*	*Diss Fe*	*Total Fe*	*Diss Li*	*Total Li*	*Diss Mn*	*Total Mn*
AR-01	Fall 2019	BDL	BDL	0.07	0.06	BDL	BDL	BDL	BDL	0.03	BDL	BDL	BDL	0.04	BDL
	Spring 2020	BDL	BDL	0.03	0.04	0.00	0.00	BDL	BDL	0.06	0.32	0.01	0.01	0.02	0.04
	Summer 2020	BDL	BDL	0.07	0.09	0.00	0.00	BDL	BDL	0.04	0.46	0.00	BDL	0.03	0.13
	Fall 2020	BDL	BDL	0.08	0.08	0.00	0.00	0.02	0.01	0.07	0.16	0.01	0.00	0.02	0.03
AR-02	Fall 2019	BDL	BDL	0.05	0.06	BDL	BDL	BDL	BDL	0.06	0.21	0.01	0.01	0.05	0.05
	Spring 2020	0.01	0.01	0.03	0.04	0.00	0.00	BDL	BDL	0.08	0.42	0.01	BDL	0.02	0.06
	Summer 2020	BDL	BDL	0.05	0.05	0.00	0.00	BDL	BDL	0.09	0.24	BDL	0.01	0.04	0.06
	Fall 2020	BDL	BDL	0.05	0.06	0.00	0.00	0.01	0.01	0.05	0.24	0.01	0.01	0.05	0.07
AR-03	Spring 2020	BDL	BDL	0.03	0.04	0.00	0.00	BDL	BDL	0.08	0.43	0.00	0.01	0.03	0.07
	Summer 2020	0.00	0.00	0.04	0.04	0.00	0.00	BDL	BDL	0.11	0.24	0.00	0.00	0.03	0.04
	Fall 2020	BDL	BDL	0.05	0.05	0.00	0.00	0.00	0.00	0.08	0.23	0.01	0.01	0.04	0.05
GWW-01	Spring 2019	BDL	BDL	0.00	0.00	BDL	BDL	BDL	BDL	0.01	0.14	BDL	BDL	BDL	BDL
	Fall 2019	BDL	BDL	0.18	0.17	BDL	BDL	BDL	BDL	BDL	0.14	0.01	BDL	BDL	BDL
	Spring 2020	0.00	0.00	0.21	0.21	BDL	BDL	BDL	BDL	0.01	0.01	0.01	0.01	BDL	BDL
	Fall 2020	BDL	BDL	0.22	0.22	0.00	0.00	0.00	0.01	0.01	0.01	0.00	0.00	BDL	BDL
GWW-03	Spring 2019	BDL	BDL	0.00	0.00	BDL	BDL	0.00	0.00	BDL	0.04	BDL	BDL	BDL	BDL
	Fall 2019	0.03	0.03	0.21	0.21	BDL	BDL	0.01	0.01	0.00	0.04	BDL	BDL	0.00	0.01
	Spring 2020	BDL	BDL	0.22	0.22	0.00	0.00	BDL	BDL	0.00	0.00	0.01	0.01	0.00	0.00
	Fall 2020	0.02	0.02	0.18	0.18	BDL	BDL	0.03	0.03	0.02	0.02	BDL	BDL	0.00	0.00
GWW-04	Spring 2019	BDL	BDL	BDL	BDL	BDL	BDL	BDL	BDL	BDL	BDL	BDL	BDL	BDL	BDL
	Fall 2019	BDL	BDL	0.03	0.03	BDL	BDL	BDL	BDL	BDL	BDL	BDL	BDL	0.00	0.00
	Spring 2020	BDL	BDL	0.03	0.03	0.00	0.00	0.01	0.01	0.01	0.01	0.01	0.01	0.00	0.00
GWW-06	Spring 2019	BDL	BDL	0.00	0.00	BDL	BDL	BDL	BDL	0.01	0.22	BDL	BDL	BDL	BDL
	Fall 2019	BDL	BDL	0.06	0.06	BDL	BDL	BDL	BDL	0.00	0.19	BDL	BDL	0.00	0.00
	Spring 2020	BDL	BDL	0.07	0.07	BDL	BDL	BDL	BDL	0.01	0.01	0.01	0.01	0.00	0.00
	Fall 2020	0.01	0.00	0.06	0.06	BDL	BDL	0.01	0.01	0.02	0.02	BDL	BDL	0.00	0.00
GWW-07	Spring 2019	BDL	BDL	0.00	0.00	BDL	BDL	BDL	BDL	BDL	0.12	BDL	BDL	BDL	BDL
	Fall 2019	BDL	BDL	0.02	0.02	BDL	BDL	BDL	BDL	BDL	0.01	BDL	BDL	BDL	BDL
	Spring 2020	0.01	0.01	0.02	0.02	BDL	BDL	0.02	0.02	0.00	0.00	0.01	0.01	0.00	0.00
	Fall 2020	0.00	0.00	0.01	0.01	0.00	0.00	0.06	0.06	0.01	0.01	0.01	0.01	0.00	0.00
GWW-10	Spring 2019	BDL	BDL	0.00	BDL	BDL	BDL	BDL	BDL	0.01	0.27	BDL	BDL	BDL	BDL
	Fall 2019	BDL	BDL	0.01	0.01	BDL	BDL	BDL	BDL	0.01	0.40	BDL	BDL	0.01	0.01
	Spring 2020	0.02	0.02	0.01	0.01	BDL	BDL	BDL	BDL	0.00	0.00	0.01	0.01	0.01	0.01
	Fall 2020	0.01	0.01	0.01	0.01	BDL	BDL	BDL	BDL	0.09	0.09	BDL	BDL	0.00	0.00

Site	*Season*	*Diss Mo*	*Total Mo*	*Diss Ni*	*Total Ni*	*Diss P*	*Total P*	*Diss Pb*	*Total Pb*	*Diss S*	*Total S*	*Diss Se*	*Total Se*	*Diss Si*	*Total Si*
AR-01	Fall 2019	BDL	0.02	BDL	BDL	BDL	BDL	BDL	BDL	11.98	11.53	BDL	BDL	4.64	4.87
	Spring 2020	0.00	0.00	0.00	0.00	0.02	0.06	BDL	BDL	4.07	4.18	0.02	0.03	2.31	2.53
	Summer 2020	0.00	0.00	BDL	0.00	0.03	0.07	BDL	0.02	17.70	17.58	0.02	BDL	2.79	3.00
	Fall 2020	0.01	0.00	0.01	0.01	0.02	0.02	BDL	BDL	16.10	16.00	0.01	0.01	2.75	2.65
AR-02	Fall 2019	BDL	BDL	BDL	BDL	0.01	BDL	BDL	BDL	17.33	17.57	BDL	BDL	3.95	4.06
	Spring 2020	0.01	0.00	0.00	0.00	0.05	0.06	BDL	0.01	6.86	6.77	0.03	0.02	2.83	3.01
	Summer 2020	BDL	0.00	BDL	BDL	0.04	0.03	BDL	BDL	19.20	19.20	BDL	0.01	3.30	3.27
	Fall 2020	0.00	0.00	0.01	0.01	0.03	0.02	BDL	BDL	20.50	21.10	0.0188	0.02	3.36	3.57
AR-03	Spring 2020	0.00	0.00	0.00	0.00	0.04	0.05	BDL	BDL	6.05	6.01	0.03	0.02	2.62	2.80
	Summer 2020	0.00	0.00	BDL	BDL	0.06	0.03	BDL	BDL	18.55	19.35	0.01	BDL	3.31	3.35
	Fall 2020	0.00	0.00	0.01	0.00	0.04	0.05	BDL	BDL	23.10	23.80	0.01	0.02	3.52	3.66
GWW-01	Spring 2019	BDL	BDL	BDL	BDL	0.04	0.03	BDL	BDL	26.97	27.36	BDL	BDL	4.32	4.52
	Fall 2019	BDL	BDL	BDL	BDL	BDL	BDL	BDL	BDL	29.39	28.56	BDL	BDL	4.93	4.76
	Spring 2020	0.00	0.0	BDL	BDL	0.03	0.03	BDL	BDL	33.61	33.61	BDL	BDL	4.62	4.62
	Fall 2020	0.00	0.00	0.01	0.01	0.02	0.03	BDL	BDL	32.50	32.50	0.02	0.02	4.19	4.19
GWW-03	Spring 2019	BDL	BDL	BDL	BDL	BDL	BDL	BDL	BDL	16.44	16.87	BDL	BDL	4.40	4.75
	Fall 2019	BDL	BDL	BDL	BDL	BDL	BDL	BDL	BDL	17.50	17.88	BDL	BDL	4.90	4.76
	Spring 2020	0.00	0.00	0.00	0.00	0.09	0.09	BDL	BDL	27.26	27.26	0.02	0.02	5.01	5.01
	Fall 2020	0.00	0.00	0.00	0.00	0.08	0.08	BDL	BDL	17.17	17.17	0.01	0.01	4.61	4.61
GWW-04	Spring 2019	BDL	BDL	BDL	BDL	0.08	0.10	BDL	BDL	5.32	5.62	BDL	BDL	11.03	11.84
	Fall 2019	BDL	BDL	BDL	BDL	0.10	0.08	BDL	BDL	5.50	5.43	BDL	BDL	11.64	11.52
	Spring 2020	BDL	BDL	BDL	BDL	0.10	0.10	BDL	BDL	5.94	5.94	BDL	BDL	12.00	12.00
GWW-06	Spring 2019	BDL	BDL	BDL	BDL	BDL	BDL	BDL	BDL	11.99	11.84	BDL	BDL	3.20	3.33
	Fall 2019	BDL	BDL	BDL	BDL	BDL	BDL	BDL	BDL	11.63	11.71	BDL	BDL	3.30	3.23
	Spring 2020	0.00	0.00	BDL	BDL	0.03	0.03	BDL	BDL	14.73	14.73	BDL	BDL	3.35	3.35
	Fall 2020	0.00	0.00	0.00	0.00	0.02	0.02	BDL	BDL	10.60	10.60	0.01	0.01	3.02	3.02
GWW-07	Spring 2019	BDL	BDL	BDL	BDL	BDL	BDL	BDL	BDL	1.83	1.88	BDL	BDL	5.34	5.67
	Fall 2019	BDL	BDL	BDL	BDL	0.02	0.01	BDL	BDL	1.86	1.87	BDL	BDL	6.07	5.69
	Spring 2020	BDL	BDL	BDL	BDL	0.04	0.04	BDL	BDL	1.35	1.35	BDL	BDL	5.83	5.83
	Fall 2020	BDL	BDL	0.00	0.00	0.04	0.04	BDL	BDL	2.26	2.26	BDL	BDL	5.39	5.39
GWW-10	Spring 2019	BDL	BDL	BDL	BDL	BDL	BDL	BDL	BDL	4.06	4.14	BDL	BDL	5.30	5.48
	Fall 2019	BDL	BDL	BDL	BDL	0.02	0.02	BDL	BDL	4.68	4.57	BDL	BDL	5.40	5.66
	Spring 2020	0.00	0.00	BDL	BDL	0.04	0.04	BDL	BDL	3.71	3.71	BDL	BDL	5.46	5.46
	Fall 2020	0.00	0.00	0.00	0.00	0.05	0.05	BDL	BDL	4.47	4.47	BDL	BDL	6.11	6.11

Site	*Season*	*Diss Sr*	*Total Sr*	*Diss Ti*	*Total Ti*	*Diss Tl*	*Total Tl*	*Diss V*	*Total V*	*Diss Zn*	*Total Zn*
AR-01	Fall 2019	0.07	0.07	BDL	BDL	BDL	BDL	BDL	BDL	0.01	0.01
	Spring 2020	0.06	0.06	BDL	0.00	0.02	0.02	BDL	BDL	0.06	0.07
	Summer 2020	0.09	0.09	BDL	BDL	BDL	BDL	BDL	BDL	0.02	0.15
	Fall 2020	0.08	0.08	BDL	BDL	BDL	BDL	BDL	BDL	BDL	BDL
AR-02	Fall 2019	0.09	0.09	BDL	BDL	BDL	BDL	BDL	BDL	0.04	0.05
	Spring 2020	0.08	0.07	BDL	0.00	0.014	0.02	BDL	BDL	0.06	0.10
	Summer 2020	0.10	0.10	BDL	0.00	BDL	0.01	BDL	BDL	0.02	0.04
	Fall 2020	0.10	0.10	BDL	0.00	BDL	BDL	BDL	BDL	BDL	BDL
AR-03	Spring 2020	0.07	0.07	BDL	0.00	0.017	0.02	BDL	BDL	0.07	0.10
	Summer 2020	0.09	0.09	BDL	BDL	BDL	BDL	BDL	BDL	0.03	0.04
	Fall 2020	0.09	0.10	BDL	BDL	BDL	BDL	BDL	BDL	BDL	BDL
GWW-01	Spring 2019	0.00	0.00	BDL	BDL	BDL	BDL	BDL	BDL	BDL	BDL
	Fall 2019	0.11	0.11	BDL	BDL	BDL	BDL	BDL	BDL	0.01	0.02
	Spring 2020	0.10	0.10	BDL	BDL	BDL	BDL	BDL	BDL	0.00	0.00
	Fall 2020	0.11	0.11	BDL	BDL	BDL	BDL	BDL	BDL	BDL	BDL
GWW-03	Spring 2019	BDL	BDL	BDL	BDL	BDL	BDL	BDL	BDL	BDL	BDL
	Fall 2019	0.13	0.13	BDL	BDL	BDL	BDL	BDL	BDL	0.01	0.01
	Spring 2020	0.21	0.21	BDL	BDL	BDL	BDL	BDL	BDL	BDL	BDL
	Fall 2020	0.12	0.12	BDL	BDL	BDL	BDL	BDL	BDL	BDL	BDL
GWW-04	Spring 2019	BDL	BDL	BDL	BDL	BDL	BDL	BDL	BDL	BDL	BDL
	Fall 2019	0.02	0.02	BDL	BDL	BDL	BDL	BDL	BDL	0.02	0.02
	Spring 2020	0.03	0.03	BDL	BDL	BDL	BDL	BDL	BDL	0.02	0.02
GWW-06	Spring 2019	0.00	0.00	BDL	BDL	BDL	BDL	BDL	BDL	BDL	BDL
	Fall 2019	0.09	0.07	BDL	BDL	BDL	BDL	BDL	BDL	0.01	0.01
	Spring 2020	0.08	0.08	BDL	BDL	0.01	0.01	BDL	BDL	0.00	0.00
	Fall 2020	0.09	0.09	BDL	BDL	BDL	BDL	BDL	BDL	BDL	BDL
GWW-07	Spring 2019	0.00	0.00	BDL	BDL	BDL	BDL	BDL	BDL	BDL	BDL
	Fall 2019	0.08	0.07	BDL	BDL	BDL	BDL	BDL	BDL	0.00	BDL
	Spring 2020	0.08	0.08	BDL	BDL	BDL	BDL	BDL	BDL	0.00	0.00
	Fall 2020	0.09	0.09	BDL	BDL	BDL	BDL	BDL	BDL	0.00	0.00
GWW-10	Spring 2019	0.00	BDL	BDL	BDL	BDL	BDL	BDL	BDL	BDL	BDL
	Fall 2019	0.08	0.08	BDL	0.00	BDL	BDL	BDL	BDL	0.01	0.00
	Spring 2020	0.07	0.07	BDL	BDL	BDL	BDL	BDL	BDL	0.00	0.00
	Fall 2020	0.09	0.09	BDL	BDL	BDL	BDL	BDL	BDL	0.00	0.00

Major Cation and Trace Metal Analysis:

Major cations and trace metals were analyzed at Colorado School of Mines Atomic Spectroscopy Laboratory (Golden, CO) by Inductively Coupled Plasma Optical Emission Spectroscopy (ICP-OES). A laboratory blank is analyzed at the beginning and end of each analytical run (~30 samples) and is acceptable if the readings are below the detection limit. A standard reference material (SRM 1643f) is used and acceptable if readings are within ±10% of known concentration. Calibration checks with known concentrations are analyzed by continuing the calibration verification (CCV) solution after every 10th primary sample, which remains acceptable if readings are within ±20% of known concentration. Lastly, an internal standard is continuously analyzed for every sample, including calibration standards, throughout the entire run; scandium is used with a target concentration and accuracy of 1 mg/L ±0.2 mg/L. The internal standard is used to monitor potential analytical drift or issues with the system.

Table B2. Isolated Fulvic Acid (DOC-03) concentrations in mg/L.

Site	*Season*	*DOC-03*	*Site*	*Season*	*DOC-03*	*Site*	*Season*	*DOC-03*
AR-01	Fall 2019	3.50	GWW-01	Spring 2019	1.57	GWW-06	Spring 2019	2.85
	Spring 2020	2.44		Fall 2019	7.70		Fall 2019	2.70
	Summer 2020	6.16		Spring 2020	1.82		Spring 2020	4.24
	Fall 2020	7.41		Fall 2020	4.52		Fall 2020	17.57
AR-02	Fall 2019	2.28	GWW-03	Spring 2019	2.21	GWW-07	Spring 2019	1.79
	Spring 2020	4.70		Fall 2019	1.30		Fall 2019	2.50
	Summer 2020	10.48		Spring 2020	2.63		Spring 2020	6.01
	Fall 2020	3.46		Fall 2020	6.36		Fall 2020	9.82
AR-03	Spring 2020	8.12	GWW-04	Spring 2019	2.22	GWW-10	Spring 2019	2.67
	Summer 2020	10.80		Fall 2019	1.80		Fall 2019	3.20
				Spring 2020	4.94		Spring 2020	2.56
	Fall 2020	4.83					Fall 2020	7.04

APPENDIX C

FULVIC ACID ISOLATION STANDARD OPERATING PROCEDURE (SOP) AND OPTICAL SPECTROSCOPY RESULTS

SOP FOR ISOLATION OF FULVIC ACID (FA)

Modified from E. M. Thurman and Malcolm (1981)

Materials and Regents

For all samples:

- 0.9cm i.d. glass columns for 1L sample H^+ saturated and clean XAD-8 (or DAX-8) resin.
- 0.9cm i.d. glass columns with H^+ saturated CEC resin (stored in 1M HCl between samples).
- Peristaltic pump with a variable speed capability of 1ml/minute to 100ml/minute
- Pre-combusted/pre-cleaned 100mL glass amber jars for DOC-03 fraction (one for each sample).
- 1L 0.1N NaOH
- 1L 0.1N HCl
- 1L 1.0M HCl
- DI water
- Calibrated pH meter
- Magnetic stir plate with Teflon coated stir bars
- Clean 100mL glass Erlenmeyer flask to catch the 0.1N NaOH back-eluent.
- 200mL glass (plastic will work if previously soaked in 1M HCl) beakers with approximately 100 cm^3 (approximately 100mL) cation exchange resin. Pre-clean with DI water and 0.1N NaOH.

In addition, for 50 L samples:

- 5cm i.d. glass columns with H^+ saturated and clean XAD-8 (or DAX-8) resin.
- Pre-combusted/pre-cleaned 1L glass amber jars for DOC-03 fraction (one for each sample).

Procedure for the hydrophobic fraction of DOM (fulvic and humic acids)

1. Acidify 1L sample, if necessary, with phosphoric acid (H_3PO_4) or hydrochloric acid (HCl). Check with pH paper to ensure that the pH is <2.0.
2. If necessary, assemble the columns and tubing. Add enough resin until you reach approximately 1-inch (0.9cm columns) from the top. Run DI water through your setup to check for leaks before proceeding to the next step.
3. Rinse the columns by alternating 0.1N NaOH for five minutes with 0.1N HCl for the same amount of time. Perform this flush a minimum of three times to ensure that the columns are cleaned out. Run DI water for the same amount of time, then finish with 0.1N HCl. Be sure all the flow valves on the columns are closed to avoid loss of pressure.
4. Collect a DOC-01 sample in one of the 30mL or 60mL sample bottles from each sample.
5. Wipe the pump tube with DI and place the tube into the DOM sample. Cover the top with Parafilm to prevent contamination.
6. Use a 1L Erlenmeyer flask to catch the effluent. Cover with Parafilm.
7. Set the pump rate for the appropriate column:
    a. 0.9cm = 4mL/min (for 1L DOC-01 sample). Approximately 4-hour isolation time.
    b. 5cm = 100mL/min (for 50L DOC-01 sample). Approximately 5-6 hours isolation time.
8. Start the pump and open the flow valve on the columns. You made need to make some adjustments to ensure that the DAX-8 resin is completely submerged in the sample during the duration of the isolation process.
9. There is no need to babysit the samples, but it is suggested to check on them every 15-20 minutes to ensure that there are no leaks and the sample tube in the DOM fraction is still submerged.

10. Once the DOM samples have completely been run through the columns, close the flow valves and stop the pump.
11. Run DI water through the columns for approximately 10 minutes to flush out any residual ions.
12. Rearrange the columns to back-eluent the now sorbed fulvic acid on the XAD-8 resin with 0.1N NaOH.
13. Run 0.1N NaOH through the bottom tube to completely fill before attaching to the column.
    a. Set the pump rate at 2mL/min. Approximately 50-minute flush time.
14. Set the pump rate for the appropriate column:
    a. 0.9cm = 3mL/min (for 1L DOC-01 sample). Approximately 30-minute flush time.
    b. 5cm = 20mL/min (for 10L DOC-01 sample). Approximately 50-minute flush time.
14. Temporarily place the exit tubes into a 1 L waste beaker. You may need parafilm to make them stay in the beaker.
15. Start the pump and open the flow valve allowing 0.1NaOH to move upward through the columns.
16. Keep an eye on the effluent tubing and place into a clean 100mL flask (for 1L) and 1000mL flask (for 50L) once you see the color change to a light to dark brown (this is the fulvic acid!). If there is no or minimal coloration at the top of the resin on the column, you will need to use pH paper to verify when the 0.1 NaOH with fulvic acid starts to leave the effluent tube.
17. It takes about 50 minutes to collect your volume.

For 50L samples only:

18. Add 10mL 85% H3PO4 into your 1L back-eluent and test with pH paper to ensure pH is approximately 2.0. You will save this sample and run it through the columns (0.9cm i.d.) again to concentrate it.

For 1L samples only:

19. During the back-eluent step, prepare the CEC resin (amber colored). Pre-clean the resin by rinsing with DI water three times, then adding approximately 1 mL 5N NaOH and fill to the 200mL level with DI water. Use a magnetic stir bar and agitate for 5 minutes. Dispose of the NaOH solution (very dilute). Rinse at least three times with DI (fill to 200mL level each time). Add 100mL of 1M HCl and agitate (with magnetic stir bar) for 5 minutes. Seal with Parafilm and set aside.
20. Once the back-eluent step is complete (you should have approximately 100ml FA isolate), stop the pump.
21. Prepare the CEC resin by pouring 1M HCl into a separate clean beaker. Pour out as much as possible, then add DI until the 200mL line is reached. Immediately decant the DI water. This step is important to remove as much excess chloride (from HCl) as possible and not release H+ from the resin.
22. Add your FA isolate in the beaker with CEC resin. Be sure and keep the magnetic stir bar in the slurry.
23. Place your sample in the CEC onto the magnetic plate. Place the calibrated pH probe into the mixture. You should have a starting pH in the range of 12-13. Keep the pH probe in the mixture and start the magnetic stir bar. Stop the magnetic stir bar once you reach a pH in the range of 3.0 – 3.5.
24. Add the now H^+ saturated DOC-03 sample into a precleaned/combusted 100mL amber jar.
25. Place your FA isolate into the refrigerator.
26. Reassemble the columns to their original orientation and rinse as described in step 2 above. Always run 0.1N HCl last for storage.
27. Neutralize any acidic waste with baking soda and dispose of it properly.
28. You will now run the 1L sample collected from the 50L by going through the entire process again.

Figure C1. Set-up for an in-line approach for H^+ saturated FA isolates for 50 L in 5cm column.

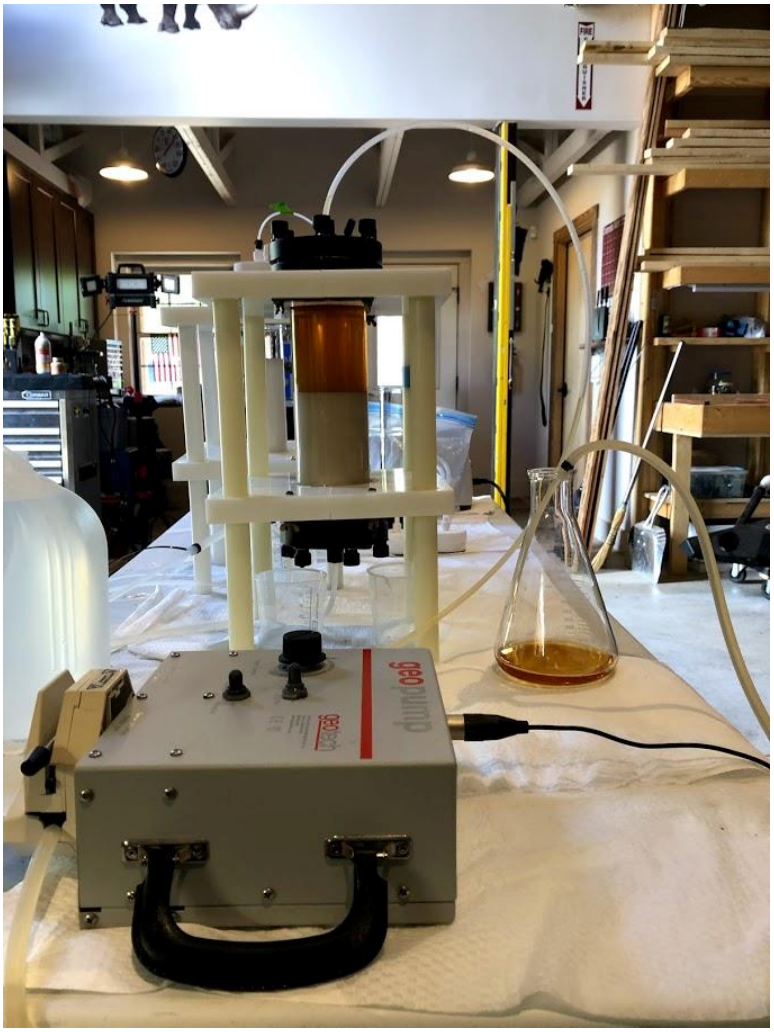

Figure C2. Example of sorbed hydrophobic acid (DOC-03) in 5cm column.

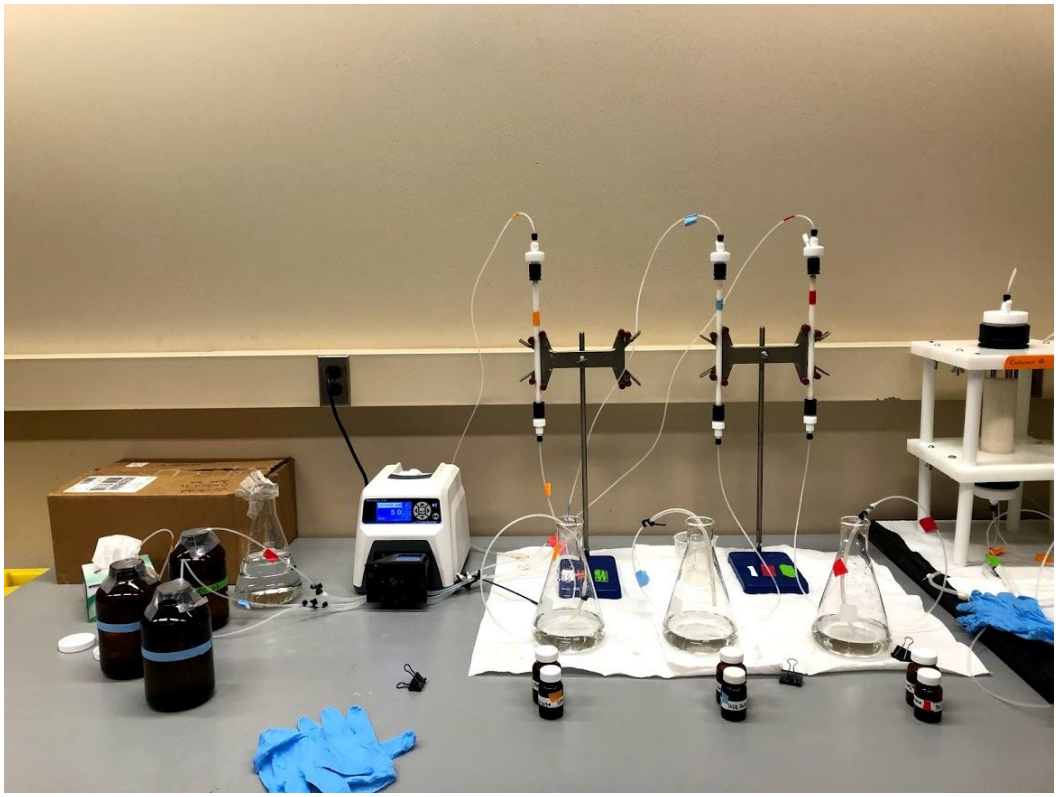

Figure C3. Set-up for an in-line approach for H+ saturated FA isolates for 1 L samples in 0.9cm columns.

EXCITATION-EMISSION MATRICES (EEMs) DATA REDUCTION ON AQUALOG

Part I. EEM data reduction in Aqualog Software

The following steps describe how to process (Rayleigh masking and inner filter effect) EEM results to be exported into a spectroscopy template to calculate spectroscopic indices:

1) Select the "Sample-Blank Waterfall Plot" tab.
2) Click on the "Rayleigh Masking" button. It is located two buttons to the left of the H_2O button used for EEM and Absorbance analysis.
3) Check the 1st and 2nd order masking boxes and hit Ok.
4) Once the masking operation is completed, click on the "Inner Filter Effect (IFE)" button located between H_2O and Rayleigh buttons.

Part 2: EEM data export

The following steps describe how to export the processed EEM results (above) to be added into the spectroscopy template:

1) Select the "Processed Data: RM_IFE" tab for your sample. The RM and IFE indicate that this EEM data has undergone Rayleigh Masking and Inner Filter Effect corrections.
2) Select the "File" pulldown menu, then "Export," then "ASCII." A window will pop up to prompt where to save and what file type.
3) Select as file type: .csv
4) Name your file as sample ID plus DOC fraction and save it in the appropriate project folder.

5) When the “Import and Export: expASC” window pops up, select Ok.
6) Double-check the project folder to ensure that all your exported data files have been successfully saved in that location.

Part 3: Absorbance data export

The following steps describe how to export the blank subtracted absorbance data:

1) Locate the blank subtracted absorbance data. The data column headings should look like the following (Excel version, but it looks exactly like this in the Aqualog software):
2) Export as a .csv file into the “Absorbance Data” folder for the respective DOC fraction (DOC-01 or DOC-03).
3) The data to use for the spectroscopy template is under the “Abs” column (Column J) header. Copy the column of data and paste it as values in the spreadsheet. Be sure the wavelength range of values (Column A) matches the template.

Part 4: Enter Data into Spectroscopy Template:

1) Add DOC concentration from TOC analysis in the “TOC and Absorbance” tab at the top.
2) Paste the absorbance data you converted and copied from the Aqualog into a blank column labeled “Abs” on the “TOC and Absorbance” tab.
3) An “Abs Spectra” graph will plot. Insert the spectral slopes ($S_{275\text{-}295}$, $S_{290\text{-}350}$, and $S_{250\text{-}400}$) into the “spectroscopy tab.”
4) Paste the EEMs Data into the “Raw EEM” tab.
5) Once everything has been transferred, the spectroscopic indices will be calculated through the template.

Table C1. Spectroscopic Indices for bulk DOM (DOC-01).

Site	*Season*	a_{254}	SAC_{340}	SAC_{350}	$S_{275-295}$	$S_{290-350}$	$S_{350-400}$	S_R ($S_{275-295}$/ $S_{350-400}$)	*BIX*
AR-01	Fall 2019	8.70	15.10	12.70	0.02	0.015	0.02	0.80	0.64
	Spring 2020	37.90	31.60	27.30	0.01	0.014	0.02	0.81	0.53
	Summer 2020	6.75	18.85	16.13	0.02	0.015	0.02	0.89	0.62
	Fall 2020	7.47	30.78	27.19	0.01	0.013	0.01	1.17	0.68
AR-02	Fall 2019	7.70	10.40	8.70	0.02	0.02	0.03	0.72	0.68
	Spring 2020	35.00	30.20	26.00	0.01	0.01	0.02	0.81	0.54
	Summer 2020	11.81	18.93	16.18	0.02	0.02	0.02	0.84	0.65
	Fall 2020	8.49	21.49	18.53	0.02	0.02	0.02	0.89	0.68
AR-03	Spring 2020	39.80	34.40	29.90	0.01	0.01	0.02	0.87	0.54
	Summer 2020	11.99	24.81	21.38	0.01	0.01	0.02	0.74	0.65
	Fall 2020	10.25	35.41	31.24	0.01	0.01	0.01	1.00	0.65
GWW-01	Spring 2019	0.53	0.18	0.17	0.03	0.02	0.03	0.81	0.74
	Fall 2019	0.90	0.30	-0.30	0.05	---	---	---	0.66
	Spring 2020	-0.36	-5.34	-3.36	---	---	---	---	1.01
	Fall 2020	1.11	39.13	33.82	0.02	0.02	0.08	0.29	0.95
GWW-03	Spring 2019	2.05	2.68	2.53	0.00	0.02	0.00	0.50	0.95
	Fall 2019	1.28	3.22	2.24	0.002	0.04	---	---	1.02
	Spring 2020	-0.50	-16.40	-15.50	---	---	---	---	1.41
	Fall 2020	1.90	18.27	16.18	0.01	0.02	0.02	0.30	1.22
GWW-04	Spring 2019	1.80	3.51	3.35	0.02	0.01	0.00	4.50	0.63
	Fall 2019	0.60	-0.50	-1.1	0.04	---	---	---	0.82
	Spring 2020	-0.10	-1.50	-0.40	---	---	---	---	0.92
GWW-06	Spring 2019	1.39	1.65	1.58	0.01	0.01	0.01	1.63	0.86
	Fall 2019	0.8	-2.70	-3.3	0.08	---	---	---	0.80
	Spring 2020	-0.65	-15.78	-14.32	---	---	---	---	1.00
	Fall 2020	0.98	8.18	6.37	0.0	0.02	---	---	0.91
GWW-07	Spring 2019	0.79	0.79	0.74	0.02	0.02	0.01	2.22	0.81
	Fall 2019	1.30	-2.70	-2.9	---	---	---	---	0.48
	Spring 2020	-0.80	-14.80	-12.70	---	---	---	---	1.96
	Fall 2020	0.90	37.48	31.32	0.02	0.03	---	---	1.25
GWW-10	Spring 2019	2.04	0.92	0.81	0.02	0.02	0.01	1.80	0.84
	Fall 2019	3.00	1.60	1.00	0.03	0.04	---	---	1.16
	Spring 2020	0.40	1.90	2.20	0.01	0.03	---	---	0.98
	Fall 2020	2.02	11.23	9.08	0.02	0.03	0.06	0.25	1.19

Table C2. Spectroscopic Indices for isolated FA (DOC-03).

Site	*Season*	a_{254}	SAC_{340}	SAC_{350}	$S_{275-295}$	$S_{290-350}$	$S_{350-400}$	S_R ($S_{275-295}$/ $S_{350-400}$)	*BIX*
AR-01	Fall 2019	14.20	7.80	6.60	0.02	0.02	0.02	0.76	0.65
	Spring 2020	26.45	31.92	27.04	0.01	0.02	0.02	0.74	0.48
	Summer 2020	18.36	4.53	3.79	0.02	0.02	0.03	0.75	0.75
	Fall 2020	34.97	10.94	9.00	0.02	0.02	0.02	0.70	0.63
AR-02	Fall 2019	10.80	10.60	8.80	0.02	0.02	0.02	0.72	0.69
	Spring 2020	23.65	15.32	12.99	0.01	0.02	0.02	0.74	0.46
	Summer 2020	43.29	9.12	7.59	0.02	0.02	0.02	0.74	0.67
	Fall 2020	15.59	10.98	9.14	0.02	0.02	0.02	0.70	0.64
AR-03	Spring 2020	23.18	8.72	7.38	0.01	0.02	0.02	0.68	0.51
	Summer 2020	54.88	11.74	9.83	0.02	0.02	0.02	0.77	0.63
	Fall 2020	26.80	13.65	11.26	0.02	0.02	0.02	0.67	0.60
GWW-01	Spring 2019	0.01	3.70	3.00	0.02	0.02	0.02	0.96	0.82
	Fall 2019	25.60	1.90	1.90	0.02	0.02	0.02	1.25	0.97
	Spring 2020	2.30	2.10	1.70	0.02	0.02	0.03	0.56	0.70
	Fall 2020	5.69	2.81	2.50	0.02	0.01	0.01	1.50	0.82
GWW-03	Spring 2019	0.03	4.70	4.00	0.02	0.02	0.01	1.43	1.03
	Fall 2019	4.10	13.90	13.70	0.01	0.01	0.01	1.80	1.01
	Spring 2020	3.80	1.40	1.10	0.03	0.01	0.09	0.30	1.02
	Fall 2020	5.20	0.60	0.40	0.03	0.03	0.00	---	1.03
GWW-04	Spring 2019	0.02	4.20	3.80	0.02	0.01	0.01	2.30	0.71
	Fall 2019	4.10	3.20	2.60	0.02	0.02	0.02	0.91	1.01
	Spring 2020	6.50	0.90	0.80	0.03	0.02	0.02	1.10	0.80
GWW-06	Spring 2019	0.02	2.90	2.40	0.02	0.02	0.03	0.81	0.84
	Fall 2019	10.30	4.70	3.90	0.02	0.02	0.02	1.17	1.02
	Spring 2020	7.30	2.50	1.90	0.02	0.03	0.03	0.61	0.70
	Fall 2020	24.98	2.36	1.97	0.02	0.02	0.02	0.90	0.87
GWW-07	Spring 2019	0.01	2.10	1.70	0.03	0.02	0.024	1.29	0.72
	Fall 2019	10.30	2.70	2.20	0.03	0.02	0.16	0.17	0.99
	Spring 2020	8.90	1.90	1.50	0.02	0.02	0.034	0.70	0.84
	Fall 2020	6.00	0.40	0.30	0.03	0.02	0.000	---	0.87
GWW-10	Spring 2019	0.03	2.60	2.00	0.03	0.03	0.03	0.94	0.92
	Fall 2019	8.90	2.40	2.00	0.02	0.02	0.02	1.44	1.11
	Spring 2020	1.60	0.00	0.00	0.05	0.00	---	---	1.17
	Fall 2020	5.80	0.90	0.70	0.03	0.02	0.03	0.94	1.05

APPENDIX D

CU-DOC BINDING EXPERIMENT PROCEDURE AND ANALYTICAL RESULTS

Cu-FA BINDING EXPERIMENT SOP

Materials and Regents

- Cupric Ion-selective Electrode (Thermo Orion ionplus Sure-Flow Cupric Electrode, #9629BNWP)
- Calibrated pH meter (Orion 8107UWMMD)
- Conductivity probe for measuring temperature (Orion 013005MD)
- Pre-cleaned (acid washed) 100mL glass volumetric flasks (four)
- Pre-cleaned 1 L volumetric flasks
- 100 mL plastic beakers (ten)
- Dilute Ionic Strength Adjuster (ISA) (Orion ionplus #940011)- 20 mL ISA and 80 mL DI water
- 10^{-1} M Cu^{2+} standard solution (Orion #942906)
- 50 mL 20% trace metal grade HNO_3
- 50 mL 0.1 M NaOH
- 50 mL 1 M HNO_3
- DI water
- 960 mg of $NaHCO_3$
- 600 mg of $CaSO_4{*}2H_2O$
- 600 mg of $MgSO_4$
- 40 mg of KCl
- Clear Orion ionplus filling solution (Orion 900063)
- Parafilm
- Polishing strips (Thermo Scientific #948201)
- 10 L Plastic Carboy

Setting up the Cupric Ion-Selective Electrode

1) Rinse the chamber of the cupric electrode with clear Orion ionplus filling solution (Orion 900063) at least three times if the probe has not been used in a while. You can decant the solution by pressing it down on the top of the electrode. Fill up the chamber and leave the solution in it.
2) Each day before use of the electrode, polish the electrode. Pour DI water over the pink polishing paper and make sure the electrode is wet. Use the textured side of the paper to polish the probe by moving in a circular motion for about 30 seconds. Do not press hard or go back and forth, or you may scratch the electrode surface.
3) When you are finished with the electrode for the day, make sure it is submerged in a standard solution you have created for your experiments, in this case, MHW (procedure to create this solution listed below), brought to a pH six using 20% trace metal grade HNO_3 (will only need a few drops). Add parafilm over the solution and electrode to minimize evaporation of the solution)

Cupric ISE Calibration Solutions

1) Prepare Cu^{2+} standard aliquots with concentrations from 10^{-5} M to 10^{-8} M in the 100 mL glass volumetric flasks. Note: You will need to make 10^{-2} M to 10^{-4} M Cu in order to create the rest of the solutions.
    a. Add roughly 50 mL of DI water to the flask.

b. Add 1mL dilute ISA (20 mL of concentrated ISA w/80 mL of nanopure water)
c. Add three drops of trace metal grade HNO_3 to bring pH to ~4.0
d. Pipette necessary volume of cupric stock solution (C_i) as indicated in the serial dilution table below
e. Bring volume to 100mL with DI water
f. Add into pre-cleaned 100 mL PP beakers

2) A new batch of calibration standards is created for each solution set, including the known Cu^{2+} concentration, deionized, ultrapure water, dilute ionic strength adjuster, and trace metal grade HNO_3.

Table D1: Serial dilution for Cu^{2+} standards

C_f (ppb)	C_f (M)	C_i (M)	V_f (mL)	V_i (mL)
635,500	10^{-2} M	10^{-1} M	100 mL	10
63,550	10^{-3} M	10^{-2} M	100 mL	10
6,355	10^{-4} M	10^{-3} M	100 mL	10
635.5	10^{-5} M	10^{-4} M	100 mL	10
63.55	10^{-6} M	10^{-5} M	100 mL	10
6.355	10^{-7} M	10^{-6} M	100 mL	10
0.6355	10^{-8} M	10^{-7} M	100 mL	10

Synthetic Moderately Hard Water (MHW)

3) Place 8 L of DI water (ASTM Type II ultrapure water) in a properly cleaned plastic carboy.
4) Weigh out using mass balance and add 0.60 g of $MgSO_4$, 0.96 g $NaHCO_3$, and 0.040 g KCl into a 1L volumetric flask and agitate with a magnetic stir bar until the salts are completely dissolved. Transfer into the plastic carboy.
5) Add 0.60 g of $CaSO_4 \cdot 2H_2O$ 1 L of DI water in the 1L flask used in step 2. Agitate with a magnetic stirrer until the calcium sulfate is dissolved, add to the plastic carboy, and mix well.
6) The measured pH, hardness, and alkalinity are listed below. Measure pH using the probe in the lab and alkalinity using the Hach Alkalinity titration kit.

For Moderately Hard Water:

Reagent Added (mg/L)				**Final Water Quality**		
$NaHCO_3$	**$CaSO_4 \cdot 2H_2O$**	**$MgSO_4$**	**KCl**	**pH**	**Hardness**	**Alkalinity**
96.0	60.0	60.0	4.0	7.4-7.8	80-100	57-64

Preparing experimental solutions

1. Prepare Cu^{2+} with concentrations of 10^{-5} M to 10^{-8} M in the glass volumetric flasks (note: Do not add acid or ISA). Create 500 mL of MHW + 3 mg C/L for each site.
    a. To create 3 mg C/L, you must first determine the amount of stock solution necessary, your initial concentration (C_1), in order to determine the volume needed to create 500 mL. Example below:

$$\frac{C_1(\frac{100\ mg}{L})}{C_2(\frac{3mg}{L})} = \frac{V_1(500\ mL)}{V_2} = 15\ mL\ from\ stock\ solution$$

    b. Once you have determined the amount necessary, add this to the 500 mL glass beaker. Add enough MHW so that the final volume is 500 mL.

c. Mix this solution and measure the pH. Bring the pH to ~6 with either 0.1 M NaOH OR 1 M HNO_3 depending on the given pH. (NOTE: if using the nitric acid, you will likely only need a drop to half a drop, be careful!)
d. Now, create 100 mL of each of the four standard concentrations (10^{-5} through 10^{-8}). You should use the 100 mL glass beakers and add the necessary amount of Cu standard, then the solution you just created to the 100 mL mark. Note: you must first create 10^{-2}, 10^{-3}, and 10^{-4} before creating the rest. For the first three, just use the cupric standard and DI water.

Table D2: Serial dilution for Cu^{2+} experiment solutions.

C_f (ppb)	C_f (M)	C_i (M)	V_f (mL)	V_i (mL)
635,500	10^{-2} M	10^{-1} M	100 mL	10
63,550	10^{-3} M	10^{-2} M	100 mL	10
6,355	10^{-4} M	10^{-3} M	100 mL	10
635.5	10^{-5} M	10^{-4} M	100 mL	10
63.55	10^{-6} M	10^{-5} M	100 mL	10
6.355	10^{-7} M	10^{-5} M	100 mL	1
0.6355	10^{-8} M	10^{-5} M	100 mL	0.1

Measurements

1) The day BEFORE taking measurements:
   a. Make sure the probe is polished and rinsed with DI water before placing it in standards.
   b. Starting with the 10^{-8} Cu^{2+} experimental solution, Place Cu ISE into the standard. Cover this with parafilm and let the site overnight to stabilize. Let the other solutions, experimental and calibration solutions, sit in room temperature overnight.
2) Next day: In order to minimalize the potential of cross-contamination and signal carry-over, the lowest standard (10^{-8} M) is measured first. Turn on the meter, and when five mV readings are within 5% of each other over a few minutes, record potential (mV) five times. Continue with measurements working your way up in concentration.
3) When ISE is removed from the solution, place pH and conductivity probe into the solution and record pH and temperature (°C). Measure through the 10^{-5} M Cu^{2+} standard. A successful calibration is when the slope is -29.0±1.0 mV and an $R^2 = 0.99$ is achieved.
4) Between each aliquot, properly rinse the three instruments with DI water before placing them into the next standard and make sure as much of the DI water is removed without wiping down.
5) When you finish the first set, rinse the probe with DI water and let it sit in the 10^{-8} sample again. This may take a while to equilibrate as you just measured a sample with a higher concentration.
6) Measure each experimental set THREE times. When all the site measurements are finished, you can measure the calibration solutions.
7) Measure the calibration the same way by starting with the 10^{-8} M solution first and working your way up. You only need to measure this set once.
8) Once all measurements are taken, place ISE into MHW water adjusted to a pH 6 to sit overnight OR move on with the next set of measurements.

Quality control:

1) When you are finished with all measurements for an experimental set, you need to save certain samples to be measured for quality control. Save these samples:
   a. For experimental solutions (all four):

- TOC vial full of each of the four samples to measure DOC concentration.
- 15 mL plastic vials for AAS analysis to measure Cu concentration.
- Leftover: 60 mL plastic bottle for cation analysis.

b. For all four calibration solutions associated with each experimental set:
- 15 mL plastic vial for AAS analysis to measure Cu concentration.

2) A follow-up Cu analysis on an Atomic Absorbance Spectrometer (AAS) is completed to obtain exact Cu concentrations from the solutions.
   a. Create AAS Cu^{2+} standards
   b. Create 1000 mg/L of Cu standard from Cu-Cl_2 salts:

$$\frac{M.W.\ of\ CuCl_2 * 2H_2O}{M.W. of\ Cu^{2+}} = \frac{170.48\ g/mol}{63.546\ g/mol} = \mathbf{2.683\ g\ Cu}$$

   c. Add 2.683 g or 2683 mg of the salt to a 1 L volumetric flask and add DI water to the 1 L line. Mix to let the salt dissolve.
   d. Create concentrations of 0.01, 0.1, 1.0, and 10.0 mg/L using the equation:

$$\frac{M_1}{M_2} = \frac{V_2}{V_1}$$

$$\frac{1000\ mg/L}{10\ mg/L} = \frac{100\ mL}{V_1} = V_1\left(\frac{100mg}{L}\right) = 100\ mL = \mathbf{1.0\ mL}$$

3) Use manual located in the lab for SOP:
   a. First, measure the AAS standards created.
   b. Then, measure the ISE calibration standard you made with the sample solutions following. Rinse tube with DI water in between each sample.
4) All experimental solutions are analyzed for major cations (Ca, Mg, Na, K), anions (SO_4, Cl). The major cations are measured through an ICP-OES through the Center for Restoration of Ecosystems and Watersheds lab at OU. Anions can be calculated based on cation results.
   - The method used through the CREW Lab at OU is USEPA SW-846 Method 6010c. They use an internal standard that allows them to correct distortions in high concentration samples.

<u>Calculating {Cu^{2+}}</u>

Step 1: Plot copper concentration vs. absorbance to get a linear equation.
1. Copper concentration on y-axis (0, 0.01, 0.1, 1.0, 10 mg/L) and absorbance values on x-axis
2. Add trendline and set linear regression to run through zero, so y = mx.
3. R^2 should equal 0.99.

Step 2: Plot total Cu concentration (calculated in step 1) vs. mV readings.
1. Total Cu concentration is from the calibration solution on the y-axis.
2. mV readings from calibration solutions
3. Create an exponential curve and use the equation to calculate {Cu^{2+}}

Step 3: Use the mV readings from each of the three runs for all samples to calculate the free copper in solution.

Step 4: Plot the value of {Cu^{2+}} on the y-axis and total copper on the x-axis.

Table D3: Suwannee River Fulvic Acid (SRFA)-Cu binding experimental results.

Suwannee River Fulvic Acid (SRFA) binding experiment			
Initial Cu Conc. (mg/L)	0.0064	0.0635	0.6355
Measured Total Cu	0.1827	0.7509	6.7239
{Cu^{2+}}	0.0000	0.0001	0.0306
DOC Conc. (mg C/L)	2.966	-0.1967	-0.1967
pH	7.817	7.798	7.286
Temp. (℃)	20.0	20.0	20.0
Alk. (mg/L as $CaCO_3$)	70.0		
Ca^{2+}	14.36		
Mg^{2+}	10.38		
K^{+}	3.48		
Na^{+}	18.77		
Cl^{-}	3.15		
SO_4^{2-}	75.49		

Figure D1. Cu-ISE in between measurements.

Figure D2. Atomic Absorbance Spectrometer used to measure absorbance of Cu in the solution used to determine the amount of free Cu in solution.

REFERENCES

Al-Reasi, H. A., Smith, D. S., & Wood, C. M. (2012). Evaluating the ameliorative effect of natural dissolved organic matter (DOM) quality on copper toxicity to Daphnia magna: improving the BLM. *Ecotoxicology, 21*(2), 524-537.

Al-Reasi, H. A., Wood, C. M., & Smith, D. S. (2013). Characterization of freshwater natural dissolved organic matter (DOM): mechanistic explanations for protective effects against metal toxicity and direct effects on organisms. *Environment International, 59*, 201-207.

Baken, S., Degryse, F., Verheyen, L., Merckx, R., & Smolders, E. (2011). Metal complexation properties of freshwater dissolved organic matter are explained by its aromaticity and by anthropogenic ligands. *Environmental Science & Technology, 45*(7), 2584-2590.

Baker, M. A., Valett, H. M., & Dahm, C. N. (2000). Organic carbon supply and metabolism in a shallow groundwater ecosystem. *Ecology, 81*(11), 3133-3148.

Barkmann, P. E., Broes, L. D., Palkovic, M. J., Hopkins, J. C., Bird, K. S., Sebol, L. A., & Fitzgerald, F. S. (2020). ON-010 Colorado Groundwater Atlas. *Colorado Geological Survey, Golden, CO*(ON-010 Colorado Groundwater Atlas). Retrieved from https://coloradogeologicalsurvey.org/water/colorado-groundwater-atlas/

Bauer, M., & Blodau, C. (2006). Mobilization of arsenic by dissolved organic matter from iron oxides, soils and sediments. *Science of the Total Environment, 354*(2-3), 179-190.

Bernal, S., Lupon, A., Catalán, N., Castelar, S., & Martí, E. (2018). Decoupling of dissolved organic matter patterns between stream and riparian groundwater in a headwater forested catchment.

Boyer, E. W., Hornberger, G. M., Bencala, K. E., & McKnight, D. (1996). Overview of a simple model describing variation of dissolved organic carbon in an upland catchment. *Ecological Modelling, 86*(2-3), 183-188.

Boyer, E. W., Hornberger, G. M., Bencala, K. E., & McKnight, D. M. (1995). *Variation of dissolved organic carbon during snowmelt in soil and stream waters of two headwater catchments, Summit County, Colorado.* Paper presented at the Biogeochemistry of seasonally snow-covered catchments. Proc. symposium, Boulder, 1995.

Brooks, P., McKnight, D. M., & Bencala, K. E. (1999). The relationship between soil heterotrophic activity, soil dissolved organic carbon (DOC) leachate, and catchment-scale DOC export in headwater catchments. *Water Resources Research, 35*(6), 1895-1902.

Butler, B. A., Ranville, J. F., & Ross, P. E. (2008). Observed and modeled seasonal trends in dissolved and particulate Cu, Fe, Mn, and Zn in a mining-impacted stream. *Water Research, 42*(12), 3135-3145.

Cabaniss, S., & Shuman, M. (1988). Copper binding by dissolved organic matter: I. Suwannee River fulvic acid equilibria. *Geochimica et Cosmochimica Acta, 52*(1), 185-193.

Cappa, J., & Bartos, P. (2007). Geology and Mineral Resources of Lake County, Colorado. Colorado Geological Survey. *Resource Series, 42*, 59.

Carroll, R. W., Bearup, L. A., Brown, W., Dong, W., Bill, M., & Willlams, K. H. (2018). Factors controlling seasonal groundwater and solute flux from snow-dominated basins. *Hydrological Processes, 32*(14), 2187-2202.

Chen, W., Smith, D., & Guéguen, C. (2013). Influence of water chemistry and dissolved organic matter (DOM) molecular size on copper and mercury binding determined by multiresponse fluorescence quenching. *Chemosphere, 92*(4), 351-359.

Chowdhury, S. (2013). Trihalomethanes in drinking water: Effect of natural organic matter distribution. *Water Sa, 39*(1), 1-8.

Cory, R. M., Miller, M. P., McKnight, D. M., Guerard, J. J., & Miller, P. L. (2010). Effect of instrument-specific response on the analysis of fulvic acid fluorescence spectra. *Limnology and Oceanography: Methods, 8*(2), 67-78.

Craven, A. M., Aiken, G. R., & Ryan, J. N. (2012). Copper (II) binding by dissolved organic matter: importance of the copper-to-dissolved organic matter ratio and implications for the biotic ligand model. *Environmental Science & Technology, 46*(18), 9948-9955.

Dee, K. T. (2016). *Dissolved organic carbon (DOC) characteristics in metal-rich waters and implications for copper aquatic toxicity.* Colorado School of Mines,

Dhar, R., Zheng, Y., Stute, M., Van Geen, A., Cheng, Z., Shanewaz, M., . . . Ahmed, K. (2008). Temporal variability of groundwater chemistry in shallow and deep aquifers of Araihazar, Bangladesh. *Journal of contaminant hydrology, 99*(1-4), 97-111.

Dorsey, A., & Ingerman, L. (2004). Toxicological profile for copper.

Dwivedi, D., Steefel, C. I., Arora, B., Newcomer, M., Moulton, J. D., Dafflon, B., . . . Spycher, N. (2018). Geochemical exports to river from the intrameander hyporheic zone under transient hydrologic conditions: East River Mountainous Watershed, Colorado. *Water Resources Research, 54*(10), 8456-8477.

EPA-821-R-02-013. (2002). Short-term Methods for Estimating the Chronic Toxicity of Effluents and Receiving Waters to Freshwater Organisms.

Findley, W. G. (2003). *Aquatic ecosystems: interactivity of dissolved organic matter*: Academic Press.

Flerchinger, G., Cooley, K., & Ralston, D. (1992). Groundwater response to snowmelt in a mountainous watershed. *Journal of Hydrology, 133*(3-4), 293-311.

Geldon, A. L. (1989). *Hydrogeology of the Leadville limestone and other paleozoic rocks in northwestern Colorado, with results of aquifer tests at Glenwood Springs* (Vol. 87): Department of the Interior, US Geological Survey.

GmbH, H. C. H. L. (2014). Alkalinity, Digital Titrator, Oil and Gas (4000 mg/L).

Godsey, S. E., Kirchner, J. W., & Tague, C. L. (2014). Effects of changes in winter snowpacks on summer low flows: case studies in the Sierra Nevada, California, USA. *Hydrological Processes, 28*(19), 5048-5064.

Green, S. A., & Blough, N. V. (1994). Optical absorption and fluorescence properties of chromophoric dissolved organic matter in natural waters. *Limnology and Oceanography, 39*(8), 1903-1916.

Hansen, A. M., Fleck, J., Kraus, T. E., Downing, B. D., von Dessonneck, T., & Bergamaschi, B. (2018). *Procedures for using the Horiba Scientific Aqualog® fluorometer to measure absorbance and fluorescence from dissolved organic matter* (2331-1258). Retrieved from

Hansen, A. M., Kraus, T. E., Pellerin, B. A., Fleck, J. A., Downing, B. D., & Bergamaschi, B. A. (2016). Optical properties of dissolved organic matter (DOM): Effects of biological and photolytic degradation. *Limnology and Oceanography, 61*(3), 1015-1032.

Hauer, F. R., Baron, J. S., Campbell, D. H., Fausch, K. D., Hostetler, S. W., Leavesley, G. H., . . . Stanford, J. A. (1997). Assessment of climate change and freshwater ecosystems of the Rocky Mountains, USA and Canada. *Hydrological Processes, 11*(8), 903-924.

Helms, J. R., Stubbins, A., Ritchie, J. D., Minor, E. C., Kieber, D. J., & Mopper, K. (2008). Absorption spectral slopes and slope ratios as indicators of molecular weight, source, and photobleaching of chromophoric dissolved organic matter. *Limnology and Oceanography, 53*(3), 955-969.

Hornberger, G., Bencala, K., & McKnight, D. (1994). Hydrological controls on dissolved organic carbon during snowmelt in the Snake River near Montezuma, Colorado. *Biogeochemistry, 25*(3), 147-165.

Hutson, S. S. (2004). *Estimated use of water in the United States in 2000*: Geological Survey (USGS).

Inamdar, S., Finger, N., Singh, S., Mitchell, M., Levia, D., Bais, H., . . . McHale, P. (2012). Dissolved organic matter (DOM) concentration and quality in a forested mid-Atlantic watershed, USA. *Biogeochemistry, 108*(1-3), 55-76.

Jasechko, S., Kirchner, J., Welker, J., & McDonnell, J. (2016). Substantial proportion of global streamflow less than three months old, Nat. Geosci., 9, 126–129. In.

Jenne, E. A. (1979). *Chemical modeling in aqueous systems*: ACS Publications.

Jiang, W., Cai, Q., Xu, W., Yang, M., Cai, Y., Dionysiou, D. D., & O'Shea, K. E. (2014). Cr (VI) adsorption and reduction by humic acid coated on magnetite. *Environmental Science & Technology, 48*(14), 8078-8085.

Kimball, B. A., Callender, E., & Axtmann, E. V. (1995). Effects of colloids on metal transport in a river receiving acid mine drainage, upper Arkansas River, Colorado, USA. *Applied Geochemistry, 10*(3), 285-306.

Kramer, K. J., Jak, R. G., Van Hattum, B., Hooftman, R. N., & Zwolsman, J. J. (2004). Copper toxicity in relation to surface water-dissolved organic matter: Biological effects to Daphnia magna. *Environmental Toxicology and Chemistry: An International Journal, 23*(12), 2971-2980.

Lee, L., & Helsel, D. (2005). Baseline models of trace elements in major aquifers of the United States. *Applied Geochemistry, 20*(8), 1560-1570.

Longnecker, K., & Kujawinski, E. B. (2011). Composition of dissolved organic matter in groundwater. *Geochimica et Cosmochimica Acta, 75*(10), 2752-2761.

Lu, Y., & Allen, H. E. (2002). Characterization of copper complexation with natural dissolved organic matter (DOM)—link to acidic moieties of DOM and competition by Ca and Mg. *Water Research, 36*(20), 5083-5101.

Lynch, L. M., Sutfin, N. A., Fegel, T. S., Boot, C. M., Covino, T. P., & Wallenstein, M. D. (2019). River channel connectivity shifts metabolite composition and dissolved organic matter chemistry. *Nature communications, 10*(1), 1-11.

Macoustra, G. K., Jolley, D. F., Stauber, J., Koppel, D. J., & Holland, A. (2020). Amelioration of copper toxicity to a tropical freshwater microalga: Effect of natural DOM source and season. *Environmental Pollution, 266*, 115141.

McKnight, D. M., & Bencala, K. E. (1990). The chemistry of iron, aluminum, and dissolved organic material in three acidic, metal-enriched, mountain streams, as controlled by watershed and in-stream processes. *Water Resources Research, 26*(12), 3087-3100.

McKnight, D. M., Bencala, K. E., Zellweger, G. W., Aiken, G. R., Feder, G. L., & Thorn, K. A. (1992). Sorption of dissolved organic carbon by hydrous aluminum and iron oxides occurring at the confluence of Deer Creek with the Snake River, Summit County, Colorado. *Environmental Science & Technology, 26*(7), 1388-1396.

McKnight, D. M., Boyer, E. W., Westerhoff, P. K., Doran, P. T., Kulbe, T., & Andersen, D. T. (2001). Spectrofluorometric characterization of dissolved organic matter for indication of precursor organic material and aromaticity. *Limnology and Oceanography, 46*(1), 38-48.

Minor, E. C., Swenson, M. M., Mattson, B. M., & Oyler, A. R. (2014). Structural characterization of dissolved organic matter: a review of current techniques for isolation and analysis. *Environmental science: processes & impacts, 16*(9), 2064-2079.

National Integrated Drought Information System, N. (2021). Conditions for Leadville, CO. *Retrieved from: https://www.drought.gov/location/80461*.

Ohno, T. (2002). Fluorescence inner-filtering correction for determining the humification index of dissolved organic matter. *Environmental Science & Technology, 36*(4), 742-746.

Pellerin, B. A., Saraceno, J. F., Shanley, J. B., Sebestyen, S. D., Aiken, G. R., Wollheim, W. M., & Bergamaschi, B. A. (2012). Taking the pulse of snowmelt: in situ sensors reveal seasonal, event and diurnal patterns of nitrate and dissolved organic matter variability in an upland forest stream. *Biogeochemistry, 108*(1-3), 183-198.

Perdue, E. M. (1998). Chemical composition, structure, and metal binding properties. In *Aquatic humic substances* (pp. 41-61): Springer.

Roline, R. A. (1988). The effects of heavy metals pollution of the upper Arkansas River on the distribution of aquatic macroinvertebrates. *Hydrobiologia, 160*(1), 3.

Saar, R. A., & Weber, J. H. (1982). Fulvic acid: modifier of metal-ion chemistry. *Environmental Science & Technology, 16*(9), 510A-517A.

Sares, A., Hauff, P. L., Peters, D. C., Coulter, D. W., Bird, D. A., Henderson III, F. B., & Prosh, E. C. (2004). *Characterizing sources of acid rock drainage and resulting water quality impacts using hyperspectral remote sensing—examples from the upper Arkansas River Basin, Colorado.* Paper presented at the Geospatial Conference.

Shen, Y., Chapelle, F. H., Strom, E. W., & Benner, R. (2015). Origins and bioavailability of dissolved organic matter in groundwater. *Biogeochemistry, 122*(1), 61-78.

Singh, S., Inamdar, S., Mitchell, M., & McHale, P. (2014). Seasonal pattern of dissolved organic matter (DOM) in watershed sources: influence of hydrologic flow paths and autumn leaf fall. *Biogeochemistry, 118*(1), 321-337.

Smith, K. S., Walton-Day, K., & Ranville, J. F. (2000). *Evaluating the effects of fluvial tailings deposits on water quality in the Upper Arkansas River Basin, Colorado: Observational scale considerations.* Paper presented at the Proceedings from the Fifth International Conference on Acid Rock Drainage (ICARD 2000), Denver, Colorado.

Smith, R., Moore, R., Weiler, M., & Jost, G. (2014). Spatial controls on groundwater response dynamics in a snowmelt-dominated montane catchment. *Hydrology and Earth System Sciences, 18*(5), 1835-1856.

Striegl, R. G., Aiken, G. R., Dornblaser, M. M., Raymond, P. A., & Wickland, K. P. (2005). A decrease in discharge-normalized DOC export by the Yukon River during summer through autumn. *Geophysical Research Letters, 32*(21).

Tchounwou, P. B., Yedjou, C. G., Patlolla, A. K., & Sutton, D. J. (2012). Heavy metal toxicity and the environment. In *Molecular, Clinical and Environmental Toxicology* (pp. 133-164): Springer.

Thorslund, J., Jarsjö, J., Wällstedt, T., Mörth, C. M., Lychagin, M. Y., & Chalov, S. R. (2017). Speciation and hydrological transport of metals in non-acidic river systems of the Lake Baikal basin: field data and model predictions. *Regional Environmental Change, 17*(7), 2007-2021.

Thurman, E. (1985). Aquatic humic substances. In *Organic geochemistry of natural waters* (pp. 273-361): Springer.

Thurman, E. M., & Malcolm, R. L. (1981). Preparative isolation of aquatic humic substances. *Environmental Science & Technology, 15*(4), 463-466.

Tiwari, T., Laudon, H., Beven, K., & Ågren, A. M. (2014). Downstream changes in DOC: Inferring contributions in the face of model uncertainties. *Water Resources Research, 50*(1), 514-525.

U.S. Climate Data, U. (2021). Leadville, Colorado *Retrieved from: https://www.usclimatedata.com/climate/leadville/colorado/united-states/usco0235*.

United States Department of Agriculture, U. (2021). Natural Resources Conservation Service, Colorado. *Retrieved from: https://www.nrcs.usda.gov/wps/portal/nrcs/detail/co/snow/products/?cid=nrcseprd1432263*.

United States Geological Survey, U. (2021). USGS 07081200 ARKANSAS RIVER NEAR LEADVILLE, CO. *Retrieved from: https://waterdata.usgs.gov/co/nwis/uv?site_no=07081200*.

Wallace, A. (1993). Geologic setting of the Leadville mining district. *Lake County, Colorado: US Geological Survey Open-File Report*, 93-343.

Walton-Day, K., & Poeter, E. (2009). Investigating hydraulic connections and the origin of water in a mine tunnel using stable isotopes and hydrographs. *Applied Geochemistry, 24*(12), 2266-2282.

Warren, L. A., & Zimmerman, A. P. (1994). The influence of temperature and NaCl on cadmium, copper and zinc partitioning among suspended particulate and dissolved phases in an urban river. *Water Research, 28*(9), 1921-1931.

Weishaar, J. L., Aiken, G. R., Bergamaschi, B. A., Fram, M. S., Fujii, R., & Mopper, K. (2003). Evaluation of specific ultraviolet absorbance as an indicator of the chemical composition and reactivity of dissolved organic carbon. *Environmental Science & Technology, 37*(20), 4702-4708.

Wellman, T. P., Paschke, S. S., Minsley, B., & Dupree, J. A. (2011). *Hydrogeologic setting and simulation of groundwater flow near the Canterbury and Leadville Mine Drainage Tunnels, Leadville, Colorado*. Retrieved from

Western Regional Climate Center, W. (2021). Leadville, Colorado. *Retrieved from: https://wrcc.dri.edu/cgi-bin/cliMAIN.pl?co4884*. Retrieved from https://wrcc.dri.edu/cgi-bin/cliMAIN.pl?co4884

Winnick, M. J., Carroll, R. W., Williams, K. H., Maxwell, R. M., Dong, W., & Maher, K. (2017). Snowmelt controls on concentration-discharge relationships and the balance of oxidative and acid-base weathering fluxes in an alpine catchment, E ast R iver, C olorado. *Water Resources Research, 53*(3), 2507-2523.

Wood, C. M., Al-Reasi, H. A., & Smith, D. S. (2011). The two faces of DOC. *Aquatic Toxicology, 105*(3-4), 3-8.

Woody, C. A., & O'Neal, S. (2012). Effects of copper on fish and aquatic resources.

Xue, H., & Sunda, W. G. (1997). Comparison of [Cu2+] measurements in lake water determined by ligand exchange and cathodic stripping voltammetry and by ion-selective electrode. *Environmental Science & Technology, 31*(7), 1902-1909.

Yang, Y., Yuan, X., Deng, Y., Xie, X., Gan, Y., & Wang, Y. (2020). Seasonal dynamics of dissolved organic matter in high arsenic shallow groundwater systems. *Journal of Hydrology, 589*, 125120.